DEVELOPMENT AND PERFORMANCE ANALYSIS OF FLAT PLATE BASE-THERMAL CELL ABSORBER

BY

MUHAMMAD AMIN BIN HARUN

A thesis submitted in fulfillment of the requirement for the degree of Doctor of Philosophy (Engineering)

Kulliyyah of Engineering
International Islamic University Malaysia

AUGUST 2023

ABSTRACT

This study aims to design, fabricate, and study the performance of a thermal cell absorber attached to a flat plate absorber collector. Flat Plate Solar Collector (FPSC) is widely used in agricultural products for drying applications. An investigation into the effect of design parameters on FPSC has been carried out. Flat Plate Base-Thermal Cell Absorber (FPBTCA) has been designed and fabricated based on the design parameters experiment results which are; absorber base materials (AL), absorber base thickness (0.5 mm), the air gap distance between glass and absorber base (10 mm), the air gap distance between glass 1 and glass 2 (0.4 mm), double glass, glass thickness (2.0 mm), thermal cell thickness (1.0 mm) and material (SS). The experiment was performed using a solar simulator with solar radiation of 700 W/m^2. The solar simulator is used as the artificial sun, which is exposed to solar radiation for 300 seconds and without solar radiation also for 300 seconds. The heat transfer rate of the collector ($\dot{Q}$) and efficiency of the collector shows that stainless steel 1.0 mm with aluminum base absorber has a higher value which is 412 kJ, 18.21 kW, and 47.08 %, respectively. The performance of the outlet temperature in the drying chamber of stainless steel with an aluminum absorber has a higher value of energy gain which is 116.08 J at 300 seconds. Evaluation under outdoor conditions revealed that the FPBTCA has a lower temperature discharge rate as compared to the FPSC. FPBTCA also shows the highest heat absorption ($\dot{Q}$), which is 96079.37 J on 4 March 2021, then FPSC, which is 49187.07 J. The highest efficiency for FPBTCA at 360 minutes is 30.24 %, and for FPSC is 21.81 %. The efficiency of FPBTCA is consistent while the solar radiation is decreased at 120 minutes and 180 minutes. Mathematical modelling analysis proved that the error for energy balance is below 5%. FPBTCA has been introduced to enhance the thermal performance and efficiency of solar thermal collector systems. It also has higher heat storage capabilities during solar radiation drops when the weather is cloudy.

خلاصة البحث

هدفت الدراسة الحالية إلى تصميم وتصنيع ودراسة أداء مُمتص للخلايا الحرارية والمرتبطة بمجمّع امتصاص لوح شمسي مسطح (FPSC)، حيث أنه يُستخدم على نطاق واسع في المنتجات الزراعية لعمليات التجفيف. وقد أُجري تحقيق لمعرفة تأثير معلمات التصميم المستخدم في البحث الحالي على FPSC والتي كانت؛ المواد الأساسية للامتصاص (AL)، سماكة قاعدة الامتصاص (0.5 مم)، مسافة فجوة الهواء بين الزجاج وقاعدة الامتصاص (10 مم)، مسافة فجوة الهواء بين الزجاج 1 والزجاج 2 (0.4 مم)، الزجاج المزدوج، سماكة الزجاج (2.0 مم)، سماكة الخلية الحرارية (1.0 مم) والمادة (SS)، وتم تصميم وتصنيع ممتص الخلايا الحرارية ذو القاعدة المسطحة (FPBTCA) بناءً على نتائج تجربة معايير التصميم. تم إجراء التجربة باستخدام جهاز محاكاة شمسي بإشعاع 700 واط/م^2، ويتم استخدام جهاز المحاكاة هذا كشمس اصطناعية، حيث تتعرض للإشعاع لمدة 300 ثانية وبدونه أيضاً لنفس المدة. يوضح معدل نقل الحرارة للمُجمّع ($\dot{Q}$ وتبلغ 412 كيلو جول) وكفاءة المجمّع (18.21 كيلو واط) أن الفولاذ المقاوم للصدأ 1.0 مم مع قاعدة الألومنيوم الممتص له قيمة أعلى بنسبة 47.08٪. درجة حرارة المخرج في حجرة التجفيف المصنوعة من الفولاذ المقاوم للصدأ مع ممتص الألمنيوم كانت له قيمة أعلى في اكتساب الطاقة وهي 116.08 جول عند 300 ثانية. أظهر التقييم في الظروف الخارجية أن FPBTCA لديه معدل تدفق أقل للحرارة مقارنة بـ FPSC. أظهر FPBTCA أعلى امتصاص للحرارة ($\dot{Q}$)، وهو 96079.37 جول، ثم FPSC وهو 49187.07 جول. أعلى كفاءة لـ FPBTCA عند 360 دقيقة هي 30.24٪ و FPSC هي 21.81٪. كفاءة FPBTCA ثابتة حينما ينخفض الإشعاع الشمسي عند 120 و 180 دقيقة. أثبت تحليل النمذجة الرياضية أن الخطأ في توازن الطاقة أقل من 5٪. تم إدخال FPBTCA لتحسين الأداء الحراري وكفاءة أنظمة تجميع الطاقة الشمسية الحرارية. كما أن لديها قدرات تخزين أعلى للحرارة أثناء انخفاض الإشعاع الشمسي عندما يكون الطقس غائماً.

APPROVAL PAGE

The thesis of Muhammad Amin Harun has been approved by the following:

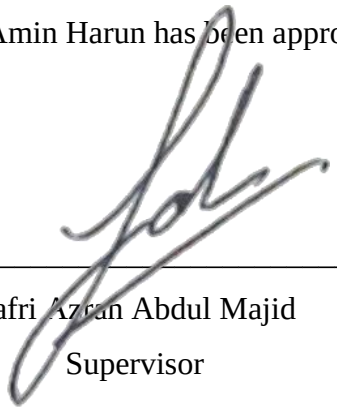

Zafri Azran Abdul Majid
Supervisor

Sany Izan Ihsan
Co-Supervisor

Sanisah Saharin
Internal Examiner

Wan Azmi Bin Wan Hamzah
External Examiner

Ahmad Faris Ismail
Chairman

DECLARATION

I hereby declare that this dissertation is the result of my own investigations, except where otherwise stated. I also declare that it has not been previously or concurrently submitted as a whole for any other degrees at IIUM or other institutions.

Muhammad Amin Harun

Signature ..... Date 09 AUGUST 2023

INTERNATIONAL ISLAMIC UNIVERSITY MALAYSIA

DEVELOPMENT AND PERFORMANCE ANALYSIS OF FLAT PLATE BASE-THERMAL CELL ABSORBER

I declare that the copyright holders of this dissertation are jointly owned by the student and IIUM.

By signing this form, I acknowledged that I have read and understand the IIUM Intellectual Property Right and Commercialization policy.

Affirmed by Muhammad Amin Harun

……..…….. ……..

Signature Date

09 AUGUST 2023

DEDICATION

This thesis is dedicated to my late father and my mother for laying the foundation of what I turned out to be in life.

ACKNOWLEDGEMENTS

Firstly, special thanks to my dear mother; Napiah Uda, my wife; Noriza Mat Hashim and my children; Muhammad Aqmar, Muhammad Afifuddin, Mohammad Asri Haiqal, and Adlina Humaira, who gave me the strength to achieve my goal to complete the research successfully.

I wish to express my appreciation and thanks to those who provided their time, effort, and support for this project. To the members of my dissertation committee, Prof. Ahmad Faris Ismail, Associate Prof. Dr. Sany Izan Ihsan and Prof. Dato' Dr. Kamaruzzaman Sopian thanks for always supporting my journey. I would also like to thank my friends and research colleagues, Dr. Iqbal Jamaludin, Dr. Ahmad Fadzil Sharol, Dr. Amir Abdul Razak and Zairul Azrul Zakaria for their constant encouragement.

My sincerest gratitude goes to my supervisor, Assistant Prof. Dr. Zafri Azran Abdul Majid, who has supported me throughout my thesis with his patience and knowledge while allowing me the room and freedom to work in my own way. He has taught me the methodology to carry out the research and to present the research work as clearly as possible. It was a great privilege and honor to work and study under his guidance. I am extremely grateful for what he has offered me.

TABLE OF CONTENTS

Abstract ..... **ii**
Abstract in Arabic ..... **iii**
Approval Page ..... **iv**
Declaration ..... **v**
Copyright ..... **vi**
Dedication ..... **vii**
Acknowledgements ..... **viii**
Table of contents ..... **ix**
List of Tables ..... **xiiiii**
List of Figures ..... **xv**
List of Symbols ..... **xixx**
List of Abbreviations ..... **xxi**

CHAPTER ONE : INTRODUCTION **1**
1.1 Background of Study 1
1.2 Research Problem 3
1.3 Research Objectives 4
1.4 Significance of Study 5
1.5 Research Scopes 5
1.6 Research Methodology 6
1.7 Thesis Structure 6
1.8 Chapter Summary 7

CHAPTER TWO : LITERATURE REVIEW **8**
2.1 Introduction 8
2.2 Solar Thermal Collector Technology 9
2.3 Types of Solar Thermal Collector 10
2.3.1 Stationary Solar Collector 11
2.3.1.1 Flat Plate Solar Collector 11
2.3.1.2 Stationary Compound Parabolic Collectors 12
2.3.1.3 Evacuated Tube Collectors 13
2.3.2 Single Axis Tracking 15
2.3.2.1 Linear Fresnel Reflector 16
2.3.2.2 Parabolic Through Collector 17
2.3.2.3 Cylindrical Through Collector 18
2.3.3 Two Axes Tracking 19
2.3.3.1 Parabolic Dish Collector 19
2.3.3.2 Heliostat Field Collector 20
2.4 Flat Plate Solar Collector (FPSC) Application 22
2.5 Types of Air Heating Flat Plate Solar Collector 24
2.5.1 Bare –Plate Solar Collector 25
2.5.2 Covered-Plate Solar Collector 25
2.6 Flat Plate Solar Collector (FPSC) 26
2.6.1 Thermal Absorber Collector Design 27
2.6.2 Materials and Thickness of Flat Plate Solar Collector 28

2.6.3 Solar Collector Glazing Materials 29
2.6.3.1 Types of Glass in Flat Plate Solar Collector 30
2.6.4 Thermal Absorber Surface Coating 30
2.6.5 Thermal Insulation 32
2.6.6 Air Gap Between Glass and Flat Plate Absorber Collector 33
2.6.7 Double Glass for Glazing.....33
2.7 The Improvement of Flat Plate Solar Collector (FPSC).....33
2.7.1 Finned Absorber Collector.....34
2.7.2 Ribbed Absorber Collector 34
2.7.3 Corrugated Absorber Collector.....35
2.7.4 Phase Change Material (PCM) as Thermal Storage 36
2.7.5 Nanofluid as Working Fluid 37
2.7.6 Porous Media in the Flat Plate Absorber Collector 38
2.8 Mathematical Modelling.....39
2.9 Chapter Summary 41

CHAPTER THREE : RESEARCH METHODOLOGY 42
3.1 Introduction 42
3.2 Flow Chart of Research.....42
3.2.1 Review the Design of Flat Plate Solar Collector 44
3.2.2 Preliminary Experiment to the Flat Plate Solar Collector (FPSC) Parameter 44
3.2.3 Design and Developed Flat Plate Base-Thermal Cell Absorber (FPBTCA).....45
3.2.4 Preparation of the Materials and Component 45
3.2.5 Fabricate Flat Plate Base-Thermal Cell Absorber (FPBTCA) 47
3.2.6 Venue for the Experiment.....47
3.2.7 Run Experiment 47
3.2.8 Mathematical Modelling.....48
3.2.9 Experiment Result Satisfies with Mathematical modelling.....48
3.3 Method to Evaluate for Flat Plate Absorber Design Parameter.....48
3.3.1 Method to Evaluate for Flat Plate Absorber Material, Glass Thickness, Air Gap Thickness and Flat Plate Absorber Base Collector.....49
3.3.2 Method to Evaluate for Different Coating Surfaces and Thermal Cell Absorber 51
3.4 Selection of Flat Plate Absorber Collector Materials 53
3.5 Selection of Coating Surface and Non Coating Surfaces 53
3.6 Selection of Flat Plate Thermal Cell Thickness.....54
3.7 Selection of Glass Thickness 55
3.8 Evaluation Air Gap Distance (Between Flat Plate Absorber Collector and Glass) 55
3.9 Selection of Flat Plate Absorber Base Collector Thickness 56
3.10 Selection of Glass Cover.....57
3.11 Preliminary 1 and 2 for Flat Plate Solar Collector and Flat Plate Base-Thermal Cell Absorber 58

3.11.1 Method to Evaluate for Flat Plate Solar Collector (Aluminum Base Absorber)....59
3.11.2 Method to Evaluate for Flat Plate Base-Thermal Cell Absorber (FPBTCA)....61
3.11.3 Evaluation of Aluminum Cell with Aluminum (Absorber Base)....64
3.11.4 Evaluation of Stainless Steel Cell with Aluminum (Absorber Base)....64
3.12 Experiment Outdoor for Flat Plate Solar Collector (FPSC) and Flat Plate Base-Thermal Cell Absorber (FPBTCA)....65
3.12.1 Method to Evaluate for Flat Plate Solar Collector (FPSC)....65
3.12.2 Method to Evaluate for Flat Plate Base-Thermal Cell Absorber (FPBTCA)....66
3.13 Uncertainty Analysis....67
3.14 Energy Balance of Flat Plate Base-Thermal Cell Absorber (FPBTCA)....68
3.14.1 Heat Transfer Loss....72
3.14.2 Heat Storage Capability....72
3.14.3 The Process of Theoretical Solution....73
3.15 Chapter Summary....74

CHAPTER FOUR : RESULT AND DISCUSSION....75
4.1 Introduction....75
4.2 Evaluation of Design Parameter....75
4.2.1 Thermal Analysis....75
4.2.2 Materials Comparison....76
4.2.3 Coating Surface Comparison....78
4.2.4 Glass Thickness Comparison....80
4.2.5 Air Gap Thickness (Between Flat Plate Absorber Collector and Glass)....82
4.2.6 Flat Plate Solar Thermal Cell Absorber....85
4.2.7 Flat Plate Absorber Base Collector....87
4.2.8 Glass Cover Comparison....89
4.3 Design Parameter for Flat Plate Base-Thermal Cell Absorber (FPBTCA)....90
4.4 Preliminary Experiment 1 for Flat Plate Solar Collector and Flat Plate Base-Thermal Cell Absorber (FPBTCA)....92
4.4.1 Performance Output Analysis of Drying Chamber....96
4.4.2 Heat Storage....97
4.4.3 Heat Transfer Rate ($\dot{Q}$)....98
4.4.4 Efficiency (%)....99
4.4.5 Energy Gain....100
4.5 Preliminary Experiment 2 for Flat Plate Solar Collector (FPSC) and Flat Plate Base-Thermal Cell Absorber (FPBTCA)....102
4.5.1 Heat Storage....105
4.5.2 Efficiency (%)....106
4.5.3 Energy Gain....106
4.6 Outdoor Experiment Performance....108
4.6.1 Day 1, 4 March 2021....108
4.6.2 Day 2, 5 March 2021....110
4.6.3 Day 3, 6 March 2021....112

4.6.4 Day 4, 7 March 2021 114
4.6.5 Day 5, 8 March 2021 116
4.6.6 Day 6, 9 March 2021 118
4.7.7 Day 7, 21 March 2021 120
4.7 Daily Performance Comparison 122
4.8 Evaluation of Thermal Cell Module Performance 123
4.8.1 Mathematical Modelling Analysis 124
4.8.2 Efficiency (%) Comparison Between FPBTCA and FPSC 124
4.8.3 Heat Conduction, Q (J) Between FPBTCA and FPSC 126
4.9 Techno-economics Evaluation of The Flat Plate Base-Thermal Cell Absorber (FPBTCA) 127
4.10 FPBTCA Economic Evaluation: Cost Savings 128
4.11 Evaluation of FPBTCA Cost-Effectiveness 129
4.12 Discussion 131
4.13 Chapter Summary 138

CHAPTER FIVE : CONCLUSION AND RECOMMENDATION 139
5.1 Conclusions 139
5.2 Recommendations 143
REFERENCES 144
APPENDIX I 160
APPENDIX II 163

LIST OF TABLES

Table 2.1: Solar Energy Collectors 11

Table 2.2: Layout method installation for single-axis tracking (Chang, 2016). 15

Table 2.3: Physical properties of conductors (Pekez et al., 2013) 29

Table 2.4: Transmittance of various glazing material (Vestlund, 2012) 30

Table 2.5: Solar absorptance, emittance and reflectance for various surfaces 31

Table 2.6: Properties of common insulation materials (M. Kehrer, 2003) 32

Table 3.1: The materials involved in this research 45

Table 3.2: Flat plate absorber materials configuration 53

Table 3.3: Experiment table for flat plate solar collector configuration 58

Table 3.4: Uncertainty of the important parameters 68

Table 4.1: Flat plate absorber temperature versus time for different flat plate absorber materials 77

Table 4.2: Summary of heat gain rate and heat discharge rate of aluminium coated and aluminum non-coated 80

Table 4.3: Summary of heat gain rate of different glass thicknesses 81

Table 4.4: Summary of heat gain rate and heat discharge rate of air gap distance between flat plate absorber and glass 84

Table 4.5: Summary of heat gain rate of different Stainless Steel 304 flat plate thermal cell absorber 87

Table 4.6: Summary of heat gain rate of different flat plate absorber base collector thicknesses 88

Table 4.7: Summary of heat gain rate of different glass covers 90

Table 4.8: Design parameter for Flat Plate Base-Thermal Cell Absorber (FPBTCA)91

Table 4.9: The maximum temperature within 300 seconds of charging process 93

Table 4.10: Heat storage (Q storage) value (in kW) for each type of absorber in drying chamber 98

Table 4.11: Heat transfer rate of the collector (Q) value (in kW) for drying chamber each case of the experiment 99

Table 4.12: Efficiency of the collector and storage in drying chamber (in %) of the collector and storage in the drying chamber of the different types of absorber thermal collector. 100

Table 4.13: Energy gain value (in KJ) of T1 and T2 for bottom plate each case of the experiment after the completion of discharging process 100

Table 4.14: Energy gain value (in J) of absorber for T1 and T ambient each case of the experiment after the completion of discharging process. 101

Table 4.15: Energy gain value (in J) of absorber for T3 and T ambient each case of the experiment after the completion of discharging process 101

Table 4.16: The maximum temperature within 600 seconds of charging process 103

Table 4.17: Heat storage (Q storage) value (in kW) for each type of absorber in drying chamber 106

Table 4.18: Efficiency of the collector and storage in drying chamber (in %) of the collector and storage in the drying chamber of the different types of absorber thermal collector. 106

Table 4.19: Energy gain value (in KJ) of T1 and T2 for bottom plate each case of the experiment after the completion of discharging process 107

Table 4.20: Energy gain value (in J) of absorber for T1 and T ambient each case of the experiment after the completion of discharging process 107

Table 4.21: Error between Qin and Qout 124

Table 4.22: Cost projection of conventional electrical household dryer and FPBTCA for the first year of installation and cost-saving by solar energy 129

Table 4.23: The cost of thermal absorber 130

Table 4.24: Cost effective parameter for FPBTCA 131

Table 5.1: Chosen design parameters for Flat Plate Base-Thermal Cell Absorber (FPBTCA) 138

LIST OF FIGURES

Figure 2.1: Flat plate solar collector component (S. A. Kalogirou, 2004). 12

Figure 2.2: Different configurations of ideal two-dimensional concentrators: 13

Figure 2.3: Glass evacuated tube solar collector with U-tube. a) Illustration of the glass evacuated tube; b) Cross section (Ma et al., 2010). 15

Figure 2.4: Schematic diagram of a Linear Fresnel Reflctor solar collector with a 16

Figure2.5: Parabolic Trough Collectors (PTC) (1) reflector, (2) receiver (Chafie et al., 2018) 17

Figure 2.6: Schematic diagram of Cylindrical Through Collector (CTC) at 30 degrees and the receiver tube (Shojaee et al., 2015) 18

Figure 2.7: Schematic diagram of Parabolic Dish Reflector (PDR) 19

Figure 2.8: Schematic diagram of a Heliostat Field Collector (Kodama, 2003). 21

Figure 2.9: Classification and indicative temperature range of solar collectors 23

Figure 2.10: Various types of flat plate collector (FPC): A–E: air-based solar 24

Figure 2.11: Schematic diagram of a bare-plate (no cover) air-heating solar energy collector (B. Norton, 1992) 25

Figure 2.12: Schematic illustration of covered air heating solar energy collectors: 26

Figure 2.13: Cross-section of a typical liquid flat plate solar collector (Saleh, 2012) 27

Figure 2.14: Types of thermal absorbers for solar air heater with stationary flat absorber (A A Razak, 2017) 28

Figure 2.15: Hottel - Whillier Bliss efficiency curves (Norton, 2006) 32

Figure 2.16: Finned absorber plate (Vengadesan & Senthil, 2020) 34

Figure 2.17: Ribbed absorber plate (Vengadesan & Senthil, 2020) 35

Figure 2.18: Different configurations of corrugated absorber: (a) V-corrugation, (b) Trapezoidal corrugation, (c) Sinusoidal corrugation, (d) Finned corrugation (Vengadesan & Senthil, 2020). 36

Figure 2.19: Different types of phase change material (PCM) 37

Figure 2.20: Schematic diagram of a flat plate solar collector (Dobriyal et al., 2020)38

Figure 2.21: Porous media assisted in flat plate solar collector 39

Figure 3.1: Flow chart of research activities. 43

Figure 3.2: Material and device used in this study 46

Figure 3.3: Experimental set-up 49

Figure 3.4: a) Top view b) Side view of flat plate solar collector diagram. 50

Figure 3.5: Experimental set-up 51

Figure 3.6: a) Top view b) Side view of flat plate solar collector diagram. 52

Figure 3.7: a) Non-Coated b) Coated for flat plate absober collector 54

Figure 3.8: Flow chart implemented in this work 54

Figure 3.9: Process flow chart implemented in this work 55

Figure 3.10: Process flow chart implemented in this work 56

Figure 3.11: Flow chart implemented in this work 57

Figure 3.12: Double glass diagram for FPSC 57

Figure 3.13: Experiment set-up for flat plate solar colelctor 59

Figure 3.14: a) Top view b) Side view of flat plate solar collector diagram 60

Figure 3.15: Temperature sensor location. 61

Figure 3.16: Experiment set-up for FPBTCA 61

Figure 3.17: a) Top view b) Side view of FPBTCA diagram 62

Figure 3.18: Temperature sensor location 63

Figure 3.19: Experiment set-up for FPBTCA and FPSC. 65

Figure 3.20: a) Top view b) Side view of FPSC 65

Figure 3.21: a) Top view b) Side view of FPBTCA 66

Figure 3.22: Energy balance diagram for FPBTCA 70

Figure 4.1: Flat plate absorber temperature versus time for different flat plate absorber materials 76

Figure 4.2: Heat charging/ heat discharging versus different flat plate absorber material 78

Figure 4.3: Flat plate absorber temperature versus time for Aluminum coated and non-coated surface 79

Figure 4.4: Flat plate absorber temperature versus time for different glass thicknesses 81

Figure 4.5: Heat charging/ heat discharging versus glass thickness 82

Figure 4.6: Flat plate absorber temperature versus time for air gap space between flat plate absorber and glass 83

Figure 4.7: Heat charging/ heat discharging versus air gap between absorber-collector and glass 85

Figure 4.8: Flat plate absorber temperature versus time for different Stainless Steel 304 flat plate thermal cell absorber 86

Figure 4.9: Flat plate absorber temperature versus time for different flat plate absorber base collector thicknesses 88

Figure 4.10: Flat plate absorber temperature versus time for different glass cover comparison 89

Figure 4.11: Flat Plate Base-Thermal Cell Absorber (FPBTCA) diagram. 91

Figure 4.12: Temperature versus time for various absorber collector configurations, 95

Figure 4.13: Temperature versus time for various absorber collector configurations, 105

Figure 4.14: Flat plate absorber temperature, T1 for FPSC and FPBTCA 109

Figure 4.15: Dummy load absorber temperature, T3 for FPSC and FPBTCA 110

Figure 4.16: Flat plate absorber temperature, T1 for FPSC and FPBTCA 111

Figure 4.17: Dummy load absorber temperature, T3 for FPSC and FPBTCA 112

Figure 4.18: Flat plate absorber temperature, T1 for FPSC and FPBTCA 113

Figure 4.19: Dummy load absorber temperature, T3 for FPSC and FPBTCA 114

Figure 4.20: Flat plate absorber temperature, T1 for FPSC and FPBTCA 115

Figure 4.21: Dummy load absorber temperature, T3 for FPSC and FPBTCA 116

Figure 4.22: Flat plate absorber temperature, T1 for FPSC and FPBTCA 117

Figure 4.23: Dummy load absorber temperature, T3 for FPSC and FPBTCA 118

Figure 4.24: Flat plate absorber temperature, T1 for FPSC and FPBTCA 119

Figure 4.25: Dummy load absorber temperature, T3 for FPSC and FPBTCA 120

Figure 4.26: Flat plate absorber temperature, T1 for FPSC and FPBTCA 121

Figure 4.27: Dummy load absorber temperature, T3 for FPSC and FPBTCA 122

Figure 4.28: Daily heat absorption for FPSC and FPBTCA. 123

Figure 4.29: Efficiency (%) versus Time (Minutes) and Solar Radiation (W/m^2) 125

Figure 4.30: Heat conduction, Q (J) versus Time (Minutes) and Solar Radiation (W/m^2). 127

LIST OF SYMBOLS

A	Cross sectional area (m^2)
A_c	Surface area of collector (m^2)
A_s	Surface area (m^2)
C_p	Specific heat capacity (kJ/kg.K)
$\dot{E}_{in}$	Rate of energy, inlet (W)
$\dot{E}_{out}$	Rate of energy, outlet (W)
$\dot{E}_{system}$	Change of rate of energy in the system (W)
S_R	Global solar radiation, total (kW/m², W/m²)
h	Convective heat transfer coefficient ($W/m^2.K$)
H	Height (m, mm)
k	Thermal conductivity (W/m.K)
L	Length (m, mm)
S_R	Solar radiation (kW/m², W/m²)
T	Temperature (K)
T_f	Temperature of fluid (K)
$T_{f,i}$	Temperature of fluid, inlet (K)
$T_{f,o}$	Temperature of fluid, outlet (K)
T_{f1}	Temperature of fluid at point 1 (K)
T_{f2}	Temperature of fluid at point 2 (K)
T_i	Temperature, inlet (K)
T_o	Temperature, outlet (K)
t	Thickness (mm)
t	Time (s)
$\dot{Q}_u$	Rate of useful energy gain (W)
V	Air velocity (m/s)
W	Width (mm)
$\dot{m}$	Air mass flow rate (kg/s)
α	Thermal diffusivity (m^2/s)
ε	Emissivity
η	Thermal efficiency

ρ	Air density (kg/m^3)
η	Thermal efficiency
$\tau\alpha$	Transmittance-absorptance product

LIST OF ABBREVIATIONS

BOM	Bills of Materials
CFD	Computational Fluid Dynamic
DAQ	Data acquisition
e.g.	*(exempli gratia)*: for example
FPBTCA	Flat Plate Base-Thermal Cell Absorber
et al.	*(et alia)*: and others
etc	*(et cetera)*: and so forth
fig./ figs.	*figure/ figures*
FPSC	Flat Plate Solar Collector
GMP	Good Manufacturing Practice
i.e.	*(id est)*: that is
ID	Inner diameter
OD	Outer diameter
PV	Photo-voltaic
PVC	Polyvinyl Chloride
SAHP	Solar Assisted Heat Pump
Vol./ Vols.	Volume/ Volumes

CHAPTER ONE

INTRODUCTION

1.1 BACKGROUND OF STUDY

The solar radiation that reaches the Earth's surface without being diffused is labeled as direct beam solar radiation. The sum of the diffused and direct solar radiation is labeled as global solar radiation. The effective blackbody temperature of the sun is about 5777 K. The central interior region's temperature is varyingly approximated at 8 x 10^6 to 40 x $10^{6,}$ and the density is approximated about 100 times water (Beckman, 2013). Solar energy is known as a renewable energy source (Bahadori & Nwaoha, 2013), and the usage of the energy could be minimized with environmental impacts (Panwar et al., 2011). Solar energy has been used in solar thermal technology such as solar air heating systems, solar water heating systems, photovaltic systems, and thermal systems.

Solar thermal technology can be considered as a reliable technology in the applications related to industry and household due to its abundant sources of energy. Based on history, in 1767, the Swiss scientist Horace Benedict de Saussure was the first man who invented and produced flat plate solar thermal collectors (Huff et al., 1950). The component inside a flat plate solar thermal collector consists of three layers of glass which are used to absorb heat energy from the sun's radiation. Flat plate solar thermal collectors are used because it has advantages such as incurring low cost in manufacturing, economical maintenance (Colangelo et al., 2016), and environmentally friendly.

The principle involved in flat plate solar collectors (FPSC) is to gain as much possible radiation energy from the sun by heat absorption. The absorber for a flat plate solar collector is coated with a flat black coating to increase the rate of energy gained from sunshine. The energy which has been collected is transferred through conduit tubes by working fluids (usually water) which are integrated with a heat absorber plate. On

that occasion, the warm water transmits the heat energy through the hot water system at the same time, stores it in the storage system, which is a backup when the sun's radiation is low (John A. Duffie and William A. Beckman, 2006). The performance of solar collectors is analyzed using Thermodynamics analysis.

There is an important issue related to the solar energy system, which is the cost of the system (S. A. Kalogirou, 2008). Basically, it is very expensive to develop solar technology systems. Based on that argument, economic analysis is a very important aspect that should be considered when developing the solar collector. The researcher has been studying the impact of solar water hot systems on the economical and environmental prospects(Ardente et al., 2005; S. A. Kalogirou, 2004; S. A. Kalogirou, 2008; Tsilingiridis, G. et al., 2004).

Malaysia consists of Peninsular Malaysia, Sabah, and Sarawak. The West and east of Malaysia are separated by the South China Sea (Muhammad-Sukki et al., 2011). Malaysia is also a tropical country located at the equator and strategically located. Based on the statistics, Malaysia has received approximately 400–600 MJ/m^2 of monthly solar radiation (Mekhilef et al., 2012). The average daily solar insulation is about 5.5 kWm^2, equivalent to 15 MJ/m (Shafie et al., 2011). Malaysia's climate is suitable for its solar energy usage as a renewable source with 10 hours of predictable daily sunlight (Gomesh et al., 2013).

The purpose of this study is to design a flat plate solar thermal Aluminum absorber (base) collector with an absorber thermal cell. The different absorber thermal cell material is investigated to find the best absorber thermal cell that can be used when designing a new design of Flat Plate Solar Collector (Aluminum and Stainless Steel). The design parameters involved in this experiment are absorber base-collector thickness, absorber collector materials, air gap distance, double glass and glass thickness, thermal cell thickness, and material. The experiment was done indoor and outdoor to determine the experimental data for Flat Plate Solar Collector (FPSC) and Flat Plate Base-Thermal Cell Absorber (FPBTCA). The development of mathematical modelling for the flat plate solar thermal Aluminum absorber (base) collector with absorber thermal cell system will be modelled. Mathematical modelling is performed

to compare with the experiment to find the correlation data. The absorber will then be integrated into an open cycle drying chamber with energy storage ability to optimize system performance for the indoor and outdoor experiment. The venue for the indoor experiment was at IIUM campus Kuantan, while for outdoor was at Beserah, Kuantan, and the experiment was conducted to gather the data and to compare it with mathematical modelling.

1.2 RESEARCH PROBLEM

i. Drying chamber system:

The design of flat plate solar collector with different locations of drying chamber has a weakness in the flat plate solar collector's performance. The heat energy is reduced when the heat is transferred from the flat plate absorber collector to the drying chamber (Choudhary et al., 2020; D. Gao et al., 2020; Nabnean et al., 2016). Basically, the current design of a flat plate solar collector is designed with extra insulation, piping, and fitting (Mohamad, 1997). Based on the situation, the performance of a flat plate solar collector is affected when air flow moves from the flat plate solar collector absorber to the drying chamber.

ii. Flat plate solar collector design parameters and materials:

The performance of a flat plate solar collector depends on parameters such as design and components. The parameters were absorber collector thickness, absorber collector materials, air gap distance, double glass, and glass thickness (M. Faizal Fauzan, 2015). Absorber material and design is the most important factor for flat plate solar collector. Therefore, the shape of the absorber collector could affect the efficiency performance of flat plate solar (Essalhi et al., 2018). Basically, the design of the absorber collector could improve heat transfer (Sharol, 2021). Obstacles' presence is an important factor for the improvement of flat plate solar collector performance. Different shapes of obstacles and positions produce different results (A A Razak, 2017; Abene et al., 2004). One of the aspects of enhancing the heat transfer capability in the collector is to increase

the heat exchanging areas of the thermal absorber (Colangelo et al., 2016). By increasing the glass thickness ,the total heat gain will be reduced (Ismail & Henr, 2003). It can be concluded that the flat plate absorber collector temperature varies with different configurations of air gap thickness (Ferahta et al., 2011). The results also indicates that double glass as glass cover for flat plate solar collector could generate a lower top loss on heat transfer coefficient than single glass configuration (Vettrivel & Mathiazhagan, 2017).

iii. Integrated thermal buffer:

Using Bi metallic cross absorber will increase the energy buffer storage, but the temperature output will be reduced (A A Razak, 2017). Therefore, thermal energy storage is an important aspect that should be considered when designing a new flat-plate solar collector. The solar collector with energy storage could make full use of solar energy to save fossil energy and protect the environment (Xu et al., 2020).

iv. Solar collector size:

The size of the solar collector depends on the drying application. There is a problem when increasing from small size to large size Flat Plate Solar Collector. The problem is to determine the size of the flat plate absorber collector. Additionally, the geometry of the flat plate absorber-collector could affect the performance of the flat plate solar collector (Manikandan & Sivaraman, 2016).

1.3 RESEARCH OBJECTIVES

This study aimed to fabricate and produce Flat Plate Base-Thermal Cell Absorber (FPBTCA). The objectives are as follows:

i. To design and develop Flat Plate Base-Thermal Cell Absorber (FPBTCA).
ii. To evaluate the effect of design parameters and materials.
iii. To develop and validate the mathematical model for FPBTCA in the passive condition.

1.4 SIGNIFICANCE OF STUDY

The research significantly improves the performance of the Flat Plate Base-Thermal Cell Absorber (FPBTCA). The enhancement was done to the flat plate solar collector by attaching a flat plate thermal cell at the top of the flat plate absorber base collector. The FPBTCA design is to meet the requirement of Good Manufacturing Practice (GMP) for food drying.

The FPBTCA was developed to reduce the weight of flat plate solar collectors so that they could be used as portable solar collectors. The results obtained from this study will serve as fundamental knowledge on the solar thermal collector, which can be utilized toward the commercialization of the FPBTCA.

1.5 RESEARCH SCOPES

i. This research is to develop a flat plat solar thermal collector, which is an absorber cell that will be used to increase the solar thermal collector efficiency. The purpose of this research is to overcome the air heating that is used in drying and heating. For heating, there is no air, and for drying, the air will be used as heating.
ii. The coating used for thermal absorber coating is matt black paint.
iii. The material used for the flat plate absorber collector is stainless steel 304 and aluminium.
iv. All types of absorber base collectors were fabricated with a dimension of 0.255-meter length and 0.185-meter width. The thermal cell collector was fabricated with a dimension of 0.01-meter length and 0.01-meter width.
v. Indoor experiments were conducted by using a simulator, and outdoor experiments were conducted during the daytime and were exposed to ambient conditions, i.e., dust, clouds, and wind.
vi. The computational and simulation of the mathematical model will be developed by using Microsoft excel.

1.6 RESEARCH METHODOLOGY

The methodology starts with studying the flat plate solar collector component and system. A study was done on reviewing the literature of previous research on solar dryer systems to determine the detailed problems and solutions for solar dryer systems. From the literature review, the details of the focus area could be explored to overcome the problem of the flat plate solar collector system.

Then the experiment was performed on the design parameters to identify the suitable design parameter that can be used when designing Flat Plate Base-Thermal Cell Absorber (FPBTCA). The experiment was conducted indoor, in a controlled environment by using a solar simulator with radiation of 450 W/m^2 and 700 W/m^2.

The material for fabricating FPBTCA was prepared based on the findings from the design parameter experiment. A preliminary experiment was done to evaluate the performance of different thermal cell absorber materials and thicknesses. Aluminum and stainless-steel material was used as thermal cell absorber material. A thermal cell absorber collector suitable for FPBTCA was identified based on the findings.

The outdoor experiment was conducted to compare the performance of FPBTCA with a flat plate solar collector (FPSC). Based on the results, it will indicate the capability of FPBTCA when applying outdoor environment conditions. A heat transfer experiment was arranged to relate it to mathematical modelling. The results will be analyzed based on the data gathered from the experiment, which will be used to compare with mathematical modelling.

1.7 THESIS STRUCTURE

This thesis consists of five chapters. The first chapter presents the background of the studies, problem statements, research objectives, the significance of the study, research scopes, and a summary of methodology. The second structures provide literature research related to the solar thermal harnessing technology with a focus on the solar

thermal collector parameters, which is the gap between glass and absorber, absorber materials, absorber thickness, and glass thickness

Chapter three covers the methodology of the experimental work conducted in this research. The details present in chapter four are the experimental setup and procedure for each experiment involved. It also involved materials and components that will be used to fabricate FPBTCA. Heat transfer analysis and mathematical modelling work for flat plate absorbers are also involved in chapter three. The theoretical analysis consists of thermodynamics energy balance, collector performance, and heat transfer analysis.

The results and discussion are presented in chapter four. This chapter consists of results and a discussion of design parameters, preliminary experiment, outdoor experiment, and heat transfer experiment. The discussion was carried out to discuss the details of the findings. In chapter five, the conclusion and recommendations are presented to elaborate on the details of the objectives achieved in this research. This chapter also discusses the findings from chapter four and then associates them with the objectives from the first chapter.

1.8 CHAPTER SUMMARY

This chapter describes the framework for designing the Flat Plate Base-Thermal Cell Absorber (FPBTCA). The framework starts with a research problem to identify the problem faced by flat plate solar collectors. Then the outcome is the research objective which is to provide the method to solve the research problem. The significance of the study explains the importance of designing FPBTCA to enhance the flat plate solar collector by improving the performance of FPBTCA.

Research scopes elaborate on the limitations applied in this study. This study was done based on the limitations when implementing the experimental work. Research methodology explores the method used in this research to evaluate the experiment with a satisfying result. The thesis structure illustrates the chapter summary from chapter one to chapter five. Based on the thesis structure, it overviews the contents of every chapter.

CHAPTER TWO

LITERATURE REVIEW

2.1 INTRODUCTION

Solar energy is known as renewable energy and can be used in different types of applications. The Sun emits energy at a rate of 3.8×10^{23} kW, of which approximately 1.8×10^{14} kW is intercepted by the earth, which is located 150 million km from the sun (Thirugnanasambandam et al., 2010). Solar energy has been used in solar thermal technology, such as solar air heating systems, solar water heating systems, photovoltaic systems, and thermal systems. The application of solar energy in the world is caused by the effect of fossil fuels on the environment ((Timilsina et al., 2012). The concept of thermal energy is the heat accumulated by absorbing sunlight captures solar radiation and converts it to thermal energy through a heat transfer mechanism. The solar dryer is an example of a solar energy application. The solar dryer is applicable for developed and developing countries to reduce harvesting crop damages in terms of increasing the crop value addition (El-Sebaii & Shalaby, 2012).

Generally, there are two types of solar dryers that have been used, which is open-air sun drying and convective solar drying (Belessiotis & Delyannis, 2011). Drying the food direct to the sun is an open-air sun drying concept. While the exposure of the food by a convective process with a collar dryer is convective solar drying. Agricultural products are dried with a solar dryer to increase shelf-life and preserve the time for drying (Musembi et al., 2016). Basically, the drying chamber has a temperature between 50 °C to 60 °C when using a solar dryer (M. Kumar et al., 2016). The solar collector is a sample application of a solar dryer that can be used to dry the product. The types of a solar collectors are flat plate solar collectors (FPSC), evacuated tubes, compound parabolic collectors and etc.

2.2 SOLAR THERMAL COLLECTOR TECHNOLOGY

Solar thermal collectors are the type of heat exchangers that transform solar radiation energy into internal energy through a transport medium. There are several types of applications utilising solar thermal collector, which are solar water heating systems, solar space heating and cooling, solar refrigeration, industrial heat processes, solar desalination systems, solar thermal power system, solar furnaces, and solar chemistry applications (S. A. Kalogirou, 2004).

The most important component is the flat plate collector, which is attached to the solar thermal system. The function of flat plate solar collectors is to absorb as much possible of any solar radiation and then convert it into heat. Basically, the flat plate solar collector component has a thermal absorber collector and thermal energy storage components (Y. Tian & Zhao, 2013). Therefore, thermal energy storage component design is important to improve efficiency and performance in flat plate solar collector systems. There are two types of flat plate solar collectors which are non-concentrating or stationary and concentrating (Naik et al., 2017). A non-concentrating collector has the same area for intercepting and absorbing solar radiation, whereas a sun-tracking concentrating solar collector usually has concave reflecting surfaces to intercept and focus the sun's beam radiation to a smaller receiving area, thereby increasing the radiation flux. The performance of the solar collector is determined by the thermal absorber as the use of the thermal absorber is to convert solar radiation energy to thermal energy (A A Razak, 2017).

The thermal absorber of flat plate solar collectors plays the main role in the efficiency and performance of flat plate solar dryers. The collector's efficiency could be improved by improving the design of the flat plate solar collector, such as having a slender configuration alongside the air flow direction, creating a small air gap between the absorber and bottom plate, using high absorptivity of coatings, and the fluid temperature should be placed close to the collector (Buker & Riffat, 2015). The absorber collector design should be considered when designing a solar dryer system in order to avoid reducing the efficiency and performance of the solar dryer. The improvement of flat plate solar collectors could be done when irradiation is low, absorber emissivity is

high, the class cover emissivity is low, and the inclination angle is low (Makhanlall & Jiang, 2015).

There are several researchers who concentrated on hybrid solar dryer systems to improve the performance of the solar dryer system. Amer et al. (2010) did their research to design and evaluate the performance of a new hybrid solar dryer system used for bananas. The advantages of implementing a hybrid solar dryer, is that the solar dryer can be operated during sunny days and during cloudy days as a hybrid solar dryer. Nabnean et al., 2016 conducted an experiment to find the best performance of a new design of solar dryer for drying osmotically dehydrated cherry tomatoes. The result, shows a reduction in drying time in the new solar dryer as compared to natural sun drying.

The location of the drying chamber and solar collector should be closed as possible because it affects the performance of the flat plate solar collector. There are several non-controllable external factors that affect the performance of flat plates solar collectors such as solar radiation, ambient air temperature, wind speed, and relative humidity of the air. The other factors that affects the performance are initial moisture content, physical properties, and surface exposed to drying air (Jain & Tiwari, 2003).

2.3 TYPES OF SOLAR THERMAL COLLECTORS

The solar thermal collector has a different type of design and depends on the applications. There are a large number of solar collectors available in the market. The types of Solar Energy Collectors are shown in Table 2.1 (S. Kalogirou, 2003). There are three types of solar thermal collectors' motion such as Stationary, Single-axis Tracking, and Two-axes tracking. Stationary Flat Plate Collector has a lower temperature in the drying chamber from 30 °C to 80 °C. The highest temperature in the drying chamber is Two-axes tracking Heliostat Field Collector, which is 150 °C to 2000 °C.

Table 2.1: Solar Energy Collectors

Motion	Collector type	Absorber type	Concentration ratio	Indicative range (T °C)
Stationary	Flat plate collector (FPC)	Flat	1	30-80
	Evacuated tube collector (ETC)	Flat	1	50-200
	Compound parabolic collector (CPC)	Tubular	1-5	60-240
Single-axis tracking			5-15	60-300
	Linear Fresnel reflector (LFR)	Tubular	10-40	60-250
	Parabolic trough collector (PTC)	Tubular	15-45	60-300
	Cylindrical trough collector (CTC)	Tubular	10-50	60-300
Two-axes tracking				
	Parabolic dish reflector (PDR)	Point	100-1000	100-500
	Heliostat field collector (HFC)	Point	100-1500	150-2000

Note: Concentration ratio is defined as the aperture area divided by the receiver/absorber area of the collector.

2.3.1STATIONARY SOLAR COLLECTOR

For the stationary collector, the collector is permanently positioned and it moves to track the sun. There are three types of collectors applied in stationary collectors, which are Flat Plate Collectors (FPC), Stationary Compound Parabolic Collectors (CPC), and Evacuated Tube Collectors (ETC).

2.3.1.1FLAT PLATE SOLAR COLLECTOR

For flat plate solar collector component, it is important to get the best performance when applied in the application. Generally, there are four components in a flat plate solar collector, which are glazing, the thermal absorber, the base of the collector, and the collector frame (S. A. Kalogirou, 2004). Glazing is used to reduce convection losses from the absorber plate through the restraint of the stagnant air layer between the absorber plate and the glass. A flat plate absorber collector is used as an absorbing plate to absorb the incoming solar radiation, convert it into heat energy then transfer it to the transport medium in the fluid tubes to be carried away for storage or use. The collector's base is used as the bottom in the drying chamber between thermal absorber collectors. Figure 2.1 represents the flat plate solar collector component. The main component is glazing, absorber plate, header tube, copper risers, insulation, and frame section.

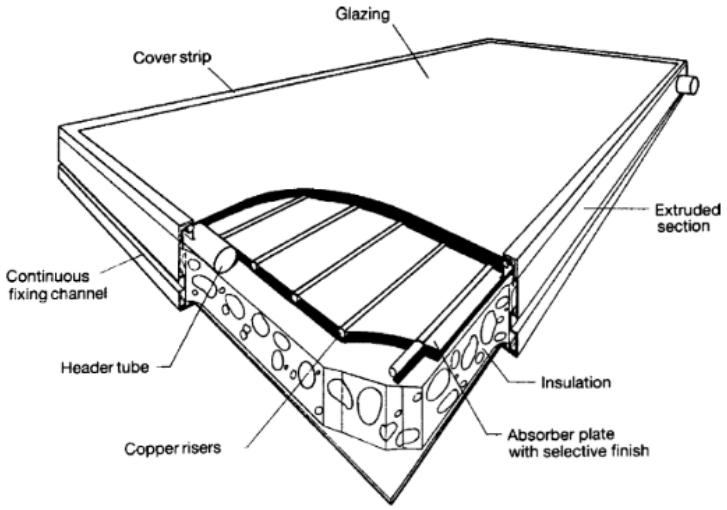

Figure 2.1: Flat plate solar collector component (S. A. Kalogirou, 2004).

2.3.1.2 STATIONARY COMPOUND PARABOLIC COLLECTORS

The mechanism of a Compound Parabolic Concentrator (CPC) is called a non-imaging concentrator which applies the concept of edge optics. Winston (1974) stated that CPC with collectors has the advantage of its application in solar energy. By using CPC, the concentrators have the capability to absorb incoming radiation from a wide range of angles. The CPC concentrator's design is from the improvement of the cone concentrator, which the ratio of concentration should be at maximum (M. Tian et al., 2018). Figure 2.2 shows the different configurations of ideal two-dimensional concentrators: (a) tubular absorber, (b) wedge receiver, one face illuminated; (c) flat horizontal receiver, fully illuminated, (d) flat vertical receiver, fully illuminated (Branda et al., 2008). CPC with fully illuminated ‘‘plane’’ and ‘‘tubular’’ is shown in (Figures 2 a, c, and d). CPC with wedge receiver and one face illuminated is shown in (figure 2 b).

Basically, there are two types of CPC which is tubular absorber or flat absorber. Based on the application, CPC with a tubular absorber is practical for fluid media and also for heating a fluid because it has higher heat collection efficiency (Jiang et al., 2020). There is a disadvantage to a tubular absorber, that it is more expensive than a plane absorber (Gordon, 1986). Zhang et al. (2017) performed experimental and

simulation studies on a novel Compound Parabolic Concentrator and found that the new improvement of CPC can improve the uniformity of light distribution on the surface of the concentrator. Based on the research, a new CPC with light compensation affects the light uniformity.

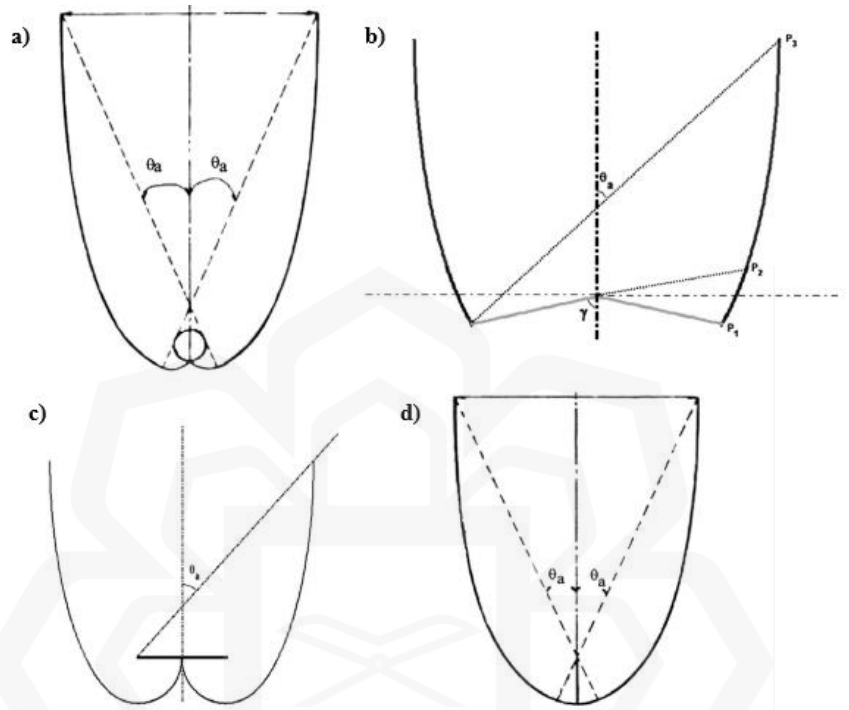

Figure 2.2: Different configurations of ideal two-dimensional concentrators: (a) tubular absorber, (b) wedge receiver, one face illuminated; (c) flat horizontal receiver, fully illuminated, (d) flat vertical receiver, fully illuminated (Branda et al., 2008).

2.3.1.3EVACUATED TUBE COLLECTORS

Evacuated tube solar collectors are the most suitable solar technology for producing useful heat in both low and medium temperature levels. Evacuated tube collectors consist of a heat pipe inside a vacuum-sealed tube. The vacuum in the glass tube will reduce convection and conduction heat loss. Therefore, the heat loss of evacuated tube collectors is less than flat plate solar collectors (Kim & Seo, 2007). Figure 2.3 shows a glass evacuated tube solar collector with U-tube. a) Illustration of the glass evacuated tube; b) Cross section (Ma et al., 2010). The evacuated tube consists of an outer glass tube, vacuum jacket, selective absorbing coating, absorber tube, copper fin, and U tube.

There are two types of evacuated tube collectors, which is single-walled glass evacuated tube and Dewar tube (Y. Gao et al., 2013).

Sato et al. (2012) performed research on numerical analysis of a modified evacuated tube solar collector. The evacuated tube solar collector has modified its geometry so that the heat removal from the tube is better and also to avoid the effect of internal circulation. Based on the improvement, the conventional collector and two geometry modifications exhibit better results, which is that the modification of solar collector geometry will produce a good thermal performance. The other improvement is by using a smaller diameter of evacuated tube solar collector to allow higher temperature heating.

Ma et al. (2010) investigated the thermal performance analysis of the glass evacuated tube solar collector with a U-tube. The method applied was to investigate the thermal performance of glass evacuated tubes is a one-dimensional analytical method. The results showed that the evacuated solar tube efficiency had increased by 10%; also, the temperature increased by 16% at the outlet fluid, if synthetical conductance increased from 5 to 40 W/m K. The surface temperature of the absorbing coating is an important parameter that should be considered.

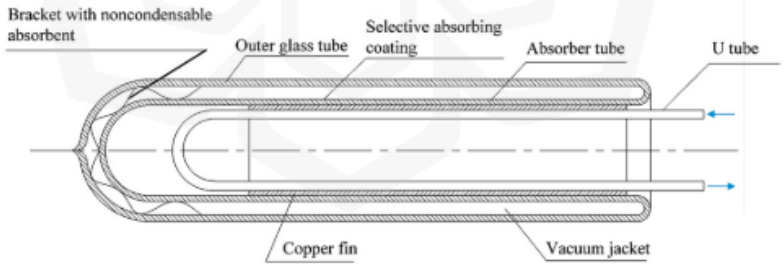

a)

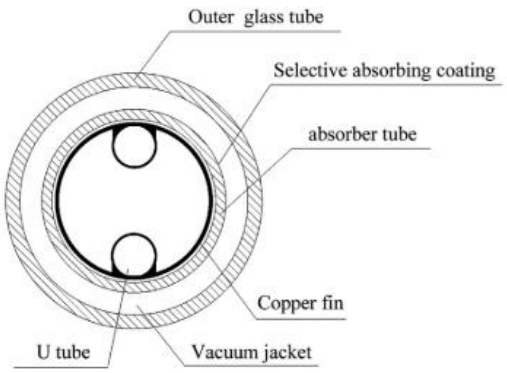

b)

Figure 2.3: Glass evacuated solar tube collector with U-tube. a) Illustration of the glass evacuated tube; b) Cross section (Ma et al., 2010).

2.3.2 SINGLE AXIS TRACKING

Single-axis tracking concept is that the solar thermal collector follows the sun's daily motion to absorb high radiation when operating. The tracking mechanism of solar thermal collectors is the ability to follow the Sun and then return back to the original position at the end of the day (Bakos, 2006). The single-axis tracker follows the Sun's East–West movement. Basically, there are two types of thermal collector in this category which is Linear Fresnel Reflector (LFR) and Cylindrical Trough Collector (CTC). Table 2.2 shows the layout installation method for a single-axis tracking system. The layout installation method is an inclined shaft, a South-North axis horizontal, and an East-West axis horizontal.

Table 2.2: Layout method installation for single-axis tracking (Chang, 2016).

No	Layout method installation	Tracking direction
1	Inclined shaft	east–west
2	South–north axis horizontal	east–west
3	East–west axis horizontal	south–north

2.3.2.1 LINEAR FRESNEL REFLECTOR

A Linear Fresnel Reflector collector is made from an array of linear mirror strips that concentrate light onto a linear receiver. Linear Fresnel Reflectors also have the potential to minimize the cost when operating (Abbas et al., 2013). Basically, there are two types of receivers which are evacuated tubes and cavities. The evacuated tubes receiver is a couple of Compound Parabolic Reflectors as secondary reflectors. The cavities receiver has a cover glass and trapezoidal shape design. Evacuated tubes receiver is more efficient than trapezoidal cavities receiver and it is economical for application (Bellos, 2019). Figure 2.4 represents the schematic representation of a Linear Fresnel Reflector (LFR) solar collector with a cavity receiver. Basically, Linear Fresnel Reflector (LFR) solar component is a mirror field, receiver, and tracking system.

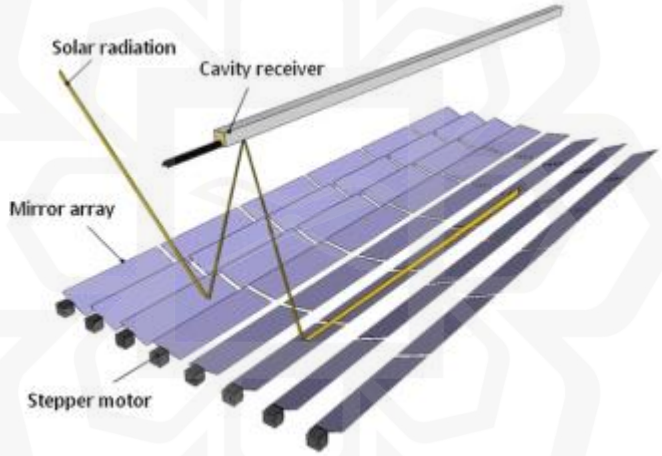

Figure 2.4: Schematic diagram of a Linear Fresnel Reflector solar collector with a cavity receiver (Lin et al., 2013)

Said et al.(2019) experimentally studied the optical performance of a small prototype of a Linear Fresnel Reflector. The results showed that optical efficiency had increased proportionally with the number of reflective mirrors applied in the experiment. The average values from the experiment are 42.65 %, 35.82 %, and 26.98 % for the 11, 09, and 07 mirrors, respectively. Thermal efficiency also affects the performance of Linear Fresnel Reflectors. It increases proportionally by using different number of reflective mirrors, which has average values exceeding 29.13 %, 27.13 %, and 20.65 % for 11, 09, and 07 mirrors.

Mokhtar et al.(2016) performed a theoretical and experimental study on Linear Fresnel Reflector as a solar system for heating water. There is a significant effect on the thermal efficiency, which exceeded 29 %, while the water temperature reached up to 347 K. Based on the results it indicates that there is a relationship between solar collector performance with direct solar radiation, and with the geometric and optical characteristics of solar collector components.

2.3.2.2 PARABOLIC THROUGH COLLECTOR

Parabolic Trough Collector (PTC) mechanism is the receiver that will convert solar beam radiation into thermal energy. It also tracks the Sun around one-axis and is on North-South oriented to get maximum performance (Brinkworth, 1974). Figure 2.5 represents the Parabolic Trough Collectors (PTC) (Chafie et al., 2018). The Parabolic Through Collector component consists of a reflector, receiver, and tracking mechanism. The reflector is made from a sheet of reflective material and covered with a glass tube. Using the glass tube as a cover, it could reduce heat losses of the reflector.

Figure 2.5: Parabolic Trough Collectors (PTC) (1) reflector, (2) receiver (Chafie et al., 2018)

Kumaresan et al. (2012) performed performance studies on a solar Parabolic Trough Collector with a thermal energy storage system. Based on the findings, the instantaneous efficiency depends on an incident of beam radiation and also the benefit of heat gain. To reduce heat loss from the system, the storage tank, piping circuit, valves,

and fittings should be insulated properly before conducting the experiment. Tzivanidis et al. (2015) employed simulation to the thermal and optical efficiency investigation of a Parabolic Trough Collector. The most important factor that affects solar collector efficiency is solar radiation direction. The -end losses in the collector occurred when the incident angle was higher.

2.3.2.3 CYLINDRICAL TROUGH COLLECTOR

Cylindrical Trough Collector is made by bending a sheet of reflective material to a cylindrical shape and covering it with a glass tube to reduce heat loss. Cylindrical shape, also known as a receiver tube, receives solar radiation form the Sun. The mechanism of a Cylindrical Trough Collector is that the collector collects heat from the sun and then reflects to the receiver tube. Basically, it is equipped with a single-axis tracking system to follow the Sun movement. Figure 2.6 shows the schematic diagram of the Cylindrical Through Collector (CTC) at 30 degrees and the receiver.

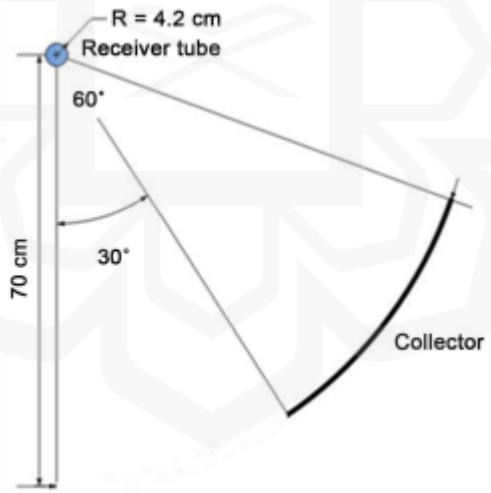

Figure 2.6: Schematic diagram of Cylindrical Through Collector (CTC) at 30 degrees and the receiver tube (Shojaee et al., 2015)

Nasir (2004) performed the design, construction, and experimental study of the thermal performance of a Cylindrical Trough Collector for a solar air heater. The results showed that the efficiency of the solar air heater is 65 % and has a higher temperature at 97 ℃. The performance is viable to be utilized domestically and also in industries.

2.3.3 TWO AXES TRACKING

Generally, there are two types of thermal collector applications for two-axes tracking thermal collector, which is parabolic dish reflector (PDR) and heliostat field collector (HFC). The two-axes concept is a tracking system that follows the Sun's changing altitude angle.

2.3.3.1 PARABOLIC DISH COLLECTOR

Generally, Parabolic Dish Reflector (PDR) has a higher temperature of operation and could be used in high-temperature applications (Mawire & Taole, 2014). An example application of a Parabolic Dish Reflector (PDR) is generating electricity (Hafez et al., 2016). Figure 2.7 represents the schematic diagram of the Parabolic Dish Reflector (PDR). Parabolic Dish Reflector's (PDR) components consists of the receiver, parabolic dish reflector, reflective support structure, and reflector tracking structure. The receiver position is fixed to the reflector's support structure. The parabolic dish reflector and receiver will be tracking the Sun movement in two axes. Parabolic dish concentrators could achieve concentration ratios of more than 2000 (Blanco & Miller, 2017).

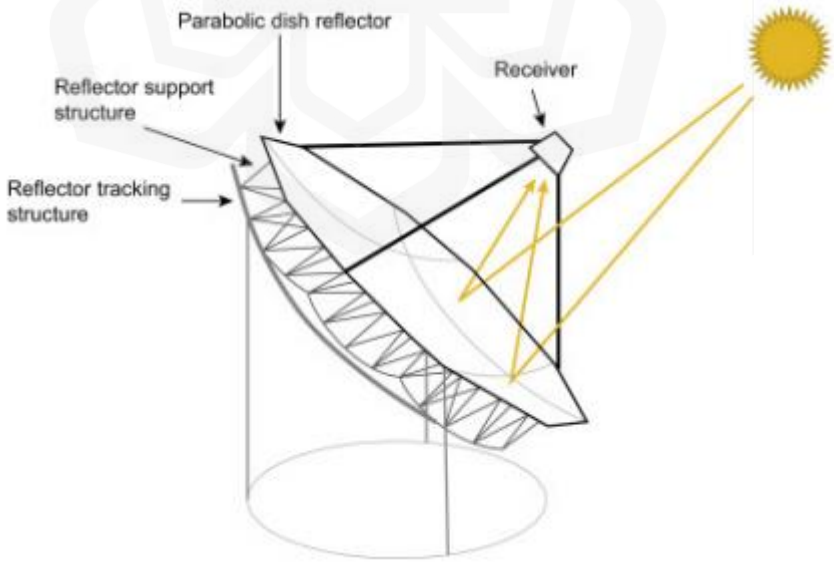

Figure 2.7: Schematic diagram of Parabolic Dish Reflector (PDR) (Blanco & Miller, 2017)

Cherif et al. (2019) investigated a receiver's geometrical effect on a solar Parabolic Dish Collector performance. The findings showed that the optimal thermal performance of the Parabolic Dish Collector is mostly affected by the properties of receiver geometry and also the inlet or outlet positions. Ab Ghani et al. (2014) studied the influence of concentrator size, reflective material, and solar irradiance on Parabolic Dish Heat Transfer. Based on the findings, increasing the concentrator size and good reflectance material of the concentrator could improve the heat transfer rate from the concentrator to the receiver.

Ramalingam Senthil and Marimuthu Cheralathan (2017) conducted an experiment to determine the effect of the phase change material on a solar receiver and on the thermal performance of a Parabolic Dish Collector. The results showed that using phase change material with the receiver could increase the Parabolic Dish Collector's efficiency by 60 % to 65 %. The advantages of using phase change material is to improve the thermal capacity of the receiver when solar radiation is absent for several minutes.

2.3.3.2 HELIOSTAT FIELD COLLECTOR

Heliostat Field Collector (HFC) uses two axis tracking system so that it follows the Sun movement to focus on the solar radiation (Saghafifar, 2016). The application of Heliostat Field Collectors (HFC) is used in power towers (Nixon et al., 2010). An array of heliostat mirrors is used to reflect the solar radiation to the receiver. Basically, the receiver is used by water-steam or molten nitrate salt as a fluid medium. Figure 2.8 shows the schematic diagram of a Heliostat Field Collector (HFC) (Kodama, 2003). Heliostat Field Collector (HFC) component consists of heliostats, a receiver, and a tower.

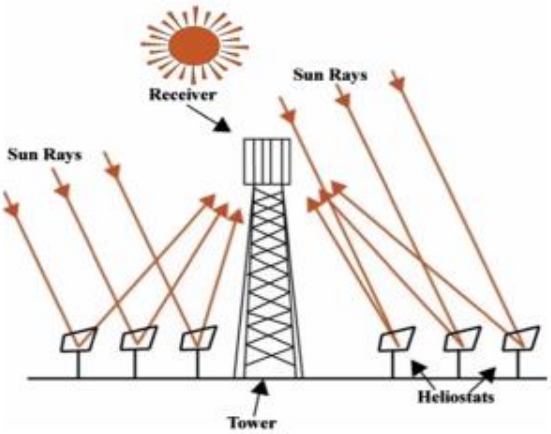

Figure 2.8: Schematic diagram of a Heliostat Field Collector (Kodama, 2003).

Saghafifar (2016) performed an experiment on thermo-economic optimization of hybrid combined power cycles using Heliostat Field Collector. The results showed that the radial-staggered and spiral field layouts have optimum weighted efficiencies, which are 58.61% and 58.38%, respectively. Based on the cost of energy, it can be concluded that the radial-staggered cost was 33.88 US$/MWh which is lower than the spiral layout cost, which is 34.03 US$/MWh.

Li et al. (2017) performed an optimization study of a Heliostat Field layout on an annual basis using a hybrid algorithm combining particle swarm optimization algorithm and genetic algorithm. Based on the findings, it can be concluded that Heliostat Field has a better improvement in annual efficiency, which increased by 5.7 %. The energy collected per unit cost (ECUC) also has an increment from 12.50 MJ/USD to 12.97 MJ/USD. The percentage of increment is about 3.8 %. Collado and Guallar (2019) exposed the quick design of regular Heliostat Fields for commercial solar tower power plants by using *Campo* code based on two parameters. Basically, the difference between the field efficiency for the 'regular' layout and the actual optimum layout is less than 1 %.

2.4 FLAT PLATE SOLAR COLLECTOR (FPSC) APPLICATION

Flat plate solar collector is widely used in commercial and domestic applications for drying, especially agricultural products. Examples of flat plates solar collectors applications are for solar water heating systems, solar space heating and cooling, solar refrigeration, industrial process heat, solar desalination systems, solar thermal power systems, solar furnaces, and solar chemistry applications (S. A. Kalogirou, 2004).

Flat plate solar collector was invented by Hottel and Woertz in 1942 and also by Hottel and Whiller in 1958, and it can be seen as the first invention of solar flat plate collector (Hottel, H.C., Whillier, 1958; Hottel, H.C., Woertz, B.B., 1942). The invented flat plate solar collector's component consists of a black flat plate absorber, a transparent cover, heat transfer fluid, and an insulating case (Pandey & Chaurasiya, 2017). The advantages of using a flat plate collector in drying is that it is easy to manufacture, is low in cost, collects both beam and diffuse radiation, is permanently fixed (no sophisticated positioning or tracking equipment is required), and requires little maintenance.

Figure 2.9 represents the classification and indicative temperature range of solar collectors. Solar collectors can be classified into two categories which are non-concentrating solar collectors (NCSC) and concentrating solar collectors (CSC). The temperature range of a flat plate collector (FPC) is between 30 ℃ and 80 ℃, and it could be passive or active FPC. A passive FPC does not require any electrical or mechanical power to run a pump or fan, whereas an active FPC requires a blower or fan to pump the air into the thermal storage. The medium of FPC also can be air or water-based. The FPC application can be associated with thermal storage and without thermal storage components.

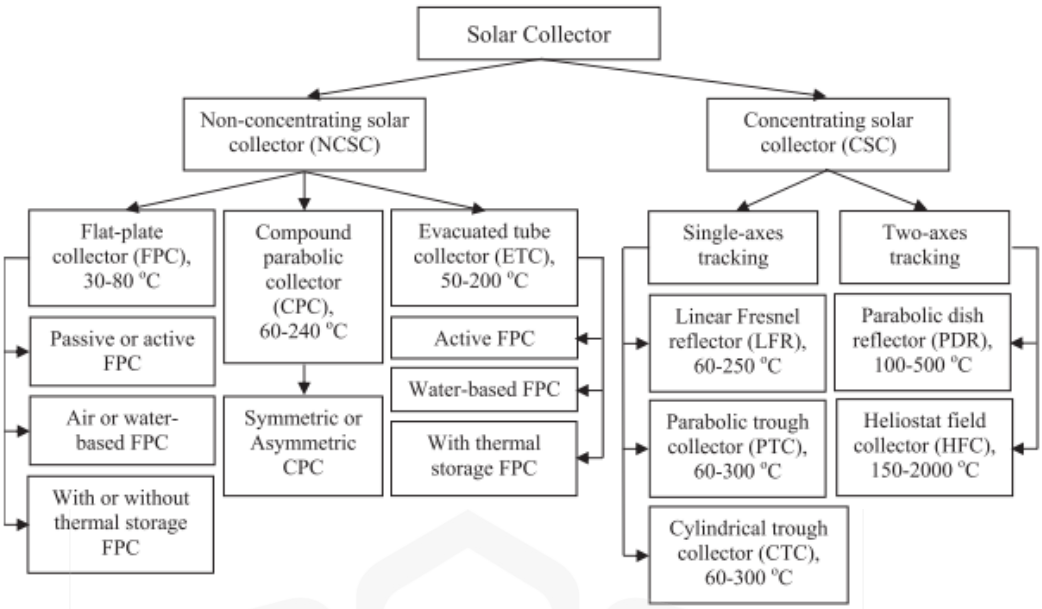

Figure 2.9: Classification and indicative temperature range of solar collectors (Fudholi & Sopian, 2019)

Figure 2.10 shows the various types of flat plate collector (FPC), which is A–E: air-based solar collectors and F–H: water-based solar collectors. The conventional FPC consists of a transparent cover, absorber, insulation, and a frame. Figures A-E presents the variant of thermal absorber types in air-based collectors, which is A: flat plate absorber, B: V-Corrugated absorber, C: U-corrugated absorber, D: finned absorber and E: flat plate absorber using porous media. Figures F-H show the different types of thermal absorber in water-based collectors, which is F: flat plate absorber with riser below, G: flat plate absorber with riser in the middle, H: flat plate absorber with riser above, and H: flat plate absorber with riser in the middle.

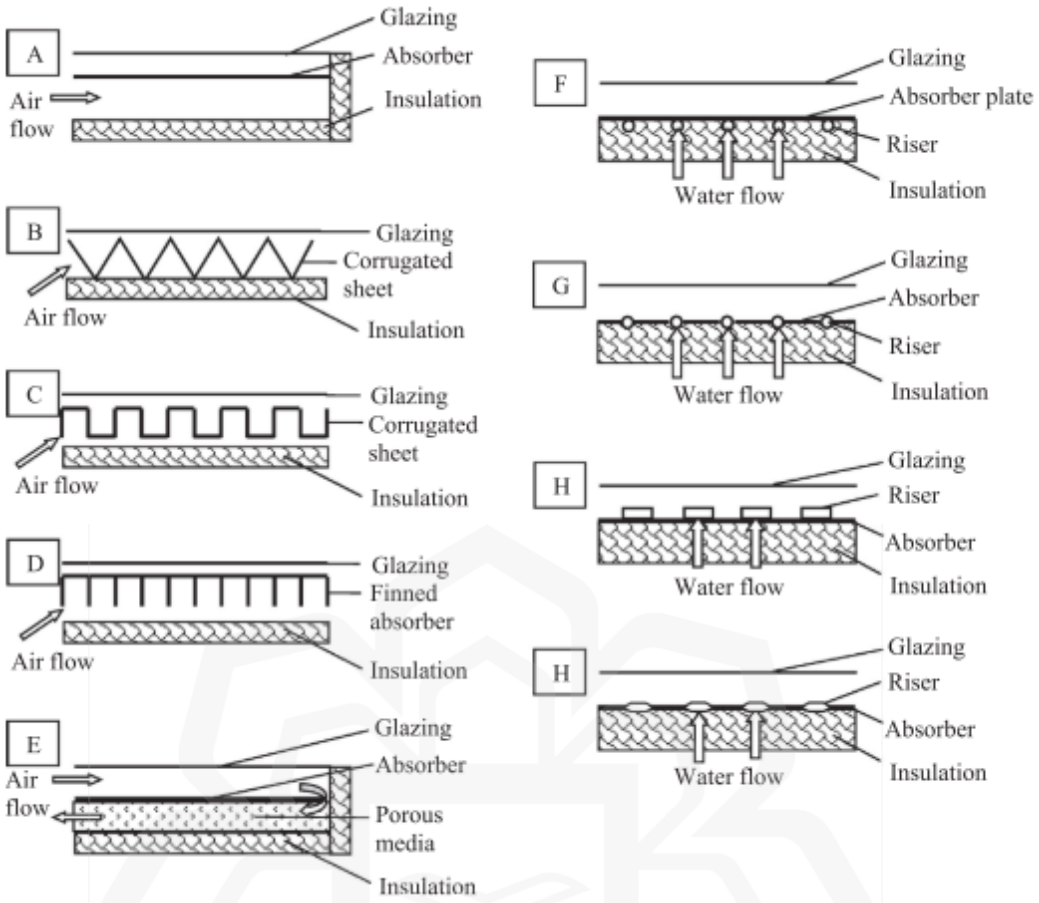

Figure 2.10: Various types of flat plate collector (FPC): A–E: air-based solar collectors, F–H: water-based solar collectors (Fudholi & Sopian, 2019).

2.5 TYPES OF AIR HEATING FLAT PLATE SOLAR COLLECTORS

There are two types of flat plate solar collectors, which is bare-plate and covered absorber plate, respectively. The difference between bare-plate and covered absorber plate is the use of glazing material at the top of the flat plate solar collector. The bare-plate does not use glazing material at the top cover in which the thermal absorber is directly exposed to the sun. Whereas the covered absorber plate uses glazing material such as glass cover at the top of the flat plate solar collector.

2.5.1 BARE –PLATE SOLAR COLLECTOR

Figure 2.11 represents the schematic diagram of a bare-plate (no cover) air-heating solar energy collector. Bare-flat plate collector components include an absorber plate, casing, and insulation. The thermal absorber plate is placed at the top of the flat plate solar collector. A bare-plate collector is used in crop-drying operations for natural and forced convection systems. The common application of bare-flat collectors is food drying in the agricultural sector (Bande & Mariah, 2014).

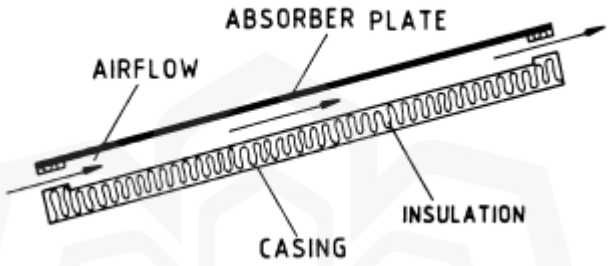

Figure 2.11: Schematic diagram of a bare-plate (no cover) air-heating solar energy collector (B. Norton, 1992)

2.5.2 COVERED-PLATE SOLAR COLLECTOR

The component of a covered-plate plate solar collector consists of glazing material, absorber plate, insulation, and casing. The glazing material as a cover material is placed at the top of the flat plate solar collector, and the position is parallel to the absorber plate. The objective of using glazing material is to allow direct falling of solar insolation to the plate, also preventing convective heat loss and cooling against the plate, especially during rain, and reduces long-wave radioactive heat losses. Glass, polycarbonate, and clear plastic are used as glazing material. Figure 2.12 shows the schematic illustration of covered air heating solar energy collectors: a-front pass, b-back pass. Figure 2.12 a) presents the front pass of the flat plate solar collector types. The airflow moves from the inlet to the outlet between the glazing and absorber plate. Figure 2.12 b) shows the back pass of the flat plate solar collector types. The airflow moves from the inlet to the outlet between the absorber plate and the insulation material. Back-pass solar air heaters have generally been found to be more efficient than front-pass types.

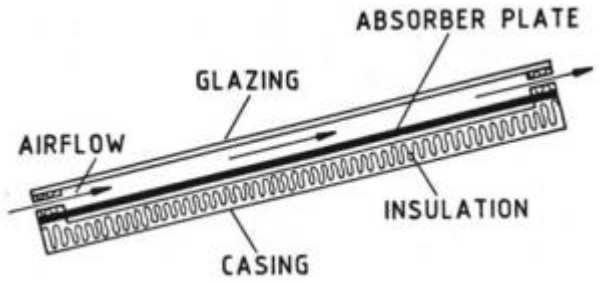

a)

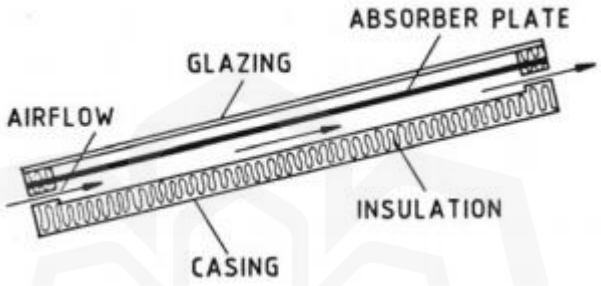

b)

Figure 2.12: Schematic illustration of covered air heating solar energy collectors: a) front pass, b)back pass (B. Norton, 1992)

2.6 FLAT PLATE SOLAR COLLECTOR (FPSC)

Figure 2.13 represents the cross-section of a typical liquid flat plate solar collector (FPSC). It consists of a flat plate absorber placed in an insulated box with a glass cover. A flat plate solar collector (FPSC) is usually permanently fixed in position and requires no tracking of the sun. The collectors should be oriented directly towards the equator, facing south in the northern hemisphere and north in the southern hemisphere. The flat plate absorber collector is the main component of FPSC which absorbs as much as possible solar radiation from the Sun. Then it is transferred to the transport medium through the fluid tubes to be carried away for storage or use.

The surface below the absorber plate and the casing are insulated to reduce conduction losses. The transparent cover is used to reduce convection losses from the absorber plate by restraining the stagnant air layer between the absorber plate and the glass. It also reduces radiation losses from the collector as the glass is transparent to the

short-wave radiation received by the sun, but it is nearly opaque to long-wave thermal radiation emitted by the absorber plate (greenhouse effect). Flat plate solar collector (FPSC) performance could be increased by applying diverse materials, different shapes and at different layouts (Akpinar & Koçyiĝit, 2010).

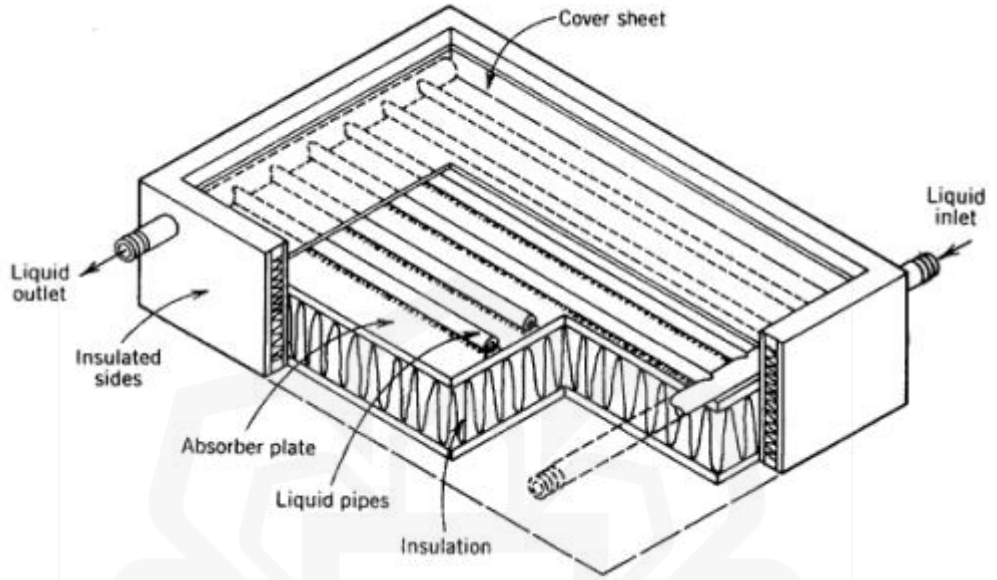

Figure 2.13: Cross-section of a typical liquid flat plate solar collector (Saleh, 2012)

2.6.1 THERMAL ABSORBER COLLECTOR DESIGN

Thermal absorber collector design should be considered when designing a new flat plate solar collector because the factors can affect the performance of the flat plate solar collector. Factors that should be considered, are thermal performance, cost, lifetime, durability, maintenance, and ease of installation (Tchinda, 2009). These factors are important when implementing the new design with the best decision-making. A flat plate absorber collector is important to increase heat transfer in flat plate solar collectors (Ahmad & Ilham, 2018).

Figure 2.14 shows the types of thermal absorbers for solar air heater with the stationary flat absorber. There are two types of stationary flat plate absorbers with physical properties which are non-permeable and permeable thermal absorbers. Non-permeable flat plate absorber is divided into two categories which are corrugated and finned. For permeable, it consists of matrix/meshes and are perforated. Both non-

permeable and permeable enhancement can expand into the flow through redirection method where air in-flow at thermal absorbers is diversified by means of the air flow path diversion.

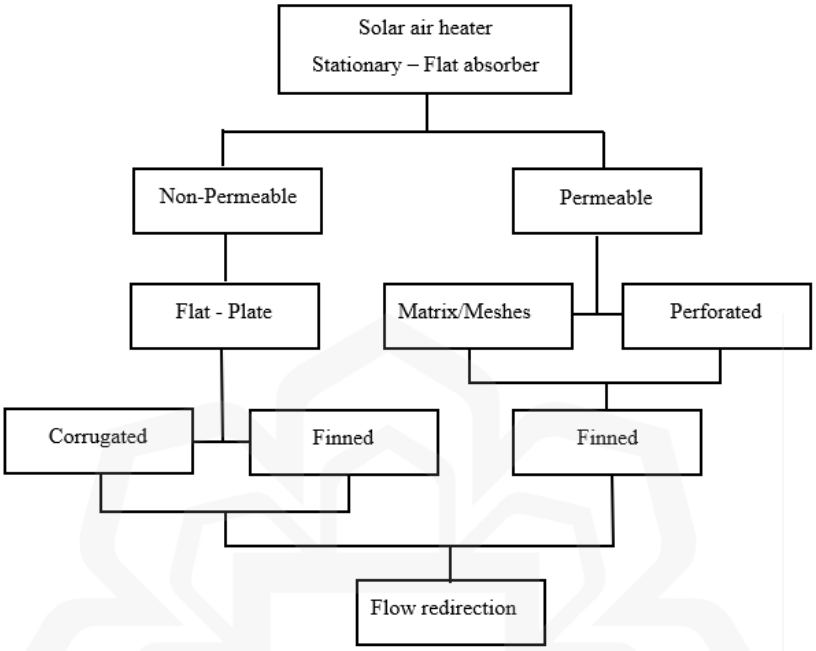

Figure 2.14: Types of thermal absorbers for solar air heater with a stationary flat absorber (A A Razak, 2017)

2.6.2 MATERIALS AND THICKNESS OF FLAT PLATE SOLAR COLLECTOR

Flat plate absorber collector material affects the thermal performance of flat plate solar collectors (FPSC) (Akpinar & Koçyiĝit, 2010). There are several criteria that should be considered when choosing the types of material for flat plate absorber collectors. They are thermal conductivity, durability, and the cost of the material. (Pekez et al., 2013). Basically, the flat plate absorber collector material is Aluminium, it has high thermal conductivity as it can increase heat transfer in flat plate absorber collector (FPSC) (Dixon-hardy et al., 2019). Copper and Stainless-Steel material also could be used as flat plate absorber collectors. Table 2.3 represents the physical properties of conductors in various material. Generally, high thermal conductivity uses silver metal, and the high specific heat capacity uses aluminium metal.

Table 2.3: Physical properties of conductors (Pekez et al., 2013)

Material	Thermal conductivity (W/m^2 ℃) at 25℃	Specific heat capacity C_p (kJ/kgK)
Silver	429	0.23
Copper	401	0.39
Gold	310	0.13
Aluminium	250	0.91
Brass	109	NA
Iron	80	0.46
Steel	46	0.5
Stainless steel	16	0.473

The thickness of the thermal absorber can produce different flat plate solar collector performance. The effect of absorber thickness on the efficiency of heat-absorbing flat plate collectors was conducted, with 2.0 millimetres thick aluminium absorber suitable for use in solar energy collectors (BILLY ANAK SUP, 2010). The results show that when designing a flat plate solar collector, the thickness of the thermal absorber should be selected based on the application of the flat plate solar collector.

2.6.3 SOLAR COLLECTOR GLAZING MATERIALS

Glass is placed on the top position of the flat plate solar collector. Glass also acts as the cover on the top of the collector casing. Glass has been very widely used as a cover material due to its high transmittance to visible light, very low transmittance to infrared radiation and its stability to high temperature. Glass is the most common glazing material because of its low transmittance of the longer wavelength. The commercially available window glass will have normal incidence transmittance of about 0.87 to 0.90.

Basically, low-iron content glass is used as a glass cover to reduce radiation and convection between flat plate absorber collectors and the atmosphere (Alvarez et al., 2010). The advantages of using low-iron glass is that it also can increase the optical efficiency of the flat plate solar collector (S. A. Kalogirou, 2002). The most important characteristics of glazing materials are reflection (r), absorption (α), and transmission (τ). The heat losses in flat plate collector come from the front of the glass, so that sides

and the back of the flat plate collector are regularly insulated (Ion & Martins, 2006). Therefore, accurate prediction of the thermal performance of solar collector systems strongly depends on how the glass cover material is analyzed.

2.6.3.1 TYPES OF GLASS IN FLAT PLATE SOLAR COLLECTOR

The different types of glass used in flat plate solar collectors will affect the performance of the flat plate solar collector. So, the selection of the glass types is important when designing a new flat plate solar collector. Table 2.4 shows the transmittance of various glazing materials. Crystal glass has the highest transmittance values of solar radiation through the glass. The capability of glass can be used in flat plate solar collectors to trap heat losses from flat plate absorber collectors.

Table 2.4: Transmittance of various glazing material (Vestlund, 2012)

Material	Transmittance (τ)
Crystal glass	0.91
Window glass	0.85
Polymethyl methacrylate (acrylic) (Acrylate, Lucite, Plexiglass)	0.89
Polycarbonate (Lexan, Merlon)	0.84
Polyethylene terephthalate (polyester, Mylar)	0.84
Polyvinyl fluoride (Tedlar)	0.93
Polyamide (Kapton)	0.80
Fluorinated ethylene propylene (FEP Teflon)	0.96
Fiberglass-reinforced polyester (Kalwall)	0.87

2.6.4 THERMAL ABSORBER SURFACE COATING

Basically, the thermal absorber surface is coated with black paint because it can increase the available solar radiation absorbed by the thermal absorber plate. When the thermal absorber is coated with flat-black paint, it can absorb 96% of the incoming solar energy from the Sun (Pekez et al., 2013). Table 2.5 shows the solar absorptance, emittance, and reflectance for various surfaces. Flat black paint and 3M Velvet black paint has high

absorbance value compared to other colours, which makes them suitable for heat absorber plate coating. The absorbance (α) for black paint is between 0.92 to 0.98. The black paint is applied by spraying on the flat plate absorber collector. These surfaces must be able to withstand repeated and prolonged exposure to the relatively high temperature.

Table 2.5: Solar absorptance, emittance, and reflectance for various surfaces (Vestlund, 2012)

Material	α	ρ	ε	α/ ε
White plaster	0.07	0.93	0.91	0.08
Fresh snow	0.13	0.87	0.82	0.16
White paint	0.20	0.80	0.91	0.22
White enamel	0.35	0.65	0.90	0.39
Green paint	0.50	0.50	0.90	0.56
Red brick	0.55	0.45	0.90	0.60
Concrete	0.60	0.40	0.92	0.68
Grey paint	0.75	0.25	0.88	0.79
Black tar paper	0.93	0.07	0.93	1.00
Flat black paint	0.96	0.04	0.88	1.09
3M Velvet black paint	0.98	0.02	0.90	1.09
Granite	0.55	0.45	0.44	1.25
Graphite	0.78	0.22	0.41	1.90
Aluminium foil	0.15	0.85	0.05	3.00
Galvanized steel	0.65	0.35	0.13	5.00

Figure 2.15 represents the Hottel-Whillier Bliss efficiency curves. The figure shows the capability of different type's solar collectors to absorb solar energy and store the energy from being lost. It can be concluded that the temperature difference between the collector outlet (T_{out}) and ambient air (T_a) can cause lower operating efficiency due to heat loss. The wavelength of radiation emitted from a surface is proportional to the temperature of the surface (Planck's Law). An ideal selective surface for solar collectors should absorb solar radiation in the visible range and emit a small amount of radiation back in the infra-red range.

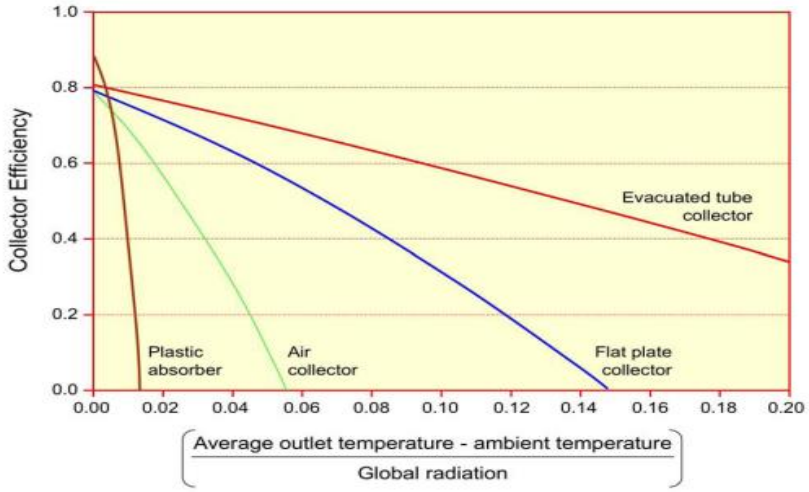

Figure 2.15: Hottel - Whillier Bliss efficiency curves (Norton, 2006)

2.6.5 THERMAL INSULATION

Flat plate solar collectors should be covered with insulated material at the back and the sides of the collector box to reduce conduction and convection losses in a flat plate solar collector. Table 2.6 show the properties of common insulation materials. Mineral wool has high relative moisture absorption compared to other insulation materials. Polyurethane foam is often used as insulation material in flat plate absorbers because it has supportive physical properties (Kaminski et al., 2019). Foam has a low thermal conductivity and is used as insulation for flat plate solar collectors (Vafaei & Sah, 2017).

Table 2.6: Properties of common insulation materials (M. Kehrer, 2003)

Insulating material	Density (kg/m^{-3})	Thermal conductivity (W/mK) at 10 °C	Compressive strength (KPa)	Relative moisture absorption
Expended polystyrene 15	15	0.4	35	Medium
Expended polystyrene 30	30	0.037	110	Medium
Expended polystyrene	32	0.27	300	Medium
Polyurethane foam	36	0.018	200	Low
Phenolic foam	32	0.027	170	Low
Cellular foam	125	0.41	700	Low
Mineral wool	24	0.0454	Negligible	Very high

2.6.6 AIR GAP BETWEEN GLASS AND FLAT PLATE ABSORBER COLLECTOR

The air gap between the glass cover and flat plate absorber collector should be considered when designing a new flat plate solar collector in order to improve performance. The effect of the air gap on the performance of a flat plate solar collector can be concluded that when the air gap parameter increased, the velocity of the air also increased (AL-Khaliffajy, M. and Mossad, 2011). Sarma et al., 2014 conducted an experiment and found that the optimum air gap between glass and flat plate absorber collector is 10 mm. There are other researchers who have suggested that the air gap of 10 mm can give an optimal performance to the flat plate solar collector (Mintsa Do Ango et al., 2013).

2.6.7 DOUBLE GLASS FOR GLAZING

The double glass is used to cover the top flat plate solar collector to trap heat loss from the flat plate absorber collector. Vettrivel & Mathiazhagan, 2017 conducted a comparative study of solar flat plate collectors with single and double glazing and reported that double glazing has a lower top loss heat transfer coefficient than single glazing cover. The findings from researchers found that double glass is more significant in the solar radiation absorption effect on heat transfer coefficient than single glass (Akhtar & Mullick, 2012). Based on other reviews, it showed that using double glass, the thermal efficiency is higher than single glass for flat plate solar water heaters (Manikandan & Sivaraman, 2016). Other researchers have suggested that the air gap parameters, should be designed with a 10 mm air gap between the glaze and thermal absorber (Subiantoro & Ooi, 2013).

2.7 THE IMPROVEMENT OF FLAT PLATE SOLAR COLLECTOR (FPSC)

The improvement of flat plate solar collector performance could be enhanced by several criteria such as fins absorber, ribbed absorber, corrugated absorber, phase change material (PCM), and nanofluids as a working fluid. By using different types of

improvement, it could increase heat transfer to the absorber collector and decrease heat loss.

2.7.1 FINNED ABSORBER COLLECTOR

Fins are used as absorber collectors for flat plate solar collectors in order to increase the surface area that is exposed to the Sun radiation. So, that by using fins, it can collect high heat radiation and increase heat transfer in the absorber collector (Hakam et al., 2016). The addition of fins is to get the maximum efficiency from the flat plate solar collectors (Wuryanti & Megawati, 2019). Using the fins also can improve thermal performance and reduce pressure losses (Youcef-Ali, 2005). Based on a review, using longitudinal rectangular fins array could increase heat transfer to 20 % enhancement (Fakoor Pakdaman et al., 2011). The outlet air temperature and efficiency could be increased when fins are applied to the flat plate solar collector (Mohammadi & Sabzpooshani, 2013). Figure 2.16 shows a finned absorber plate in a flat plate solar collector. The fins absorber plate is attached to the flat plate absorber plate.

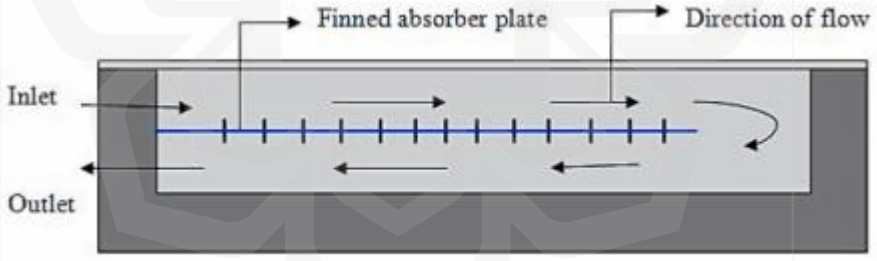

Figure 2.16: Finned absorber plate (Vengadesan & Senthil, 2020)

2.7.2 RIBBED ABSORBER COLLECTOR

A ribbed absorber was used to enhance the flat plate absorber collector's performance. The ribs are attached to the top and bottom of the flat plate absorber collector. The ribs are also known as artificial roughness and the use of ribs is to improve heat transfer in the duct (Varun et al., 2008). The existence of ribs in the flat plate absorber collector can create a uniform temperature and improve heat absorption (Abu-Hamdeh et al.,

2020). Using ribs also could improve the heat transfer rate from the absorber plate to air so that it can improve the flat plate solar collector's efficiency (Utekar & Navadagi, 2016). Figure 2.17 represents the ribbed absorber in the flat plate solar collector. The ribs are attached to the flat plate absorber collector.

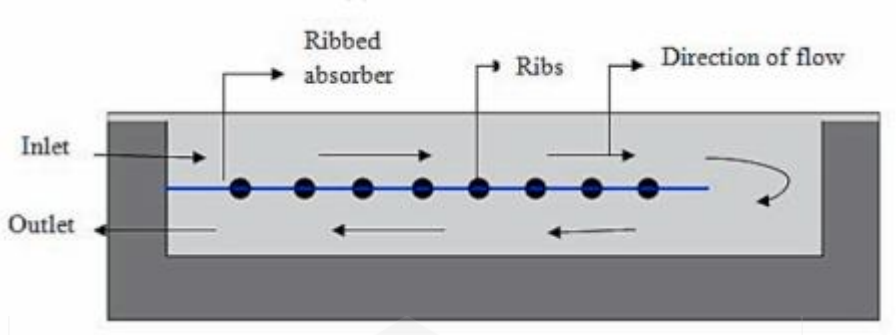

Figure 2.17: Ribbed absorber plate (Vengadesan & Senthil, 2020)

2.7.3 CORRUGATED ABSORBER COLLECTOR

A corrugated absorber was used as an absorber collector to gain higher heat at higher temperatures (R. Kumar & Rosen, 2010). An example of corrugated absorber collector is a V-corrugated absorber collector. Basically, using V-corrugated as an absorber collector is more efficient if compared to a flat plate absorber collector (Kabeel et al., 2016). Heat transfer coefficient and heat removal factor also increases by using a V-corrugated absorber collector (J.Shbailat & A. Jassim, 2018)). The solar radiation absorption could be increased by applying a V-corrugated absorber as an absorber collector (Fan et al., 2019). A corrugated absorber collector is applied, in buildings and cruise ships (Álvarez et al., 2016). Figure 2.18 represents the different configurations of corrugated absorber which are a) V-corrugation, b) Trapezoidal corrugation, (c) Sinusoidal corrugation, and (d) Finned corrugation.

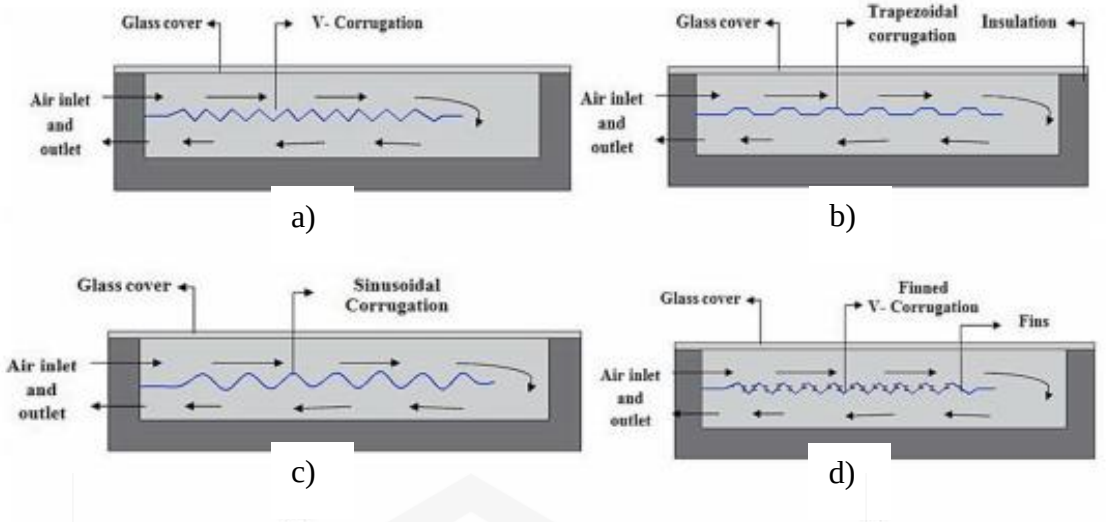

Figure 2.18: Different configurations of corrugated absorber: (a) V-corrugation, (b) Trapezoidal corrugation, (c) Sinusoidal corrugation, (d) Finned corrugation (Vengadesan & Senthil, 2020).

2.7.4 PHASE CHANGE MATERIAL (PCM) AS THERMAL STORAGE

The phase change materials (PCM) objective is to store energy which is the heat that is transferred from the flat plate absorber. The advantages of using phase change material, is that if it's integrated with a flat plate solar collector, and it can eliminate separate energy storage components (Dobriyal et al., 2020). The absorber collector section could be filled with a phase change material that has a high phase change temperature to increase the efficiency (Kürklü et al., 2002). Phase change material, which has a lower melting temperature, is good in terms of electrical properties for flat plate solar collectors (Su et al., 2017). Figure 2.19 shows the different types of phase change material that can be used for the solar collector. There are three types of phase change material which is organic, inorganic, and eutectic. Example of organic phase change material is paraffin and non-paraffin. For inorganic, the material is salt hydrate and metallic. A combination of organic and organic is eutectic.

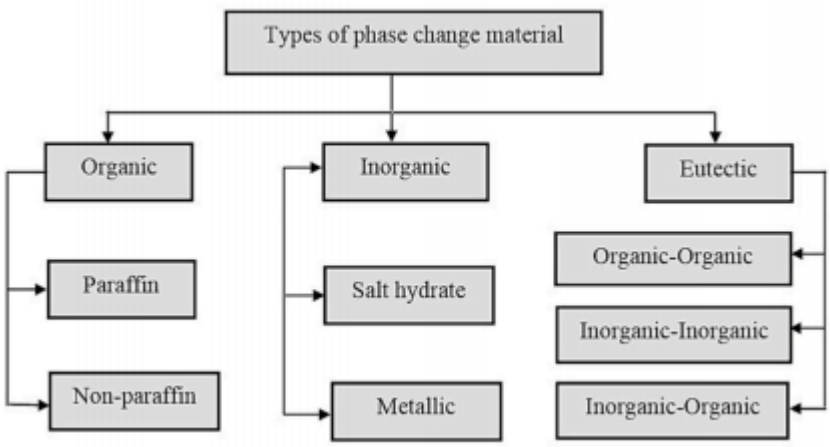

Figure 2.19: Different types of phase change material (PCM) (Vengadesan & Senthil, 2020)

2.7.5 NANOFLUID AS WORKING FLUID

Nanoparticles in liquids is defined as a mixture of fluid such as (water, oil, ethylene glycol, and molten salts) combined with a very small amount of solid metallic(carbon, metals, metal oxides) (Choi, S U.S., & Eastman, 1963). Nanofluid has good properties of radiation absorption, and it has a high thermal conductivity so that it can increase the overall conductivity of the working fluid (Chieruzzi et al., 2013, Pandey & Chaurasiya, 2017). From the researcher's review, nano particle size could have a major effect on the efficiency performance of flat plate solar collectors (Hussein, 2016). Using nanofluids in the tubes of the flat plate collector could enhance the heat transfer in the flat plate absorber collector (Dobriyal et al., 2020). Figure 2.20 shows the schematic diagram of a flat plate solar collector. From the figure, the tubes containing fluid are filled with nanofluids as working fluid.

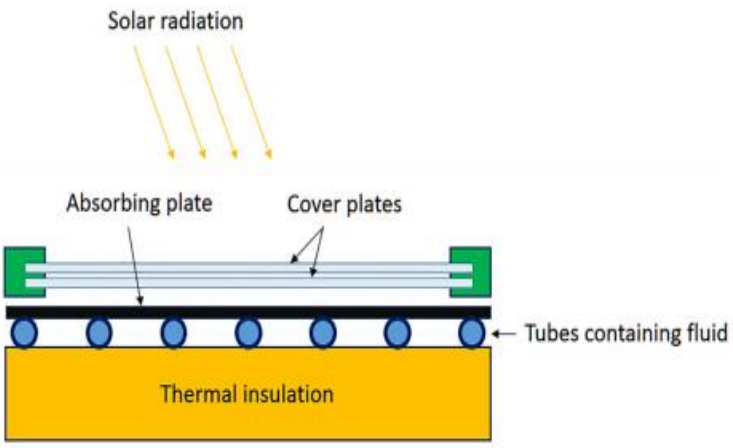

Figure 2.20: Schematic diagram of a flat plate solar collector (Dobriyal et al., 2020)

The experiment based on nanofluid is conducted by using CuO–H2O as working fluid and it was reported that the flat plate solar collector efficiency increased by 16.7 % as compared to water working fluid (Moghadam et al., 2014). Silver nanofluid is used as a working fluid. The results show that the thermal performance of flat plate solar collectors could be improved than water working fluid at high inlet temperature conditions (Polvongsri & Kiatsiriroat, 2011). Sharafeldin et al., 2017 studied the effects of using WO3 as nanofluids on the efficiency of a flat plate solar collector and found that the efficiency of solar collectors increased by 13.48%. Hawwash et al., 2018, used Alumina nanofluids as a working fluid, and the results revealed that the collector efficiency improved by about 3 % and 18 % at low and high-temperature differences.

2.7.6 POROUS MEDIA IN THE FLAT PLATE ABSORBER COLLECTOR

Porous media is used in the flat plate solar collector to increase the temperature of the air at the outlet. Figure 2.21 represents the porous media assisted in double pass flat plate solar collector. Basically, high-conductive material is used as porous media in flat plate solar collectors (N. Kumar et al., 2019). Using porous metal foam for the absorber collector could improve the thermal performance of flat plate solar collectors (Anirudh & Dhinakaran, 2020). Other results showed that using porous matrix media in flat plate absorber collectors could improve the thermal performance of flat plate solar collectors (Venu & Arun, 2013).

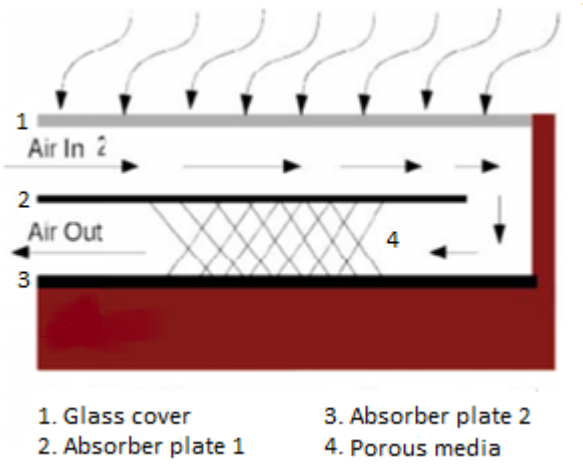

Figure 2.21: Porous media assisted in flat plate solar collector
(N. Kumar et al., 2019)

2.8 MATHEMATICAL MODELLING

The solar collectors' stationary models were presented by Hottel and Woertz [1942], and Hottel and Whillier [1958].(Hottel, H.C., Whillier, 1958, and Hottel, H.C., Woertz, B.B., 1942) which is based on a zero-capacitance model. Based on the model, the effects of thermal capacitance on the collector performance are neglected, and a single value of the collector's overall heat loss coefficient is considered. The collector is considered to be in equilibrium with its environment at any instant time. A single value of the collector's overall loss coefficient is considered in the model, independent of the variable ambient conditions.

Modelling saves cost and improves reliability, so it can possibly test a range of data and from a widely varying conditions than experimentation, which is limited by the cost of materials employed. At times the accuracy of some instruments employed in experimentation becomes an issue; thus, engineers have come to be familiar with modelling system behavior's so that specific predictions of one or more characteristics of the system can be made without an option for experimentation. To do this, it is necessary to correlate the data to obtain predictive equations.

Saleh (2012) performed a modelling of flat-plate solar collector operation in a transient state. Based on the results, the efficiency was validated by an experiment and showed the existence of a better agreement between measured and numerical values. The numerical value parameter is predicted for different running conditions and flow rates. Modelling method has solved the limitation between existing models and distributed models. The models also apply low and high flow rates of operations.

Hamed et al., 2014) have done parametric sensitivity studies on the performance of a flat plate solar collector in transient behaviour. Based on the study, the researcher developed a model regarding the energy balance analysis. The results indicate that increment in water flow rates will decrease the output water temperature and the overall heat loss coefficient. It can be concluded that the input temperature augments with the output water temperature.

Amankwah et al. (2017) conducted an experiment of distributed mathematical models supporting the design and construction of solar collectors for drying. The collector's length had increased beyond a certain limit and has not affected the solar collector because of the driving force decrease in heat transfer between plate and air. The absorber plate and glass temperatures are independent of the length. Based on the results of temperature distribution from the experiment, it was proposed that simplification of the model should be feasible by spatial lumping of the glass cover and plate temperatures. The generic spatially discretized model is verified as a good tool when designing solar collectors and operations. It can be concluded that the overall heat loss coefficient, heat gain, and efficiency depend on the air velocity.

Wahida Khalili et al. (2019)conducted a study on mathematical modelling and simulation of the performance of PV/T air solar collector. The mathematical model was developed by using a one-dimensional energy balance equation. MATLAB software was used to run the simulation to find out the effect of solar radiation and temperature on the performance of the solar collector. The findings showed that removing heat through working fluid, can reduce solar collector temperature while improving performance. Solar radiation also affects the solar collector's efficiency.

Zima and Dziewa (2010) performed mathematical modeling of heat transfer in liquid flat-plate solar collector tubes. A comparison was made between the model and the experiment results of the transient states. There are two numerical verifications carried out to validate that the model. Basically, the inlet fluid temperature and also the heat flux on the outer tube surface were determined as a step function. For real application, the fluid temperature always changes, but the solar radiation heat flux does not change rapidly.

2.9 CHAPTER SUMMARY

This chapter reviews the solar thermal technology that exists as well as also the types of solar thermal collectors. Flat Plate Solar Collector (FPSC) is commonly used in drying applications. It is also categorized as a non-concentrating solar collector (NCSC). The conclusion is that the performance of FPSC depends on several aspects such as thermal absorber design, materials and thickness of absorber collector, solar collector glazing, types of glass, thermal absorber surface coating, thermal insulation, an air gap between glass and flat plate absorber collector and double glass.

There are different techniques that could be used to improve the performance of absorber collectors such as finned absorber collector, ribbed absorber collector, corrugated absorber collector, phase change material (PCM) as thermal storage, nanofluid as working fluid and porous media in Flat Plate Absorber Collector (FPSC). Using these techniques, could improve heat transfer and thermal energy storage in the absorber collector of FPSC. The gap found from the previous studies was identified. However, there is current research being conducted to study and analyze the thermal performance and FPSC's techno-economics using a thermal cell attached at the top surface of the flat plate absorber collector.

CHAPTER THREE

RESEARCH METHODOLOGY

3.1 INTRODUCTION

This chapter discusses the details of materials, devices, and methods used in this research. There are two types of experiments involved, using a solar simulator and an outdoor experiment. A solar simulator was used to provide an artificial solar simulation in indoor conditions. The experiment was done under sun radiation as an outdoor experiment.

3.2 FLOW CHART OF RESEARCH

Figure 3.1 shows the flow chart of research activities that applies to this research project. The research work was conducted mainly in several sections, which are (i) FPBTCA design parameter, (ii) material selection experiment, (iii) heat transfer experiment, and (iv) mathematical modelling of heat transfer.

It started by reviewing the design of a flat plate solar collector (FPSC). Then the preliminary experiment was done on the flat plate solar collector design parameter. Followed by the designing and developing a Flat plate solar thermal collector (Base) with an absorber thermal cell. The materials and components were prepared based on the design that has been done. A flat Plate Solar Thermal Collector (Base) With Absorber Thermal Cell was fabricated. Then the experiment was performed, and the results were compared to mathematical modelling.

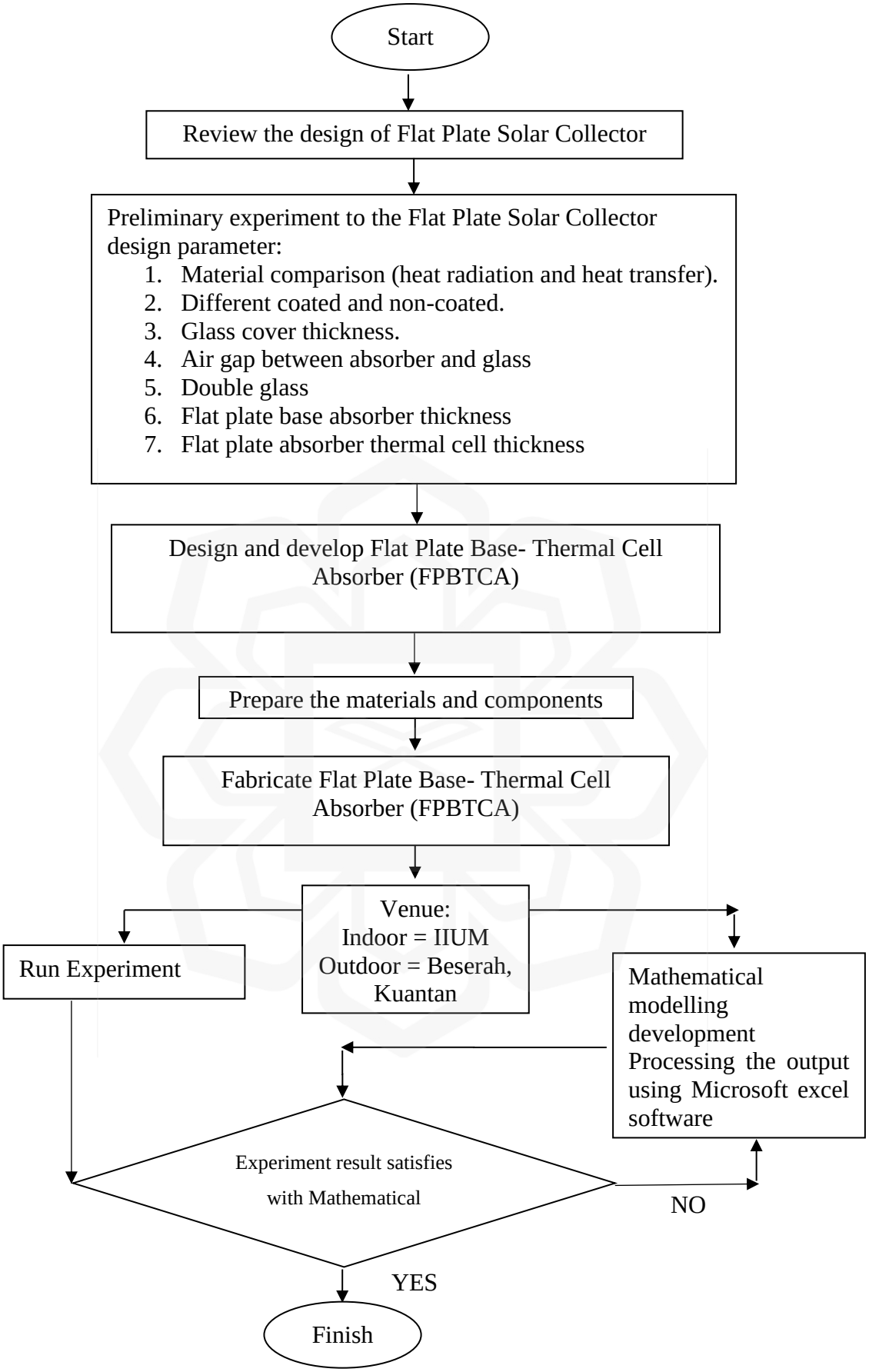

Figure 3.1: Flow chart of research activities.

3.2.1 REVIEWING THE DESIGN OF THE FLAT PLATE SOLAR COLLECTOR

Figure 3.1 shows the flow chart of research activities in this research project. The research starts with a review of the design parameter of flat plate solar collectors. The design parameter was studied based on the significant effect to the performance of flat plate solar collectors. From the literature review, the details of the focus area could be explored to enhance the problem of the solar dryer system. The objective of this research also could be pursued. The methodology of the project can be determined by reviewing the relevant literature.

3.2.2 PRELIMINARY EXPERIMENT TO THE FLAT PLATE SOLAR COLLECTOR (FPSC) PARAMETER

There are several parameters chosen in the preliminary experiment of flat plate solar collectors. The parameters were selected based on the effect on the flat plate solar collector performance. The parameters are:

1.Material comparison (heat radiation and heat transfer).
2.Different coated and non-coated flat plate thermal cell absorber
3.Glass cover thickness.
4.An air gap between the absorber and the glass
5.Selection of glass cover
6.Double glass
7.Flat plate absorber thickness
8.Flat plate absorber Thermal cell thickness

3.2.3 DESIGN AND DEVELOPED FLAT PLATE BASE-THERMAL CELL ABSORBER (FPBTCA)

The Flat Plate Base-Thermal Cell Absorber (FPBTCA) parameter is determined based on the preliminary experiment. The preliminary experiment was conducted indoors by using artificial solar radiation. Then the flat plate solar collector with an absorber thermal cell was designed and developed according to the parameter.

3.2.4 PREPARATION OF THE MATERIALS AND COMPONENT

The equipment is prepared based on Flat Plate Base- Thermal Cell Absorber (FPBTCA), which is a glass cover, data logger, pyranometer, stainless steel Cell, aluminum base absorber, ventilation fan, and weight measurement.

Table 3.1: The materials involved in this research

No	Materials	Dimension	Unit	Price (Rm)	Nett Price
1	Stainless steel 304	10 cm x 10 cm ($0.01\ m^2$) Thickness = 1.0 mm	1	24.50 (Rm/m^2)	2.50
2	Aluminium	18.5 cm x 25.5 cm ($0.0471\ m^2$) Thickness = 0.5 mm	1	19.50 (Rm/m^2)	0.92
3	Plastic box	15.5 cm x 15.5 cm	1	3.00	3.00
4	Glass	29.9 cm x 23 cm Thickness = 2.0 mm	1	4.00	4.00
5	Insulation	18.5 cm x 25.5 cm ($0.0471\ m^2$) Thickness = 1.0 mm	1	53.20	2.51
				Total Rm	12.93

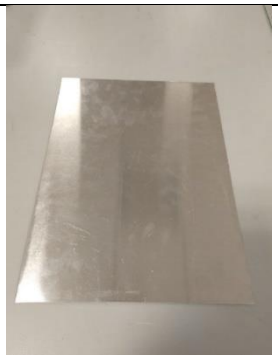

a) Aluminium flat plate

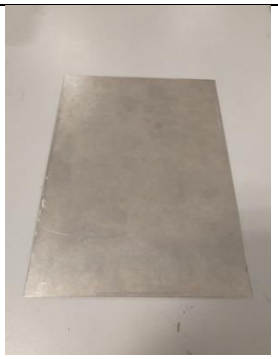

b) Stainless steel flat plate

c) Low-iron glass

d) Data logger

e) Pyranometer

f) Ventilation fan

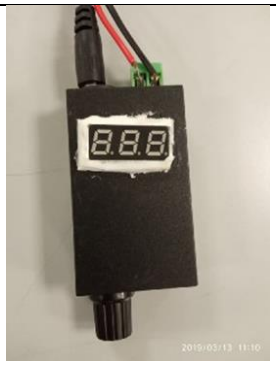

g) Fan speed controller

h) Weight measurement

Figure 3.2: Material and device used in this study

3.2.5 FABRICATION OF FLAT PLATE BASE-THERMAL CELL ABSORBER (FPBTCA)

The fabrication of the Flat Plate Base- Thermal Cell Absorber (FPBTCA) system is built part by part. Firstly, the flat plate aluminium base absorber collector is cut to the size of 18.5 cm width and 25.5 cm length. Then thermal cell absorber was cut to the size of 10 cm width and 10 cm length, next the thermal cell absorber is attached to the aluminium base absorber collector's surface.

3.2.6 VENUE FOR THE EXPERIMENT

The experiment was conducted at Pelindung Damai, 26100 Beserah, Kuantan, Pahang Darul Makmur, under actual sunshine conditions. Its setup is under an open area to get the maximum radiation from the sun. The most important is the location of the test experiment to avoid disturbance of radiation from the sun.

3.2.7 RUN EXPERIMENT

The experiments were run under the setup condition. The data gathered from the experiment were used to analyze and compare with Mathematical modelling. The weather during the outdoor experiment and the readings taken will be on ambient conditions throughout the experiment. The assumption for the experiment is:

i. The pyranometer and temperature meter used should be in good condition.
ii. The stability of airflow in the dryer chamber and absorber was stable when the experiment was done, which is the mathematical modeling was assumed as in a steady state condition.
iii. During the experiment, heat loss in the drying chamber is assumed to be minimal.

3.2.8 MATHEMATICAL MODELLING

Mathematical modelling is derived from the formulae, and then the development of mathematical modelling is done to compare with the experiment results. Development and processing of the output was by using Microsoft excel.

3.2.9 EXPERIMENT RESULTS CONCURS WITH MATHEMATICAL MODELLING

The results will be analyzed based on the data gathered from the experiment, which will be used to compare with mathematical modelling. If the results are different, it will be analyzed again. If the results are the same, then the experiment is completed.

3.3 METHOD TO EVALUATE FOR FLAT PLATE ABSORBER DESIGN PARAMETER

A preliminary experiment was done to determine the optimum parameter of a flat plate solar collector. The FPSC was exposed to the solar simulator. The devices used in this experiment were selected based on their ability to conduct the experiment and obtain data for analysis. An AT4208 Multi-Channel Temperature Meter (8-Channel, Applent Technology, China) and a pyranometer (Apogee Instruments, USA) were used to measure the temperature of the absorber's wall and solar radiation. For calibration purposes, the real-time solar radiation flux was measured using the TES-1333R Solar Power Meter (Datalogging, TES Electrical Electronic Corp., China). The readings recorded by the pyranometer and data logger were calibrated for their validity and reliability before conducting the experiment.

3.3.1 METHOD TO EVALUATE FLAT PLATE ABSORBER MATERIAL, GLASS THICKNESS, AIR GAP THICKNESS, AND FLAT PLATE ABSORBER BASE COLLECTOR

Figure 3.3 shows the experimental set-up of the study before the experiment. The figure represents the flat plate absorber material set-up, glass thickness, air gap distance, and flat plate absorber base-collector. The flat plate solar collector has a distance of 18 cm between the solar simulator.

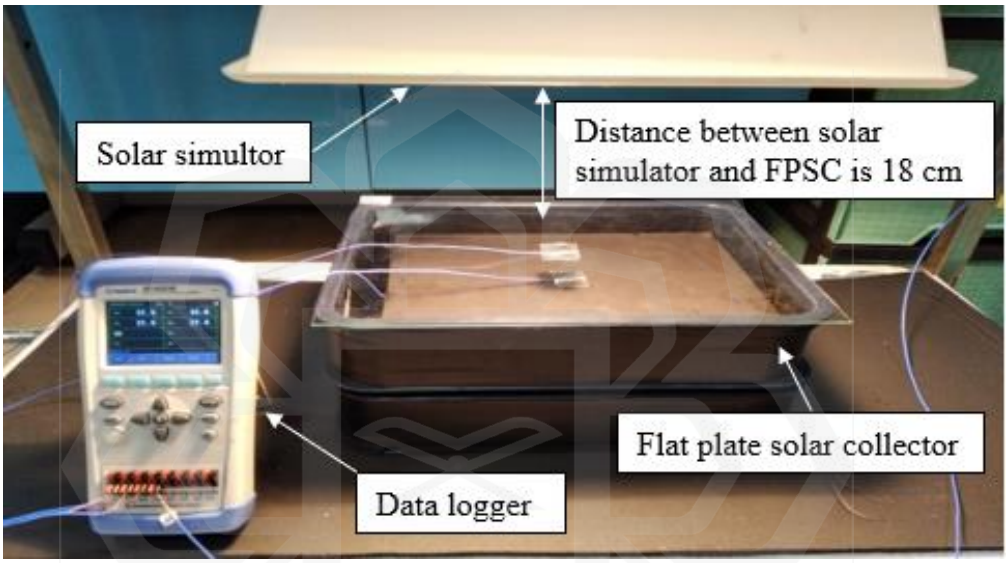

Figure 3.3: Experimental set-up

Figure 3.4 represents the flat plate solar collector diagram used in the experiment. Figure 3.4 a) shows the top and figure 3.4 b) shows the side views of the flat plate solar collector diagram. The size of the flat plate absorber collector used is 18.5 cm in width and 25.5 cm in length. The flat plate solar collector box size is 22.0 cm in width and 29.5 cm in length.

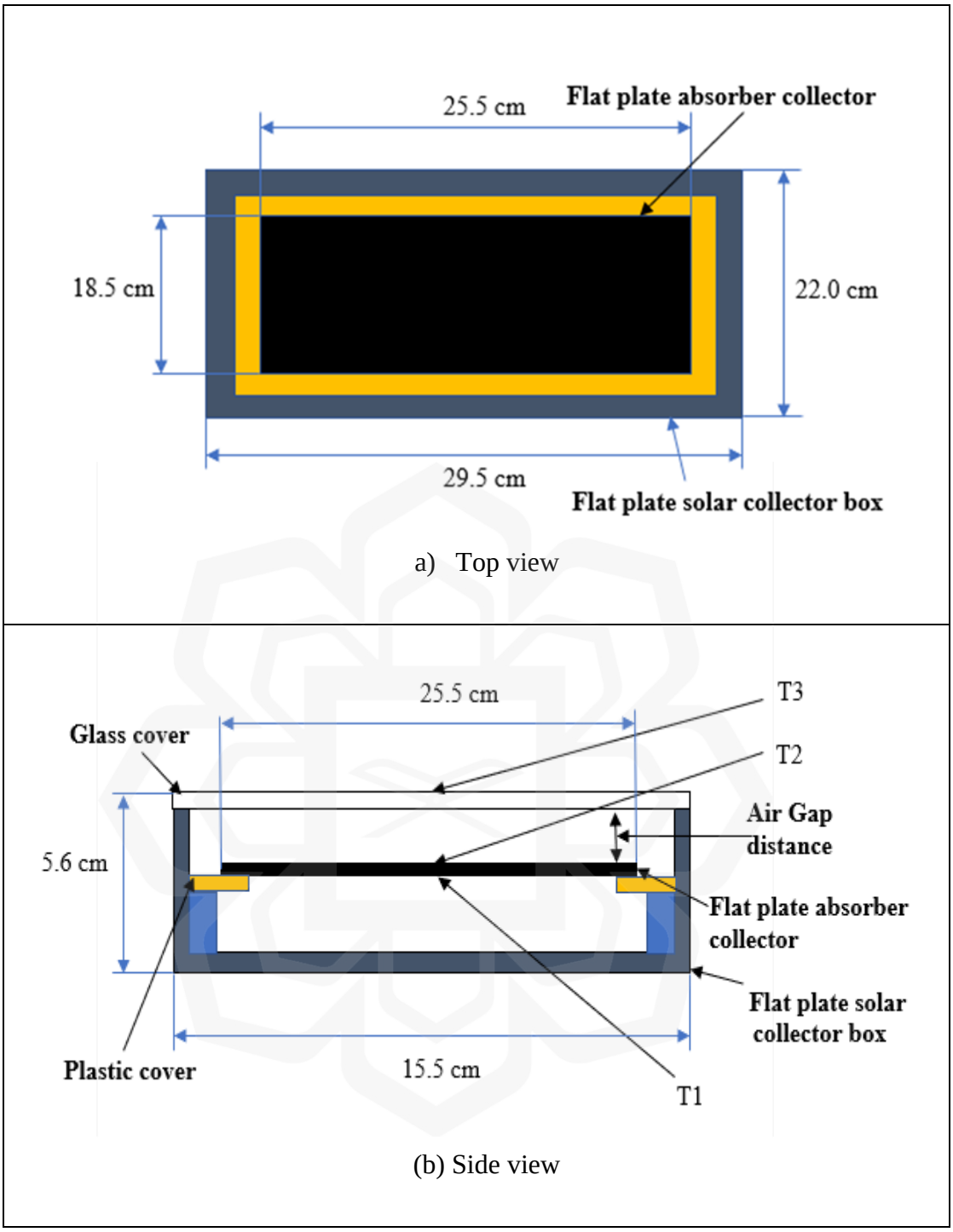

Figure 3.4: a) Top view b) Side view of flat plate solar collector diagram.

3.3.2 METHOD TO EVALUATE DIFFERENT COATING SURFACES AND THERMAL CELL ABSORBERS

Figure 3.5 represents the experimental set-up of the experiment. The figure represents the set-up for different coating surfaces and thermal cell absorbers. The data was recorded every 1 second using the data logger and the 8-channel Temperature Meter. The distance between the flat plate solar collector and the solar simulator is 19 cm.

Figure 3.5: Experimental set-up

Figure 3.6 shows the flat plate solar collector diagram used in the experiment. The figure shows the top and side views of the flat plate solar collector diagram. The flat plate absorber-collector size is 10.0 cm in width and 10.0 cm in length, and the flat plate solar collector box size is 15.5 cm × 15.5 cm.

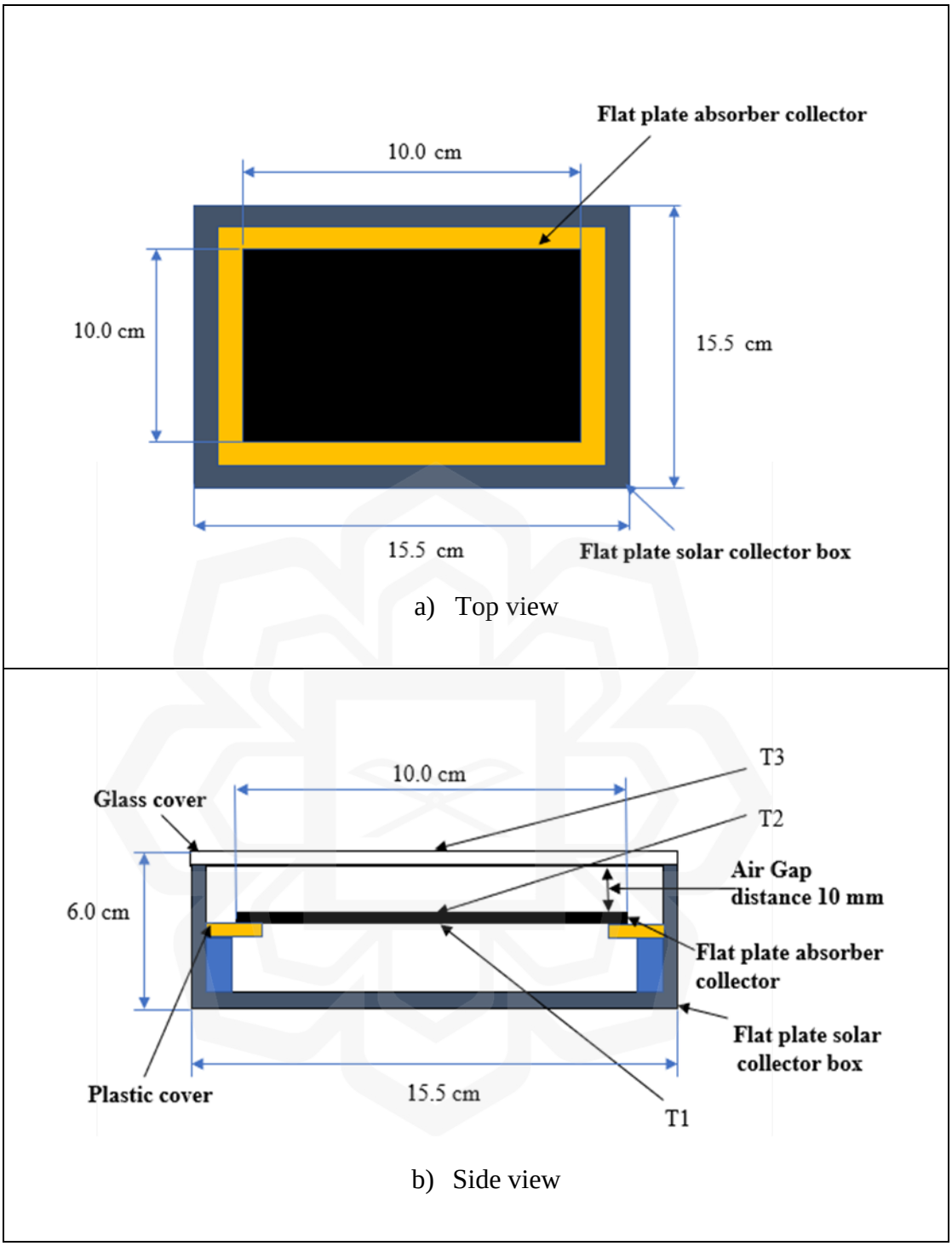

Figure 3.6: a) Top view b) Side view of flat plate solar collector diagram.

3.4 SELECTION OF FLAT PLATE ABSORBER COLLECTOR MATERIALS

Solar simulator radiation of 450 W/m^2 was applied in this experiment. Table 3.2 shows the flat plate absorber materials configuration used in the experiment. Aluminum and stainless steel were used as flat plate absorber-collector materials. The aluminum and stainless-steel size is 18.5 cm × 25.5 cm and the area is 471.75 cm^2. A flat plate absorber-collector thickness of 0.8 mm was selected for the configuration of both materials, and the weight is 0.101 kg and 0.271 kg for aluminum and stainless steel, respectively.

Table 3.2: Flat plate absorber materials configuration

Material	Size (WxL)(cm)	Area (cm^2)	Thickness (mm)	Weight (kg)
Aluminium	18.5 x 25.5	471.75	0.8	0.101
Stainless Steel	18.5 x 25.5	471.75	0.8	0.271

3.5 SELECTION OF COATING SURFACE AND NON-COATING SURFACES

Aluminum flat plate absorber-collector with 0.5 mm thickness was used in the experiment to compare the coating surface and non-coating surface. The size of the flat plate absorber-collector is 10.0 cm in length and 10.0 cm in width, and it weighs 0.015 kg. Solar simulator radiation of 450 W/m^2 was applied in the experiment. Figure 3.7 shows the non-coated and coated flat plate thermal cell absorber used in this study. Matt black paint has been used for coating the surface of the flat aluminum plate absorber. The experiment was conducted for 5 minutes of charging under solar radiation and 5 minutes of discharging by removing the solar simulator for 5 minutes.

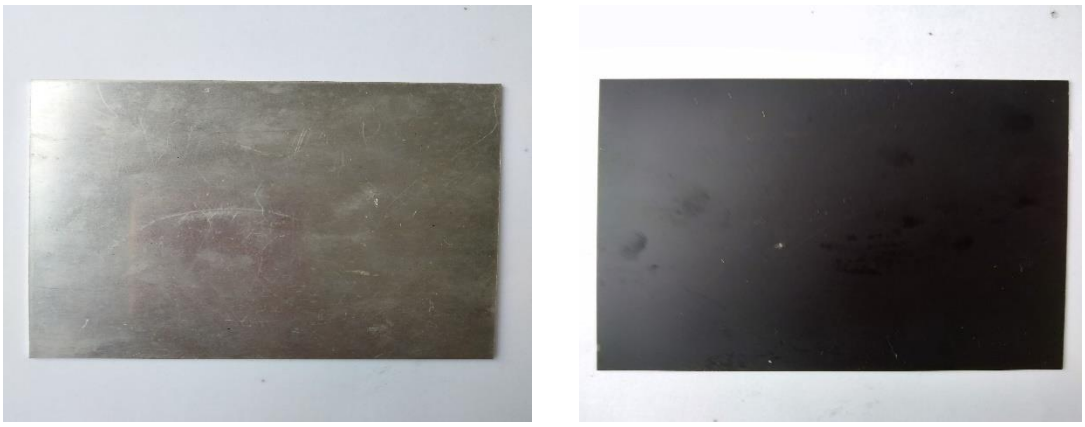

a) b)

Figure 3.7: a) Non-Coated b) Coated for flat plate absorber collector

3.6 SELECTION OF FLAT PLATE THERMAL CELL THICKNESS

The constant parameters used in this experiment were the air gap space and glass thickness. The flat plate absorber-collector and glass cover have an air gap space of 10.0 mm. Glass thickness of 2.0 mm was used in this experiment. Stainless steel 304 was used for the flat plate thermal cell absorber. The solar simulator used in this experiment has 450 W/m^2 radiation. Figure 3.8 presents the flow chart of the experiment executed. Three types of flat plate thermal cell absorbers of 0.5 mm, 1.0 mm, and 2.0 mm thickness were used in this experiment. The weight of the flat plate thermal cell thickness was 0.5 mm, 1.0 mm, and 2.0 mm is 0.038 kg, 0.073 kg, and 0.172, respectively.

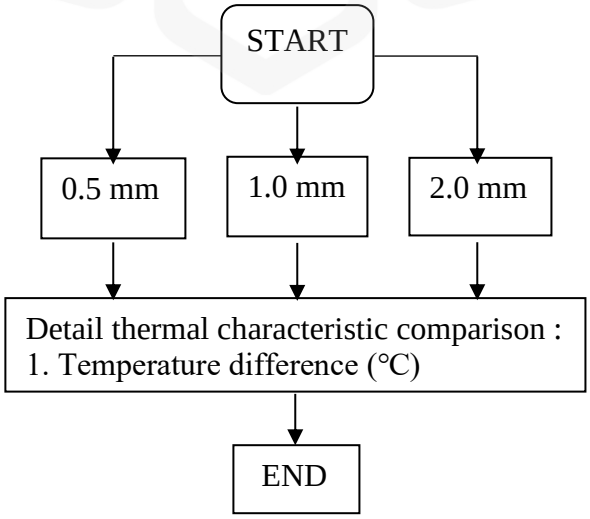

Figure 3.8: Flow chart implemented in this work

3.7 SELECTION OF GLASS THICKNESS

The constant parameters used in this experiment were flat plate absorber thickness and the air gap space (air gap between the absorber and glass). Stainless Steel 304 flat plate absorber thickness was 1.2 mm, and its weight was 0.415 kg. The flat plate absorber-collector and glass cover have an air gap thickness of 10.0 mm. The solar simulator used in this experiment emits a constant rate of 750 W/m^2 radiation. The high solar radiation rate was meant to simulate the behavior of glass thickness. Figure 3.9 shows the flow chart of the experiment carried out. The glass thickness used in this experiment is 2.0, 3.0 mm, 4.0 mm, 5.0 mm, and 10.0 mm, as top cover of the flat plate solar collector (FPSC).

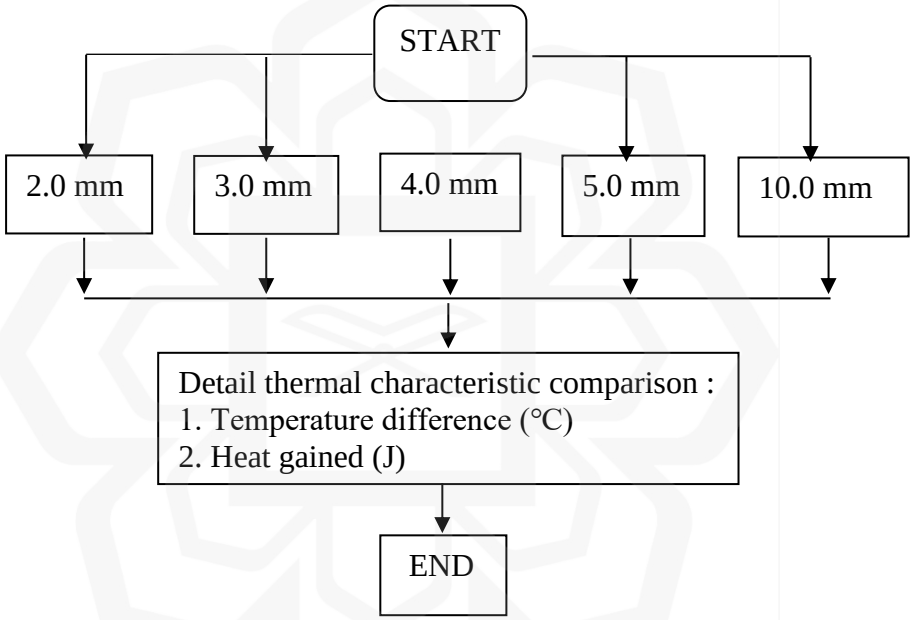

Figure 3.9: Process flow chart implemented in this work

3.8 EVALUATION OF AIR GAP DISTANCE (BETWEEN FLAT PLATE ABSORBER COLLECTOR AND GLASS)

The thickness of the flat plate absorber and glass was used as the constant parameters in this experiment. The stainless steel 304 flat plate absorber thickness was 1.2 mm, and the weight was 0.415 kg. Glass cover thickness of 2.0 mm was used for the flat plate solar collector. The solar simulator used in this experiment has 450 W/m^2 radiation. Figure 3.10 shows the process flow chart implemented in this work. The air gap distance

of 0 mm, 5.0 mm, 10.0 mm, 20.0 mm, and 30.0 mm was applied for the air gap distance configuration in this experiment.

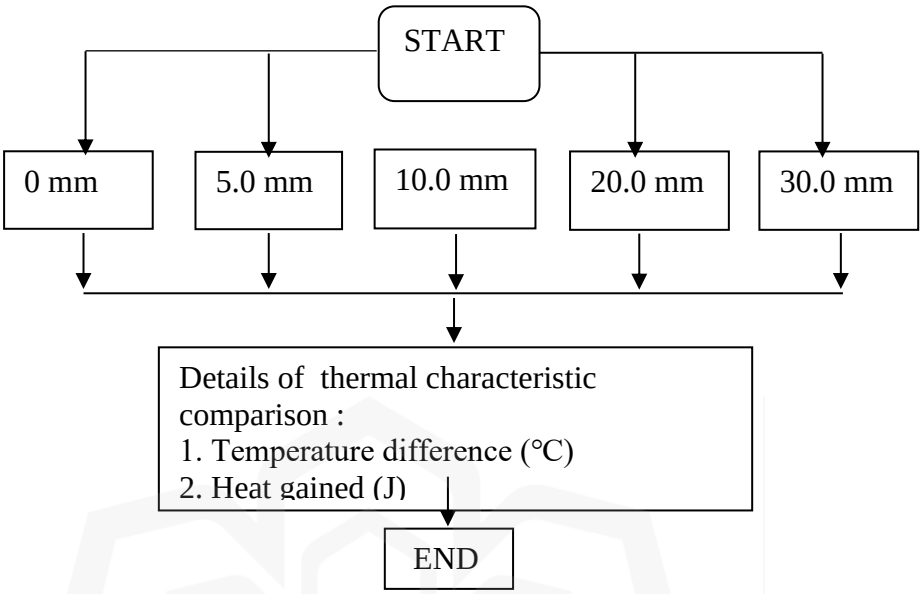

Figure 3.10: Process flow chart implemented in this work

3.9 SELECTION OF FLAT PLATE ABSORBER BASE-COLLECTOR THICKNESS

Constant parameters used in this experiment were the glass thickness and air gap space, where the glass thickness was 2.0 mm, and the air gap distance was 10.0 mm. Solar radiation of 450 W/m^2 was applied in this experiment. Figure 3.11 presents the process flow chart of the experiment. The flat plate aluminum absorber base-collector size applied in this experiment was 18.5 cm in width and 25.5 cm in length. Flat plate aluminum absorber base-collector thickness and weight used in this experiment were 0.5 mm (0.073 kg), 0.8 mm (0.101 kg), and 1.0 mm (0.119 kg). The thickness was selected based on the application of the absorber collector in a solar collector.

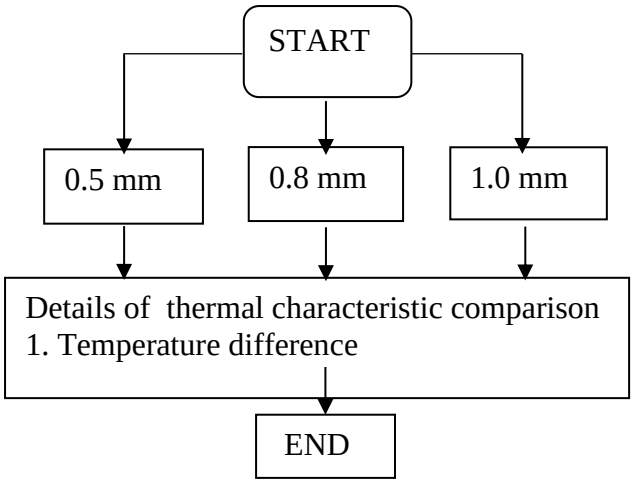

Figure 3.11: Flow chart implemented in this work

3.10 SELECTION OF GLASS COVER

Flat plate absorber thickness and glass thickness were used as constant parameters in this experiment. Stainless Steel 304 flat plate absorber thickness is 1.2 mm, and its weight is 0.415 kg. Glass thickness of 2.0 mm was used as a glass cover for the flat plate solar collector. The radiation of the solar simulator was set at 450W/m^2. The air gap distance between the flat plate absorber-collector and glass cover 1 is 10.0 mm. Figure 3.12 shows the double glass diagram for FPSC. The air gap distance between glass cover 1 and glass cover 2 is 0.4 mm.

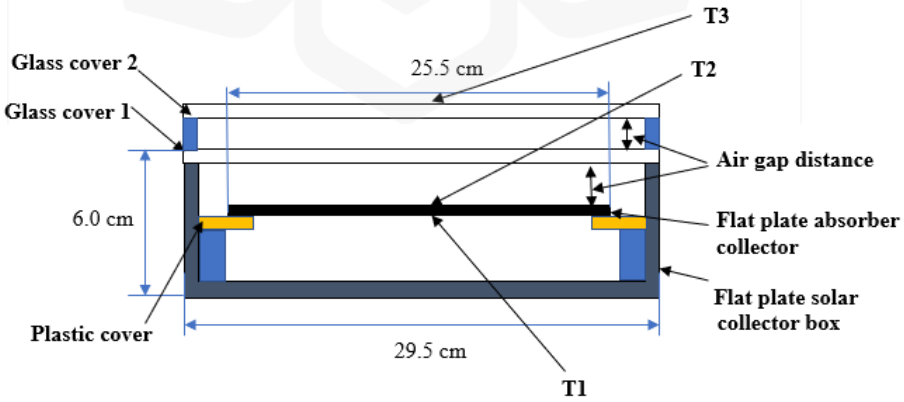

Figure 3.12: Double glass diagram for FPSC

3.11 PRELIMINARY 1 AND 2 EXPERIMENTS FOR FLAT PLATE SOLAR COLLECTOR AND FLAT PLATE BASE-THERMAL CELL ABSORBER

Preliminary 1 experiment was done by exposing the solar radiation for 300 s, while preliminary 2 experiment was done by exposing the solar radiation for 600 s period. All experimental works were conducted indoors and under a controlled environment. The details of each experiment conducted are explained in the following sub-sections. The fan speed used in this experiment is 0.62 m/s. The glass cover thickness is 2 mm. All the recorded data was analyzed, and the graph was plotted after the experiment was done.

The data logger, 8-Channel Temperature Meter, was used to record the data when the experiment was performed. The temperature data was collected and recorded at every 1 second using a data logger. The radiation used in this experiment is 750 W/m^2. Table 3.3 shows the experiment table for flat plate solar collector configuration. Aluminum was used as an absorber base-collector. There are two types of thermal cell material which are aluminum and stainless steel.

Table 3.3: Experiment table for flat plate solar collector configuration

No	Types of Absorber (Base)	Thermal cell	Thickness (mm)	Total Weight (g)	Size (m)
1	Aluminum	NA	0.5	73	0.185 x 0.255
2	Aluminum	Aluminum	0.5	95	0.010 x 0.010
3	Aluminum	Aluminum	1.0	102	0.010 x 0.010
4	Aluminum	Stainless Steel	0.5	115	0.010 x 0.010
5	Aluminum	Stainless Steel	1.0	148	0.010 x 0.010

3.11.1 METHOD TO EVALUATE THE FLAT PLATE SOLAR COLLECTOR (ALUMINUM BASE ABSORBER)

Figure 3.13 shows the setup for aluminum base absorber of a flat plate solar collector. The flat base plate absorber material is aluminum, the thickness is 0.5 mm, and the weight is 73 g. The absorber size is 0.185 m in width and 0.245 in length.

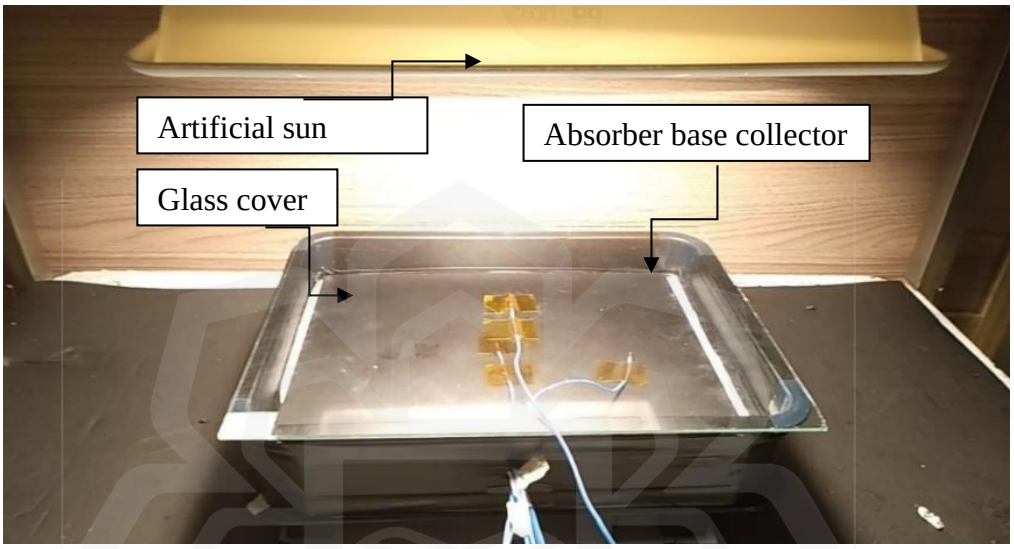

Figure 3.13: Experiment set-up for flat plate solar colelctor (Aluminum base collector).

Figure 3.14 shows a) Top view b) Side view of the flat plate solar collector diagram, based on the figure, it represents the position of the solar plate collector (Aluminum base collector). There are several parameters that should be considered, which are glass cover, air gap distance, and flat plate absorber collector. The parameters were determined based on the experiment.

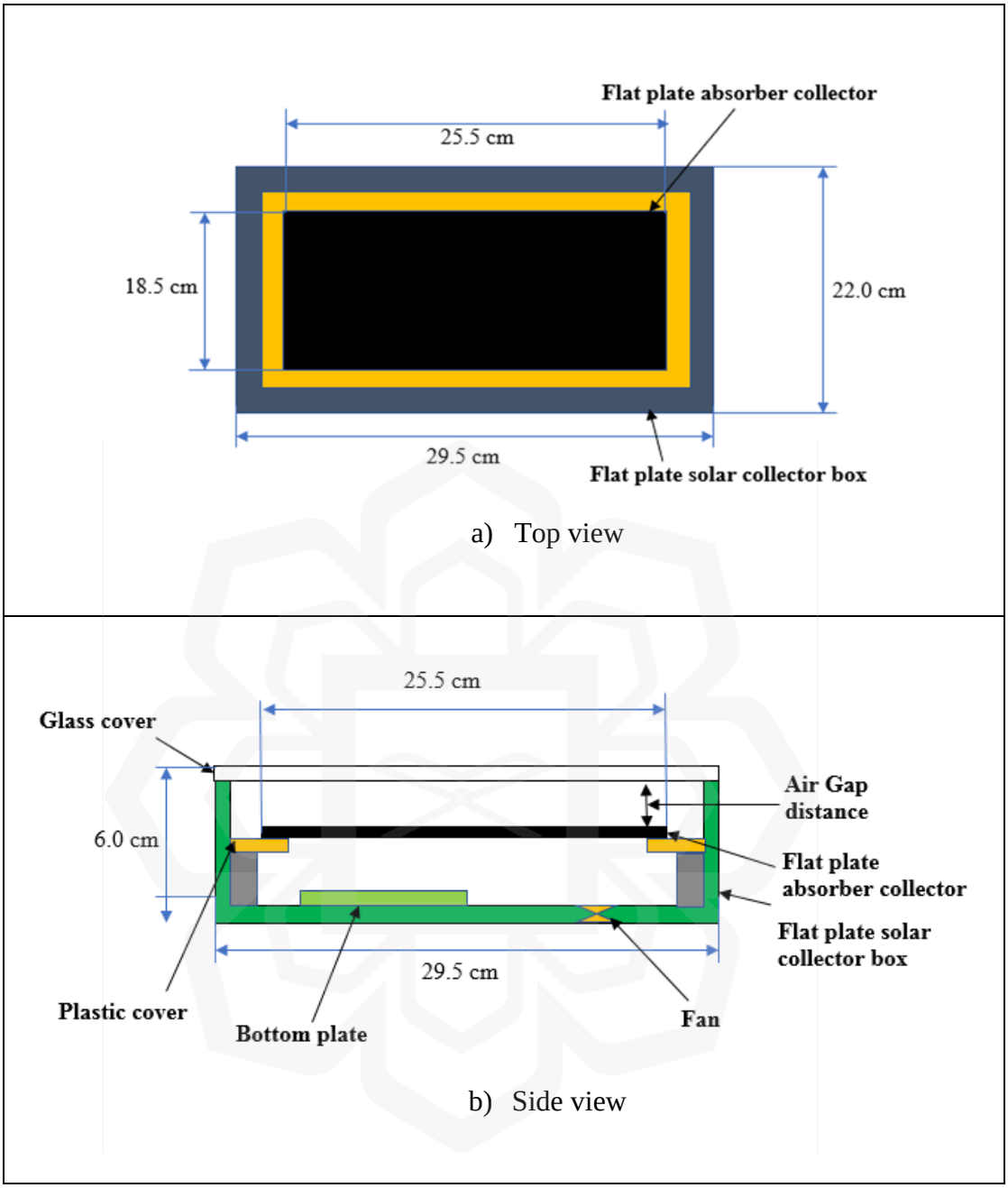

Figure 3.14: a) Top view b) Side view of flat plate solar collector diagram

Figure 3.15 represents the temperature location for the flat plate solar collector (aluminum base absorber). There are eight sensors located at the surface of the flat plate solar collector component. The sensors are T1(Bottom Temperature), T2 (Drying Temperature), T3(Outlet Temperature), T4(Absorber Temperature (Below)), T5 (Absorber Temperature (Below)), T6 (Absorber Temperature (Top)), T7(Drying Temperature) and T8 (Glass cover Temperature).

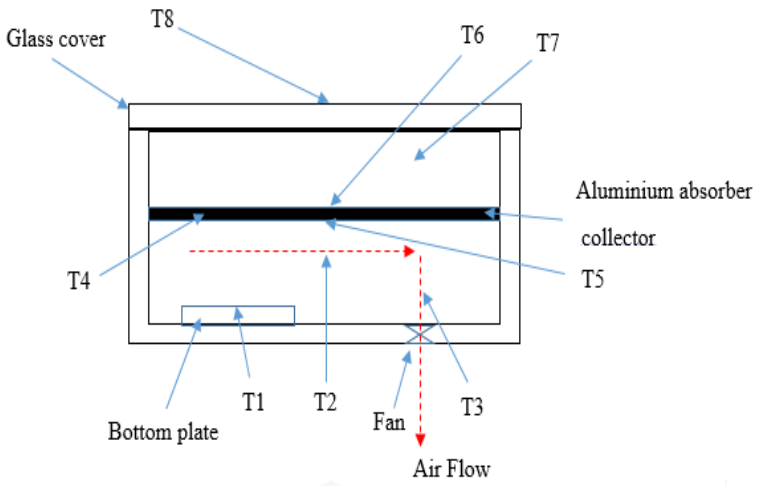

Diagram outline:
T1=Bottom Temperature
T2=Drying Temperature
T3=Outlet Temperature
T4=Absorber Temperature (Below)
T5=Absorber Temperature (Below)
T6=Absorber Temperature (Top)
T7=Drying Temperature
T8=Glass cover Temperature

Figure 3.15: Temperature sensor location.

3.11.2 METHOD TO EVALUATE THE FLAT PLATE BASE-THERMAL CELL ABSORBER (FPBTCA)

Figure 3.16 shows the experiment setup for Flat Plate Base-Thermal Tell Absorber (FPBTCA). There are two types of thermal cell material used in this experiment which are stainless steel and aluminium. The size of the thermal cell is 10.0 cm in width and 10.0 cm in length. Aluminium material is used as a flat plate absorber base-collector which is below the thermal cell.

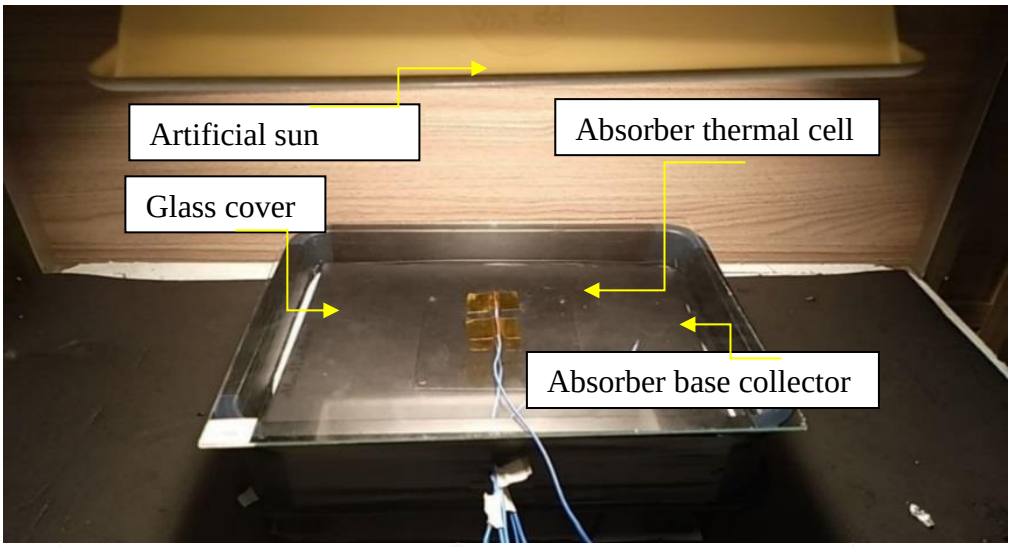

Figure 3.16: Experiment set-up for FPBTCA

Figure 3.17 shows the FPBTCA diagram. Figure a) represents the Top view, and figure b) shows the side view of FPBTCA. The FPBTCA component consists of a flat plate absorber collector, thermal cell absorber, glass cover, flat plate solar collector box, bottom plate, outlet fan, and insulation at the bottom sides. The air gap distance used in this experiment is 1.0 cm. Aluminum and stainless-steel thermal cell absorber is located at the top of the flat plate absorber collector.

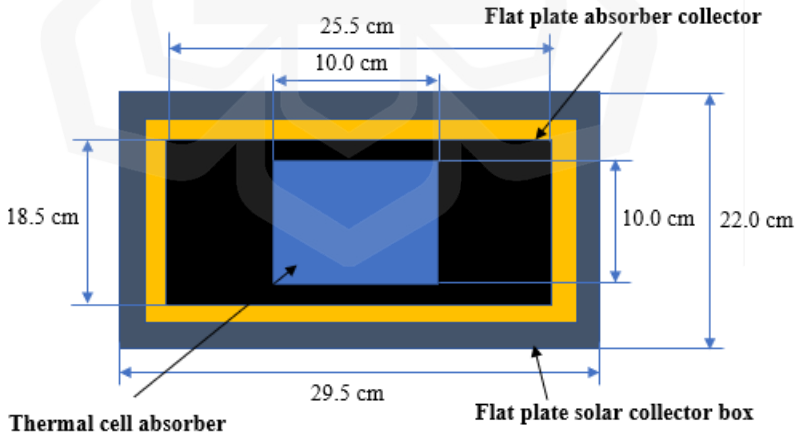

a)

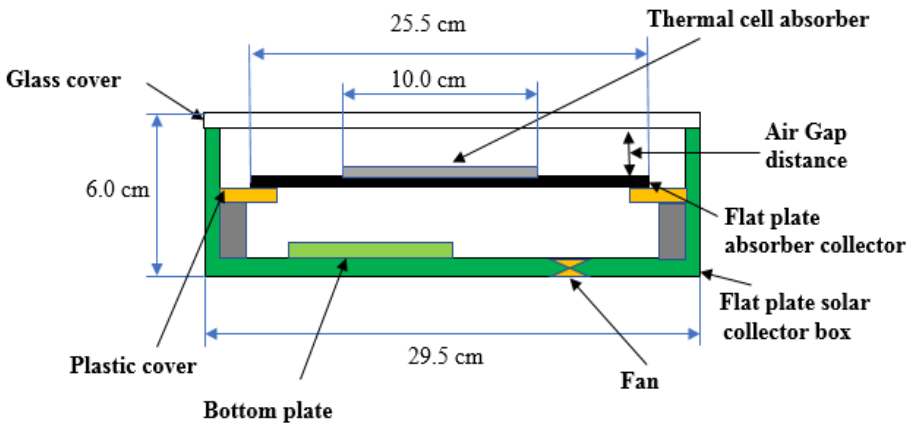

b)

Figure 3.17: a) Top view b) Side view of FPBTCA diagram

Figure 3.18 shows the temperature location for Flat Plate Base-Thermal Cell Absorber (FPBTCA). The sensors are located on the different surfaces of the FPBTCA component. There are eight sensors located at the surface of the flat plate solar collector component. The sensors are T1(Bottom Temperature), T2 (Drying Temperature), T3(Outlet Temperature), T4(Absorber Temperature (Below)), T5 (Absorber Temperature (Below)), T6 (Absorber Temperature (Top)), T7(Drying Temperature) and T8 (Glass cover Temperature).

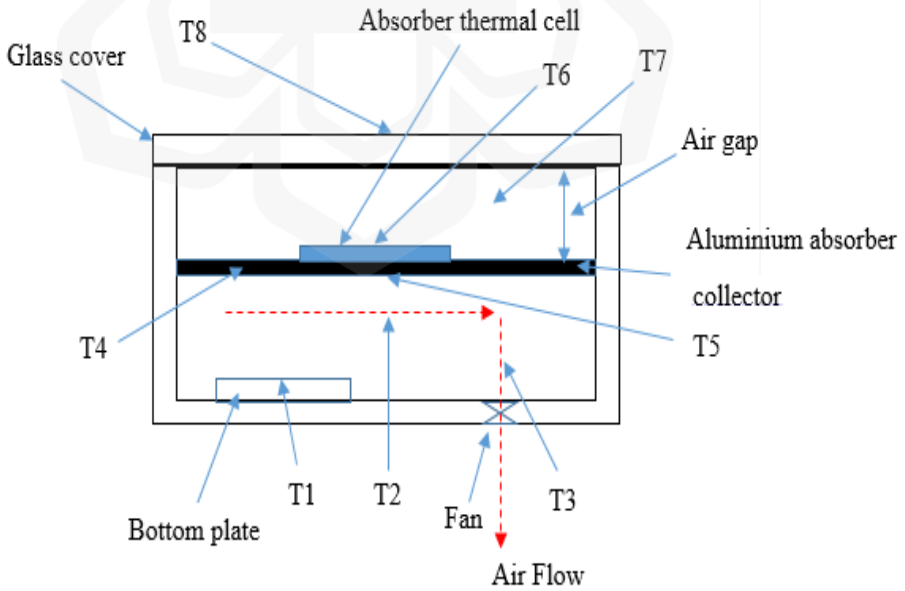

a)

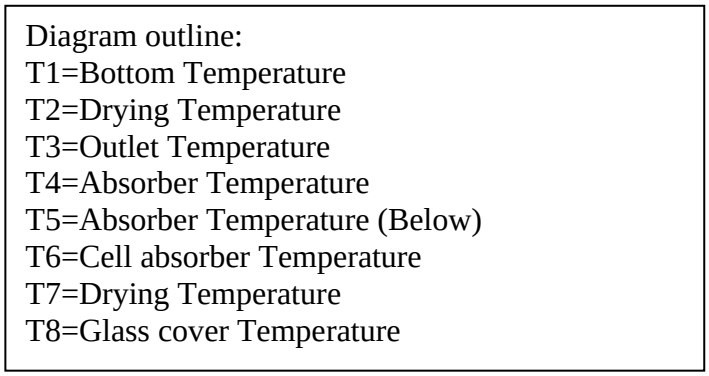

Figure 3.18: Temperature sensor location

3.11.3 EVALUATION OF ALUMINUM CELL WITH ALUMINUM (ABSORBER BASE)

Figure 3.18 shows the setup for aluminium absorber base with the solar thermal collector. The flat base plate absorber is Aluminium, and the thickness is 0.5 mm, and the weight is 73 g. The absorber base area is 0.18 m in width and 0.245 m in length. The area of aluminium cell is 0.01 m in width and 0.01 m in length. The aluminium cell is attached at the top of aluminium absorber (absorber base). The aluminium cell thickness used is 0.5 mm, and the total weight is 95 g, respectively. For aluminium cell thickness of 1.0 mm, the total weight is 102 g.

3.11.4 EVALUATION OF STAINLESS-STEEL CELL WITH ALUMINUM (ABSORBER BASE)

Figure 3.18 (a) and (b) show the experimental setup for aluminum base absorber with a stainless-steel cell solar thermal collector. The base flat plate absorber is aluminium and the thickness is 0.5 mm, and the weight is 73 g. The absorber base area is 0.18 m in width and 0.245 m in length. The area of the stainless-steel cell is 0.01 m in width and 0.01 m in length. The stainless-Steel cell is attached at the top of aluminium absorber (absorber base). The stainless-steel cell thickness used is 0.5 mm, and the total weight is 115 g, respectively. For stainless steel thickness of 1.0 mm, the total weight is 148 g.

3.12 OUTDOOR EXPERIMENT FOR FLAT PLATE SOLAR COLLECTOR (FPSC) AND FLAT PLATE BASE-THERMAL CELL ABSORBER (FPBTCA)

Figure 3.19 shows the outdoor experiment set-up for FPBTCA and FPSC. The experiment was done at Pelindung Damai, 26100 Beserah, Kuantan, Pahang Darul Makmur.

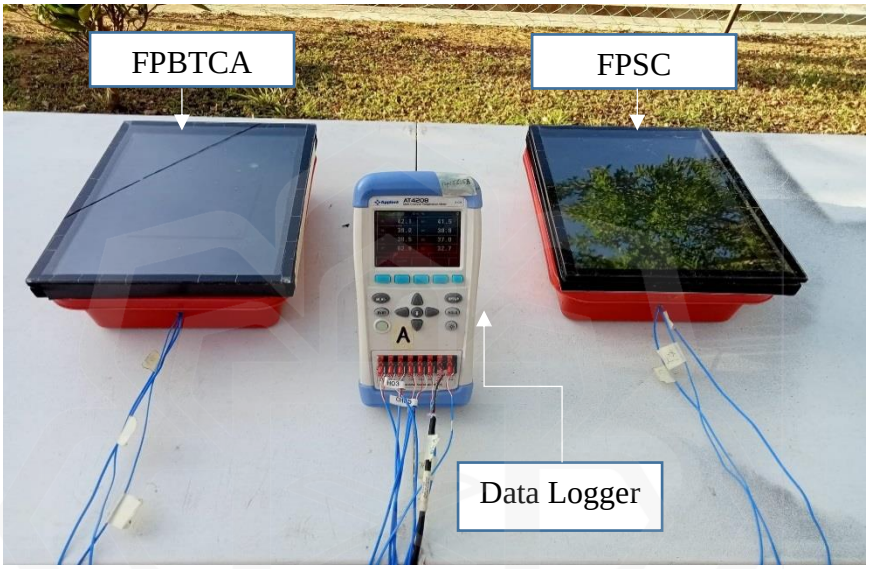

Figure 3.169: Experiment set-up for FPBTCA and FPSC.

3.12.1 METHOD TO EVALUATE THE FLAT PLATE SOLAR COLLECTOR (FPSC)

Figure 3.20: a) Top view b) Side view of FPSC for the experiment configuration. Aluminum material is used for flat plate absorber collectors. The flat plate absorber collector width is 18.5 cm, and the length is 25.5 cm. There are three temperature sensors used in this experiment which are T1, T2, and T3. T1 is the temperature sensor at the centre of the flat plate absorber collector. T2 is the temperature sensor located at the side of the flat plate absorber collector. While T3 is the temperature sensor placed at the dummy load.

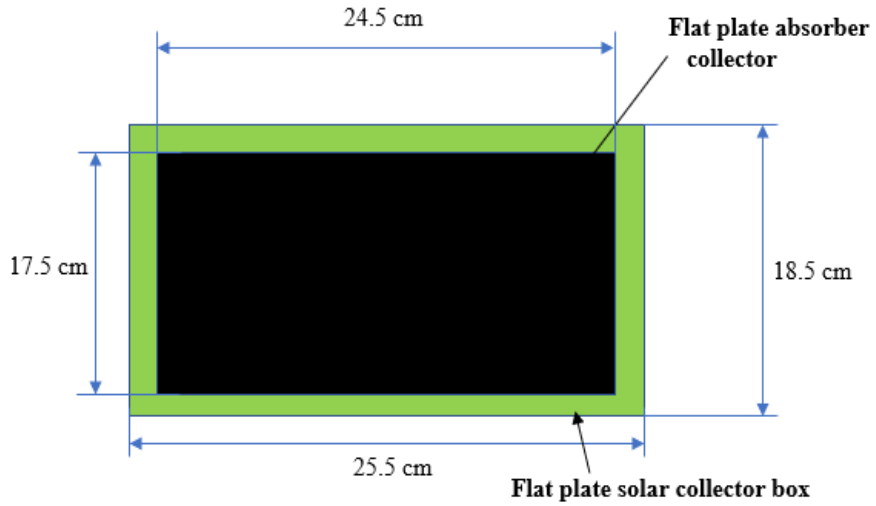

a) Top view

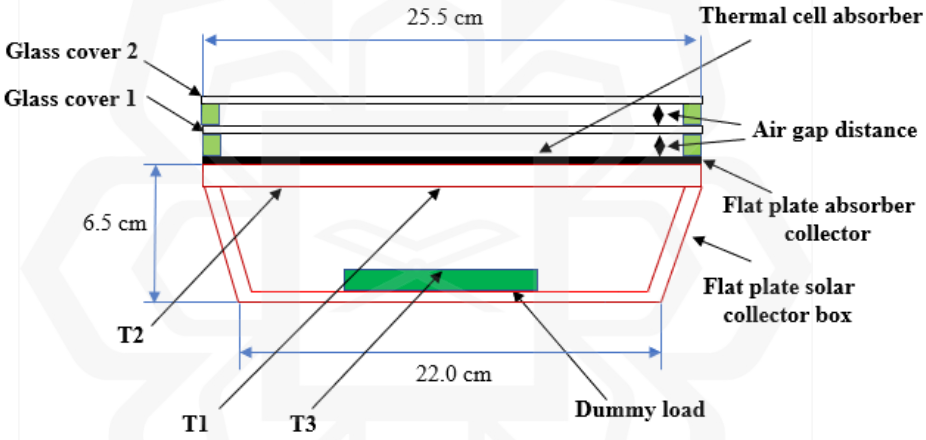

a) Side view

Figure 3.20: a) Top view b) Side view of FPSC

3.12.2 METHOD TO EVALUATE THE FLAT PLATE BASE-THERMAL CELL ABSORBER (FPBTCA)

Figure 3.21 shows the a) Top view b) Side view of FPBTCA for the outdoor experiment. Aluminium material is used as an absorber base-collector. The absorber base-collector's width is 18.5 cm, and the length is 25.5 cm. Stainless steel is used as a thermal cell and is placed at the top of the flat plate absorber collector. The thermal cell's width is 10.0 cm, and the length is 10.0 cm.

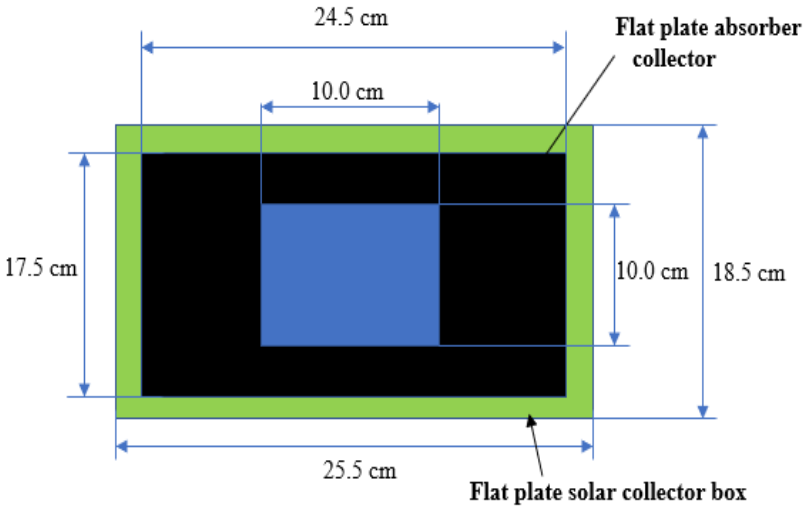

a) Top view of FPBTCA.

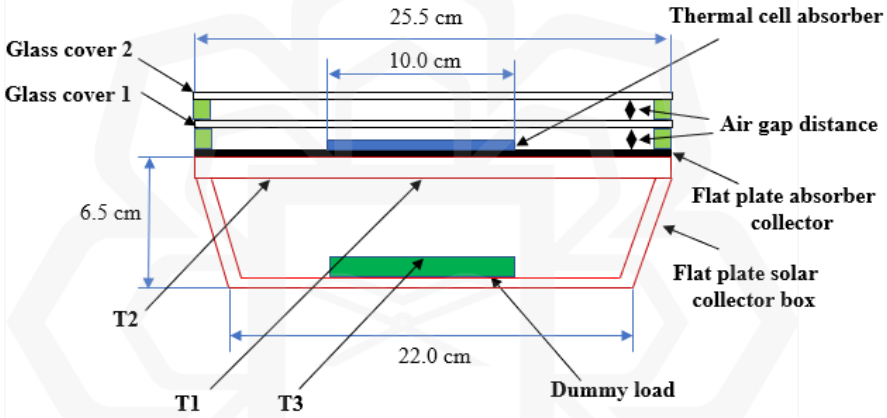

b) Side view

Figure 3.21: a) Top view b) Side view of FPBTCA

3.13 UNCERTAINTY ANALYSIS

The most important factor that should be determined in the process of recording the experimental data is uncertainty analysis. There are several factors that could affect the accuracy of the data taken from the experiment, such as the measurement apparatus. To ensure the data are recorded properly, uncertainty analysis was performed in this work to determine the measurement apparatus's reading accuracy and are at an acceptable condition. The measurement apparatus's are thermocouple, pyranometer, hot wire anemometer, and digital temperature sensor. For x_n number of measurements, each

reading has the tolerance of σ_n, and the uncertainty of the measurement parameters denoted by U_R can be calculated using the following expression (Yahya et al., 2017):

$$U_R = \sqrt{\left(\frac{U_R}{dx_1}\sigma_1\right)^2 + \left(\frac{U_R}{dx_2}\sigma_2\right)^2 + \left(\frac{U_R}{dx_3}\sigma_3\right)^2 + \cdots + \left(\frac{U_n}{dx_n}\sigma_n\right)^2} \quad 3.1$$

Table 3.4 shows the uncertainty of the evaluation of the parameters used in this study. There are four types of parameters involved in this experiment which are outer temperature, internal temperature, ambient temperature, and solar radiation. The uncertainty was used as guidance in this study to evaluate the data from the experiment.

Table 3.4: Uncertainty of the important parameters

Description	**Unit**	**Uncertainty**	**Relative uncertainty**
Outer temperature	℃	±0.10	0.48
Internal temperature	℃	±0.15	0.72
Ambient temperature	℃	±0.5	1.93
Solar radiation	W/m^2	±7.75	0.99

3.14 ENERGY BALANCE OF FLAT PLATE BASE-THERMAL CELL ABSORBER (FPBTCA)

Heat can be defined as the energy which could be transferred from one system to another if there is a temperature difference that exist in the system. Heat is the transfer from one equilibrium state to another state. The energy balance of the system could be derived from equation (3.2).

$$\dot{E}_{in} - \dot{E}_{out} = \frac{dE_{system}}{dt} \quad 3.2$$

There are several assumptions that should be considered to describe the behaviour of the FPBTCA. The below assumptions simplify the complexity with minimum error (Duffie, J. A., & Beckman, 1991):

a. Temperature gradient through the cover is negligible
b. There is one-dimensional heat flow through the back and side insulation and through the cover system
c. There is no absorption of solar energy by cover
d. There is a negligible temperature drop through the cover
e. The cover is opaque to infrared radiation
f. The sky can be considered a blackbody for long-wavelength radiations at an equivalent sky temperature
g. The temperature gradient in the direction of flow and between the tubes can be treated independently
h. Properties are independent of temperature
i. Loss through front and back are to the same temperature
j. Dust and dirt on the collector are negligible
k. Shading of the collector absorber plate is negligible
l. The collector is assumed as a short collector (Less than 10 m) (Fudholi et al., 2008)

Figure 3.4 shows the energy balance diagram of Flat Plat Base-Thermal Cell absorber (FPBTCA). The layer structure of heat transfer is Glass 1, Glass 2, Thermal cell, Absorber base, Dummy load and Bottom.

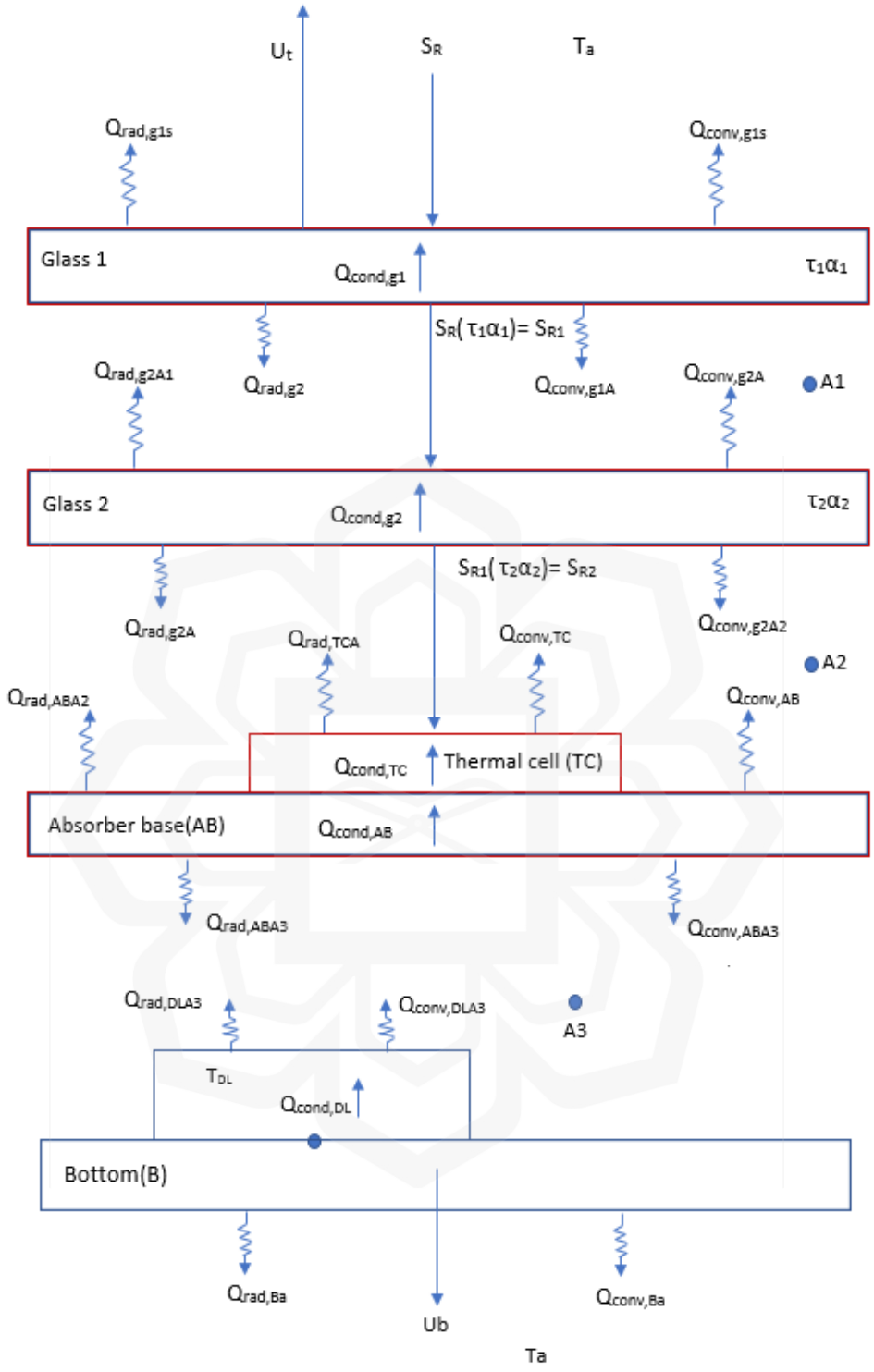

Figure 3.22: Energy balance diagram for FPBTCA

Energy balance for glass glass 1,

Energy in to the glass glass 1= Energy out of glass glass 1

$$S_R\tau_g\alpha_g + \dot{Q}_{rad,g1A1} + \dot{Q}_{conv,g1A1} = \dot{Q}_{rad,g1s} + \dot{Q}_{conv,g1s} + \dot{Q}_{cond,g1} \quad 3.3$$

Energy balance for glass glass 2,

Energy in to the glass glass 2= Energy out of glass glass 2

$$S_{R1}\tau_g\alpha_g + \dot{Q}_{rad,g2A2} + \dot{Q}_{conv,g2A2} = \dot{Q}_{rad,g2A1} + \dot{Q}_{conv,g2A1} + \dot{Q}_{cond,g2} \quad 3.4$$

Energy balance for thermal cell absorber,

Energy in to the thermal cell absorber= Energy out of thermal cell absorber

$$S_{R2}\tau_g\alpha_p = \dot{Q}_{rad,TCA2} + \dot{Q}_{conv,TCA2} + \dot{Q}_{cond,TC} \quad 3.5$$

Energy balance for base absorber,

Energy in to the base absorber = Energy out of base absorber

$$S_{R2}\tau_g\alpha_p + \dot{Q}_{rad,ABA3} + \dot{Q}_{conv,ABA3} = \dot{Q}_{rad,ABA2} + \dot{Q}_{conv,ABA2} + \dot{Q}_{cond,AB} \quad 3.6$$

Energy balance for dummy load,

Energy in to the dummy load = Energy out of dummy load

$$\dot{Q}dummy = \dot{Q}_{rad,DLA3} + \dot{Q}_{conv,DLA3} + \dot{Q}_{cond,DL} \quad 3.7$$

Energy balance for bottom,

Energy in to the bottom = Energy out of bottom

$$U_b = \dot{Q}_{rad,Ba} + \dot{Q}_{conv,Ba} \quad 3.8$$

$$Ut = \dot{Q}_{rad,g1s} + \dot{Q}_{conv,g1s} \quad 3.9$$

$$UTotal = Ut + Ub + Ue \quad 3.10$$

3.14.1 HEAT TRANSFER LOSS

There are three separate components which is the top loss coefficient, the bottom loss coefficient, and the edge loss coefficient in overall heat transfer loss in solar collector system. The empirical relations for these coefficients are shown (Duffie, J. A., & Beckman, 1991) below:

$$UTotal = Ut + Ub + Ue \quad 3.11$$

Regarding equation 3.13, Ut is the heat loss coefficient at the top, Ub is the heat loss coefficient at the bottom, and Ue is the heat loss coefficient at the edges of the solar collector. Based on the condition, it can be simplified that the solar energy absorbed by the absorber plate collector is distributed to useful heat gain and also thermal losses through the top, bottom, and edges.

The energy loss through the back of the collector is due to the resistance to heat flow through the insulation, U_b, therefore,

$$\text{Ub} = \frac{k}{z} \quad 3.12$$

Based on equation 3.14, k is the insulation of thermal conductivity (W/m.℃), and z is insulation thickness (m).

3.14.2 HEAT STORAGE CAPABILITY

Basically, the physical parameter of the absorber plate collector is determined by total surface areas and total mass. The design and arrangement of the absorber plate collector affects the performance of the solar collector. Heat storage is sensitive to the change in the storage material temperature (Cengel, 2007). The energy that can be used as heat storage material can be calculated by using the energy balance equation below.

$$Q_{12} = \rho V \int_{T1}^{T2} c_p\,(\text{T})\text{dT} \;=\; \text{m} \int_{T1}^{T2} c_p\,(\text{T})\text{dT} \quad 3.13$$

Regarding equation 3.15, Q_{12} is heat energy stored in the material. T_2 is denoted as the temperature at the end of the thermal energy absorbing process, and T_1 is the initial temperature. Based on the equation, the thermal mass, m, which is related to density ρ and volume, V of material is correlated linearly with the total energy storage.

3.14.3 THE PROCESS OF THEORETICAL SOLUTION

The process of theoretical solution was applied to solve the energy balance equation of the FPBTCA. Basically, the main heat transfer interactions between nodes in the collector are fundamentally based on a one-dimensional form. The energy balance equation was used as the linear equation to predict the model of FPBTCA. The heat loss values will be numerically determined by using the iteration approach. After that, once the new heat loss is found, the energy balance equations given can be used.

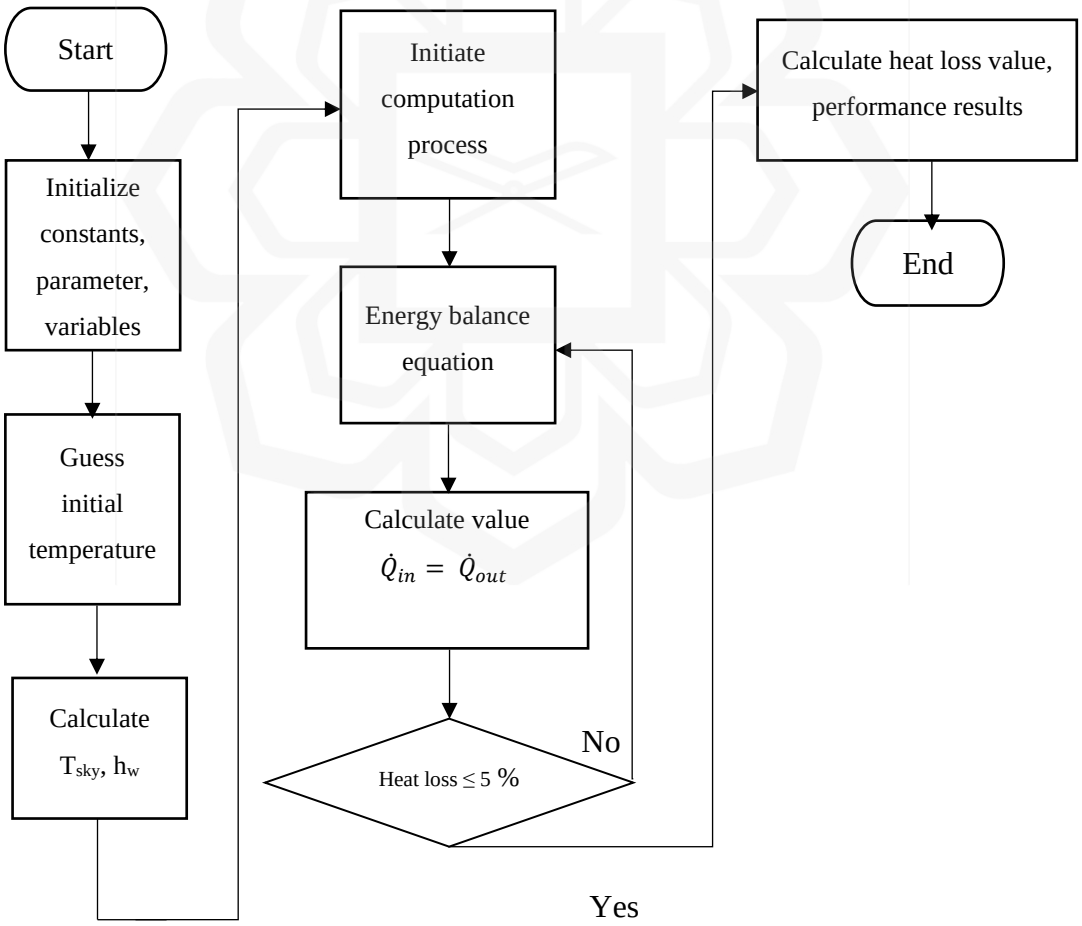

Figure 3.5: Flowchart for theoretical solution process

Microsoft Excel® software is used for solving the equation, including the iteration. The flowchart for the theoretical solution process is outlined in Figure 3.5. Before applying the initial process, there are required constant parameters that should be determined. The parameters are solar radiation, ambient temperature, optical properties of the glazing and the thermal absorber, thermophysical of the air, and physical dimension of the solar collector. Then, the temperature of the main node, including glazing 1, glazing 2, thermal cell absorber, base absorber, and bottom plate temperature, are initially predicted.

Energy balance equations were developed based on the FPBTCA heat transfer diagram. After that, the calculation of the new heat loss value was determined until the new and old heat loss was equal to/or less than 5 %. The obtained temperature value, which meets the process criteria, will then be used to compute the performance parameters of the FPBTCA.

3.15 CHAPTER SUMMARY

This chapter illustrates the detailed methodology applied in the theoretical solution process. The performance of FPBTCA was done through outdoor experiments. The mathematical model evaluation was also deliberated in this chapter. These performance parameters are calculated and validated, with their results presented in the next chapter.

This chapter presented the methodology of the experiment involved in the research. Based on the flowchart, the research is divided into two stages: indoor and outdoor experiment. The indoor experiment was done to determine the suitable design parameter that can be used to design a flat plate base-thermal cell absorber (FPBTCA). The outcome of the results was used to fabricate a flat plate base-thermal cell absorber (FPBTCA). Then, the outdoor experiment was conducted to carry out the performance comparison between flat plate solar collector (FPSC) and flat plate base-thermal cell absorber (FPBTCA). The modelling is done to compare the heat transfer between the experiment and mathematical modelling.

CHAPTER FOUR

RESULTS AND DISCUSSION

4.1 INTRODUCTION

This chapter presents the results obtained from the research experiment based on a flat plate solar collector (FPSC) and flat plate base-thermal cell absorber (FPBTCA). The experimental setup was done under artificial solar radiation and outdoor solar radiation. A discussion of the findings also has been carried out.

4.2 EVALUATION OF DESIGN PARAMETER

4.2.1 THERMAL ANALYSIS

Thermal analysis is an important factor in evaluating the performance of Flat Plate Solar Collectors. The analysis is focused on the absorber collector of the Flat Plate Solar Collector.

The heat transfer rate of the thermal absorber storage can be obtained from Equation 4.1 (Duffie, J. A., & Beckman, 2013):

$$Q_{Store} = \frac{m_{ab} C_{p(ab)} (T_2 - T_1)}{t_2 - t_1} \quad 4.1$$

where,

m_{ab}	=	mass of thermal absorber (kg)
$C_p(ab)$	=	specific heat of thermal absorber (kJ/kgK)
T_2	=	temperature of thermal absorber after heat gain (K)
T_1	=	temperature of thermal absorber before heat gain (K)
t_2	=	time after heat gain (s)
t_1	=	time before heat gain (s)

4.2.2 MATERIALS COMPARISON

Figure 4.1 shows the flat plate absorber temperature versus time for different flat plate absorber materials. The flat aluminum plate absorber-collector responds more rapidly in charging behavior than the stainless steel 304 flat plate absorber. The aluminum and stainless-steel flat absorbers have similar values of maximum temperature which is 66 °C at t = 600 seconds. Stainless steel has a lower temperature drop than aluminum flat plate absorber-collector in a discharging condition. Aluminum material has higher thermal conductivity and is a good heat reflector than stainless steel. It also could be used as an absorber base-collector. Based on the thermal conductivity advantages, it can rapidly transfer heat from the absorber surface to the drying chamber. Aluminum has a high reflectivity, which helps to maximize the amount of sunlight absorbed by the collector. Aluminum also is lightweight compared to stainless steel and could reduce the weight of flat plate solar collectors. Aluminum is a relatively low-cost material, making it a cost-effective choice for solar thermal systems. Aluminum is resistant to corrosion, making it a durable choice for outdoor applications.

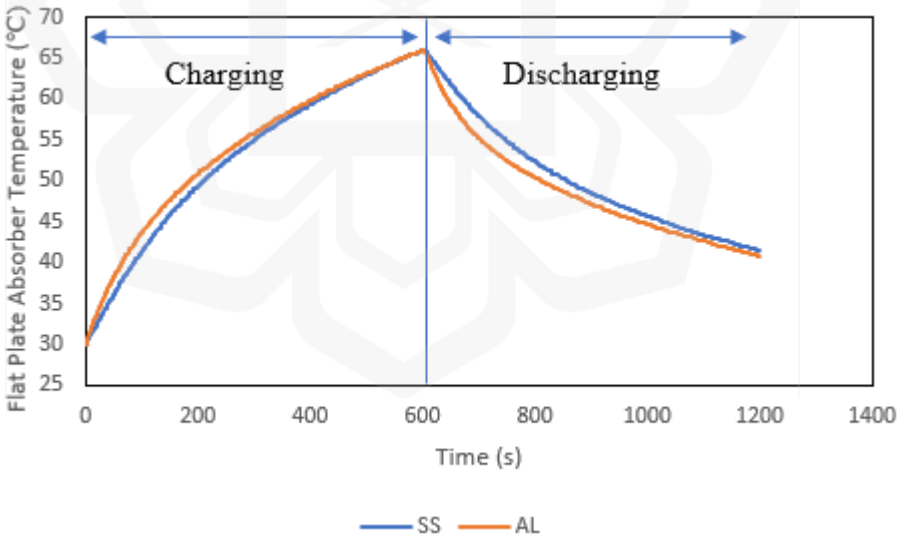

Figure 4.1: Flat plate absorber temperature versus time for different flat plate absorber materials

Table 4.1 summaries the heat gain rate of different flat plate absorber-collector materials. The results show that aluminum and stainless-steel flat plate absorber collectors have similar heat gain rate values which is 0.06 ℃/s. Stainless steel flat plate absorber-collector has more advantages during discharging period, possessing more heat storage capability than aluminum flat plate absorbers. The stainless-steel flat plate absorber-collector is chosen as the thermal cell absorber collector. The heat gain rate is an important factor that should be considered when the absorber collector is exposed to solar radiation. The increase in solar radiation of the solar collector could affect the heat gain rate absorbed by the absorber collector. The heat gain rate is proportional to the increase in solar radiation.

Table 4.1: Flat plate absorber temperature versus time for different flat plate absorber materials

Materials	Heat gain rate (˚C/s) (±0.002)	Maximum absorber temperature (˚C) (±0.01)
Aluminium	0.06	66.0
Stainless Steel	0.06	66.0

Figure 4.2 shows heat charging/heat discharging capacity versus different flat plate absorber materials. Stainless steel 304 flat plate absorber-collector has a higher heat charging capacity (with a value of 4653.61 J) than Aluminum flat plate absorber capacity (with a value of 3283.31 J). Stainless steel 304 flat plate absorber also has the highest total heat gain, which is 1499.50 J. Aluminum flat plate absorber collector has the lowest total heat gain at just 984.99 J. This result signifies that stainless steel has high energy storage and could be used favorably with fluctuations in solar radiation. Stainless steel is selected as a thermal cell absorber as the focus is to store heat and could be used in the absence of solar radiation. Stainless steel is highly resistant to rust and corrosion, making it ideal for harsh environments or exposure to moisture or chemicals. It is a strong and durable material that can withstand high stress and heavy use, making it ideal for products that need to last a long time. It is easy to clean and

maintain, requiring little to no special treatment to keep it looking new. Stainless steel is a recyclable material, making it an environmentally friendly product choice. It has a smooth surface that does not harbor bacteria or other microorganisms, making it a popular choice for use in medical, food and beverage, and hygiene-sensitive applications.

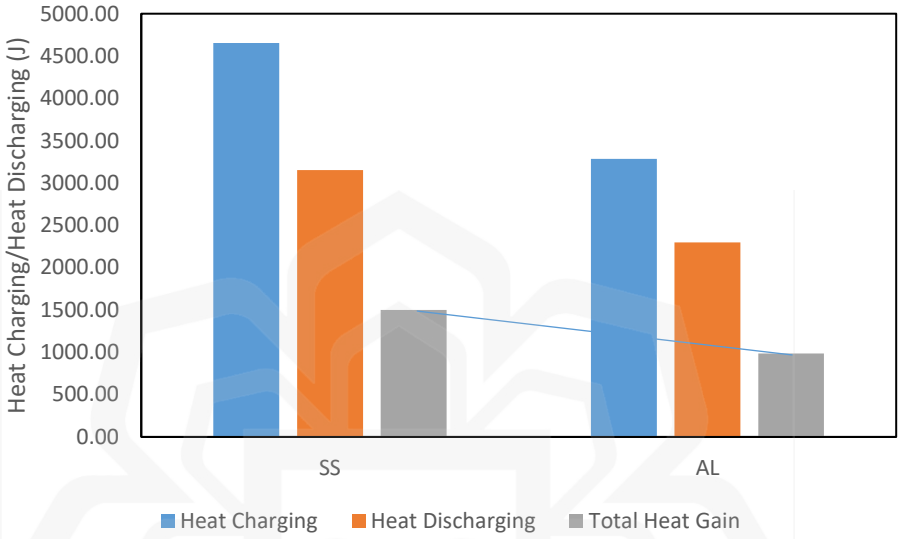

Figure 4.2: Heat charging/ heat discharging versus different flat plate absorber material

4.2.3 COATING SURFACE COMPARISON

Figure 4.3 presents the flat plate absorber temperature versus time for the coated and non-coated aluminum surfaces. A significant effect on the flat plate absorber temperature was noted on the surface coated with black paint. Based on the results, the aluminum-coated plate showed a fast response to the charging process and indicated the highest temperature for the flat plate absorber was 85.8 ℃ at t = 300 seconds. The non-coated aluminum plate has a maximum flat plate absorber temperature of 68.4℃ at t = 300 seconds. During the discharging period, the aluminum-coated plate has a higher temperature drop than non-coated aluminum, and this depends on the ambient temperature and initial max temp. Coated surfaces are more resistant to wear, tear, and corrosion, thus increasing the lifespan of the surface. Coated surfaces require less maintenance compared to uncoated surfaces, as they are more resistant to dirt, grime, and other contaminants.

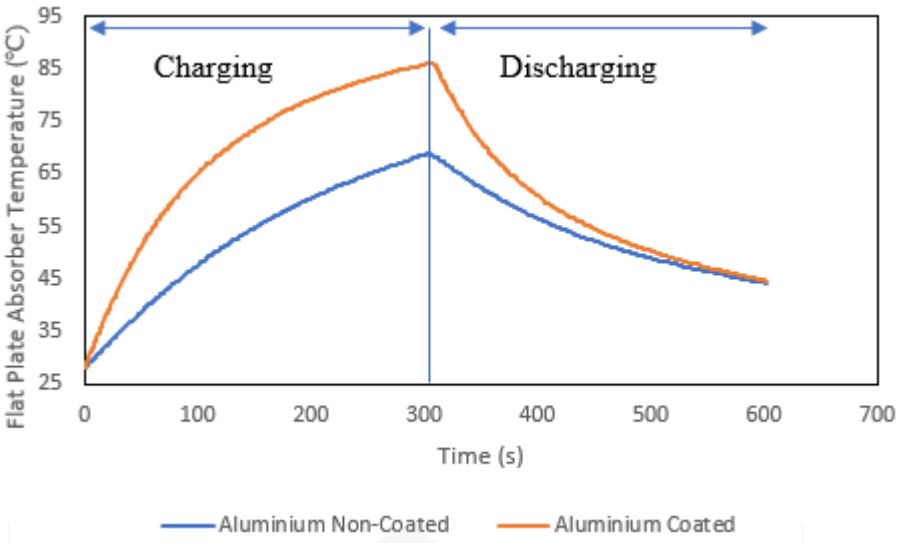

Figure 4.3: Flat plate absorber temperature versus time for Aluminum coated and non- coated surface

Table 4.2 shows the summary of the heat gain rate of coated aluminum and non-coated aluminum for flat plate absorber-collector material. The results shows that coated aluminum with matt black paint has a higher heat gain rate of 0.192 ℃/s than non coated aluminium (0.136 ℃/s). It can be concluded that coated aluminum has absorbed higher heat energy than non-coated aluminum. Solar radiation significantly affected the performance of the coated and non-coated surfaces. Coatings can protect surfaces from harmful ultraviolet rays, moisture, and other environmental factors, preserving the surface and extending its lifespan. Coatings can be used to improve the aesthetics of a surface, giving it a polished and attractive look. Coatings can be used to increase the safety of a surface by providing better traction, reducing the risk of slips and falls, and preventing the spread of fire or bacteria. The flat plate absorber-collector surface should be coated with a matt black coating to absorb high heat energy rate from solar radiation. There are greater differences in maximum absorber temperature between coated aluminum and non coated aluminum, which is 17.4 C. It can be concluded that coated aluminum contributed to the thermal performance of flat plate solar collectors.

Table 4.2: Summary of heat gain rate and heat discharge rate of coated aluminum and non-coated aluminum

Materials	Heat gain rate (℃/s)	Maximum absorber temperature (℃)
Coated Aluminum coated	0.192	85.8
Non-coated Aluminum	0.136	68.4

4.2.4 GLASS THICKNESS COMPARISON

Figure 4.4 shows the temperature behavior for different glass thicknesses. The results show that the flat plate absorber temperature configuration for 2.0 mm glass thickness has increased rapidly during the charging period. The flat plate absorber-collector of 2.0 mm glass thickness reached a maximum temperature of 88.1°C at t = 600 seconds. The maximum temperatures of the flat plate absorber for glass thickness of 3.0 mm, 4.0 mm, 5.0 mm, and 10 mm gain temperature are 81.6 °C, 82.6 °C, 78.6 °C, and 70.5 °C, respectively, at t = 600 seconds. Using different thicknesses of glass could contribute to the thermal performance of solar collectors. When the glass thickness is increased, then the temperature of the absorber also decreases.

Basically, for most installations, the following glass properties should be evaluated such as color and appearance, visible light transmission and reflection (from both sides), solar transmission (Solar Heat Gain Coefficient) and absorption, thermal and acoustic insulation, and also strength. When the thickness is lower, solar radiation could transmit more heat energy through the glass. The handling should be considered when using a low thickness of glass thickness as a glass cover in a solar collector. The cost of using low glass thickness has also reduced other glass thickness configurations.

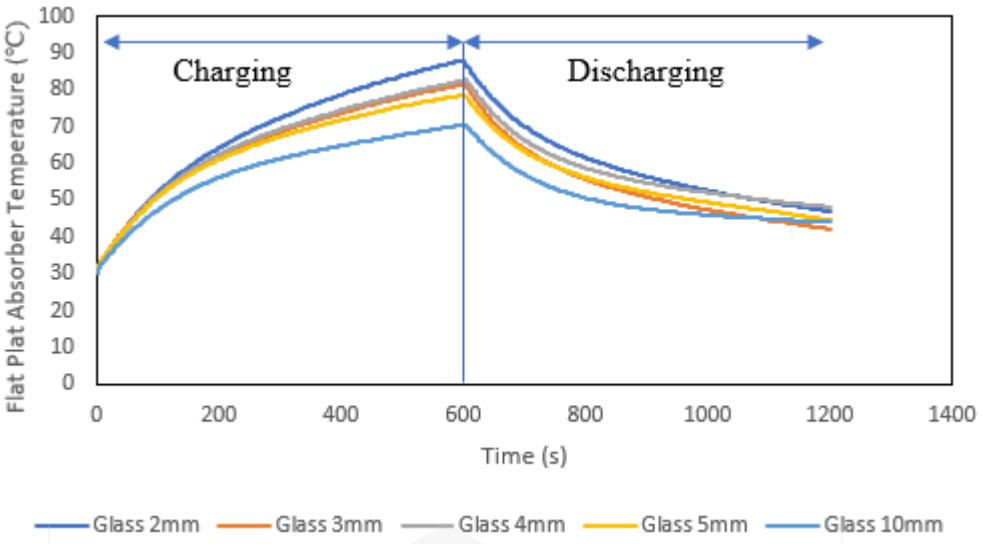

Figure 4.4: Flat plate absorber temperature versus time for different glass thicknesses

Table 4.3 summaries the heat gain rate of different glass thicknesses. Glass thickness of 2.0 mm has a higher heat gain rate (0.097 ℃/s) than other glass thickness configurations. The heat gain rate for glass thickness of 3.0 mm, 4.0 mm, 5.0 mm, and 10.0 mm is 0.083 ℃/s, 0.087 ℃/s, 0.078 ℃/s, and 0.067 ℃/s, respectively. It can be concluded that during the charging period for flat plate absorber-collector with glass thickness 2.0 mm absorbs high heat energy than other glass thicknesses. The capability of 2.0 mm glass thickness provides more advantages to trap heat loss from the flat plate absorber-collector. Thicker glass can provide greater insulation, making it more energy efficient. Thicker glass also generally has a higher thermal mass, which means it can absorb and store more heat.

Table 4.3: Summary of heat gain rate of different glass thicknesses

Glass Thickness (mm)	Heat gain rate (˚C/s)	Maximum absorber temperature (˚C)
2.0	0.097	88.1
3.0	0.083	81.6
4.0	0.087	82.6
5.0	0.078	78.6
10.0	0.067	70.5

Figure 4.5 presents the heat charging/heat discharging capacity versus glass thickness. The glass thickness of 2.0 mm has a higher heat charging capacity than other configurations at 3922.13 J. The lower heat charging occurs with a glass thickness of 10.0 mm, at 2632.94 J. Glass thickness of 2.0 mm has the highest total heat gain which is 1207.33 J compared to other configurations. It can be concluded that by increasing the glass thickness, the total heat gain will be reduced (Ismail & Henr, 2003). The 2.0 mm thick glass also has higher transmittance than other configurations. The flat plate absorber-collector can absorb high heat energy from solar radiation. The 2.0 mm thick glass is selected as the glass cover of the Flat Plate Base-Thermal Cell Absorber (FPBTCA)

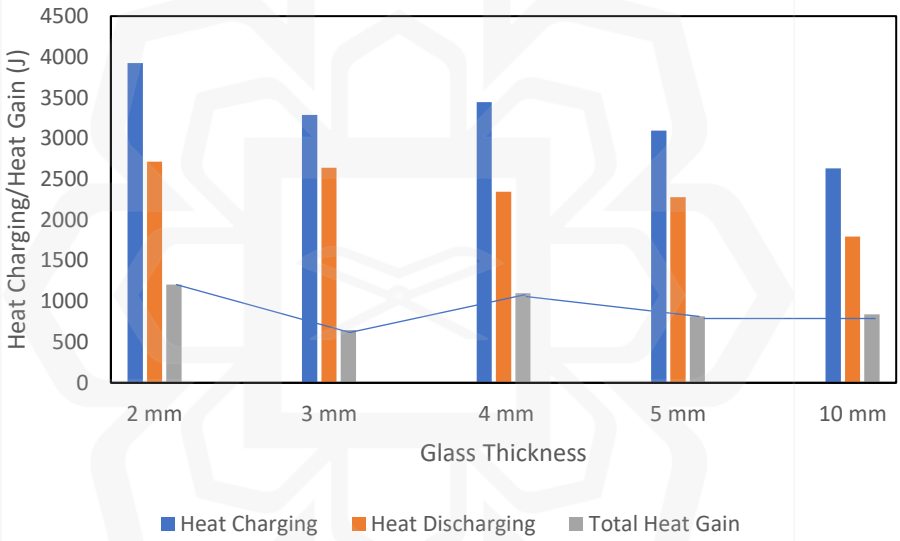

Figure 4.5: Heat charging/ heat discharging versus glass thickness

4.2.5 AIR GAP THICKNESS (BETWEEN FLAT PLATE ABSORBER COLLECTOR AND GLASS)

The parameters used in this experiment for the air gap thickness are 0, 5.0, 10.0, 20.0-, and 30.0-mm. Figure 4.6 shows the air gap thickness temperature behavior in the flat plate absorber collector. During the initial stage of the charging period, the flat plate absorber temperature for an air gap distance of 10.0 mm increased rapidly. The air gap distance achieved a maximum temperature of 64.6 °C at t = 600 s. The 0, 5.0, 20.0, and

30.0 mm air gap distance showed the maximum flat plate absorber temperature of 59.1 °C, 62.4 °C, 60.9 °C, 60.6 °C at t = 600 seconds. The temperature drop for an air gap thickness of 10.0 mm is slightly higher for the discharging period than for other air gap thickness configurations. It can be concluded that the flat plate absorber-collector temperature varies with different configurations of air gap thickness (Ferahta et al., 2011). The air gap acts as an insulation, reducing heat loss and increasing the efficiency of the solar collector. The air gap distance is one of the factors that determines the thermal performance of the solar collector. A larger air gap distance leads to higher insulation and greater efficiency but also results in a lower temperature difference between the absorber plate and the cover glass. In order to optimize the thermal performance of a solar collector, it is important to find the right balance between the air gap distance and other factors, such as the absorber plate material, the cover glass type, and the glazing angle. For example, using a low-emissivity (low-E) glass with a high transmissivity can improve the performance of the solar collector even with a smaller air gap distance.

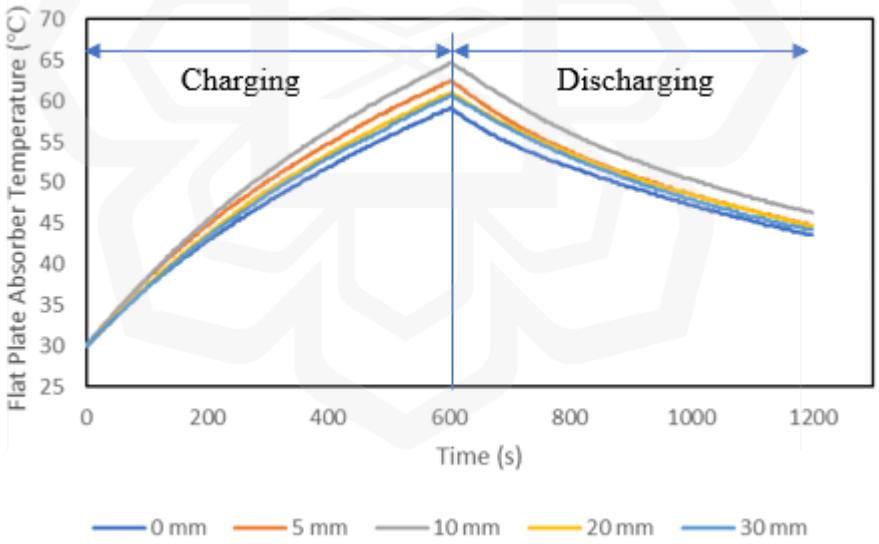

Figure 4.6: Flat plate absorber temperature versus time for air gap space between flat plate absorber and glass

Table 4.4 summaries the heat gain rate of air gap space between the absorber and glass. The air gap space of 10.0 mm has a higher heat gain rate (0.058 ℃/s) than other air gap configurations. The heat gain rate for 0, 5.0, 20.0-, and 30.0-mm air gap thickness yield values of temperature increase of 0.049 ℃/s, 0.054 ℃/s, 0.052 ℃/s, and 0.051 ℃/s, respectively. Air gap space of 10.0 mm shows the optimum performance in terms of charging period for flat plate absorber-collector to gain high heat energy from solar radiation. Hence, 10.0 mm air gap thickness is selected as the optimum design parameter for FPBTCA. The air gap distance can also be influenced by environmental factors, such as wind and atmospheric pressure, which can affect the airflow within the gap. A proper design of the solar collector should take these factors into account and include features such as airflow channels or venting systems to maintain a stable air gap distance and prevent air pockets from forming.

Table 4.4: Summary of heat gain rate and heat discharge rate of air gap distance between flat plate absorber and glass

Gap distance (mm)	Heat gain rate (℃/s)	Maximum absorber temperature (℃)
0	0.049	59.1
5.0	0.054	62.4
10.0	0.058	64.6
20.0	0.052	60.9
30.0	0.051	60.6

Figure 4.7 shows the heat charging/heat discharging capacity versus the air gap thickness between the absorber and glass. The highest heat charging capacity occurs when the air gap distance is 10.0 mm, at 6770.06 J. Meanwhile, the lowest heat charging is noted at an air gap thickness of 0 mm, which is 5641.72 J. The highest total heat gain is 4750.92 J at an air gap thickness of 10.0 mm. It can be concluded that an air gap thickness of 10.0 mm between the flat plate absorber and glass, stores high heat energy in the flat plate absorber collector than in other configurations. An air gap distance of 10.0 mm is selected as the air gap in FPBTCA. In conclusion, the air gap distance is a crucial element in the design of a solar collector. By optimizing the air gap distance and other factors, it is possible to improve the thermal performance and efficiency of the solar collector, increasing the overall effectiveness of solar energy systems.

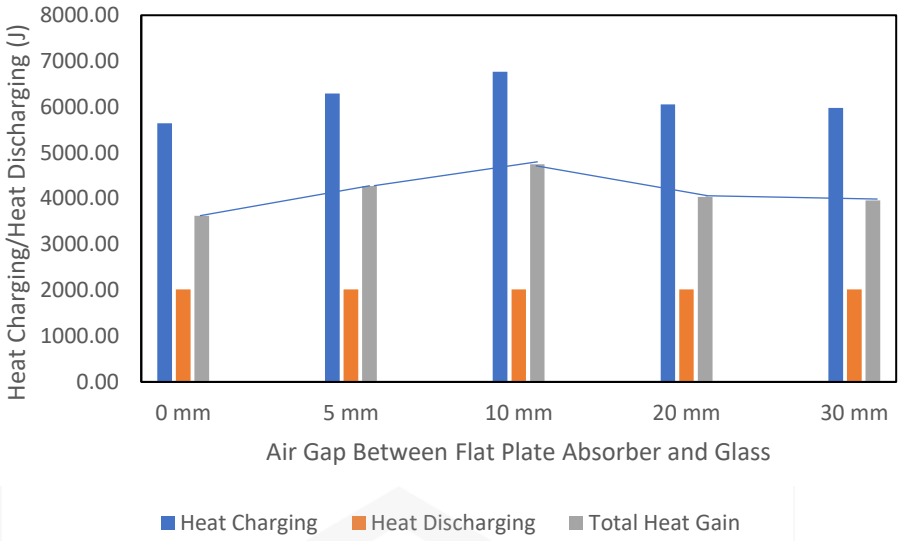

Figure 4.7: Heat charging/ heat discharging versus air gap between absorber-collector and glass

4.2.6 FLAT PLATE SOLAR THERMAL CELL ABSORBER

Figure 4.8 presents the stainless steel 304 flat plate absorber temperature versus time for different flat plate thermal cell absorbers. The results show that the stainless-steel flat plate absorber-collector temperature with 1.0 mm thickness changed rapidly during the charging period. The 1.0 mm stainless steel plate has a higher flat plate absorber-collector temperature of 76.2 ℃ at t = 600 seconds. Meanwhile, the maximum temperature of flat plate absorber temperature at t = 600 seconds for the 0.5 mm thickness is 68.6 ℃ and 66 ℃ for the 2.0 mm thickness. Solar radiation affects the thermal performance of solar collectors in terms of absorber collector temperature. Stainless steel material is advantageous as it is a good conductor of heat, which makes it an excellent material for use in absorber collectors.

The metal's high thermal conductivity helps to quickly and efficiently transfer the captured solar energy to the absorber base-collector that is being heated. This helps to improve the overall efficiency of the solar collector and reduces the time it takes to heat up the absorber base-collector. One of the main advantages of using stainless steel in solar collectors is its excellent corrosion resistance. Stainless steel can withstand exposure to various environmental elements, including rain, snow, and high

temperatures, making it an ideal material for outdoor applications. Solar collectors are often exposed to the elements, and using a material that is resistant to corrosion helps to ensure the longevity and reliability of the system. Stainless steel is also known for its durability, which makes it a popular choice for solar collectors. The material is strong, hard-wearing, and can withstand high pressure, making it ideal for high-stress applications. Solar collectors are subjected to high temperatures and pressure changes, and the use of stainless steel helps to ensure that the collector remains functional for a long time.

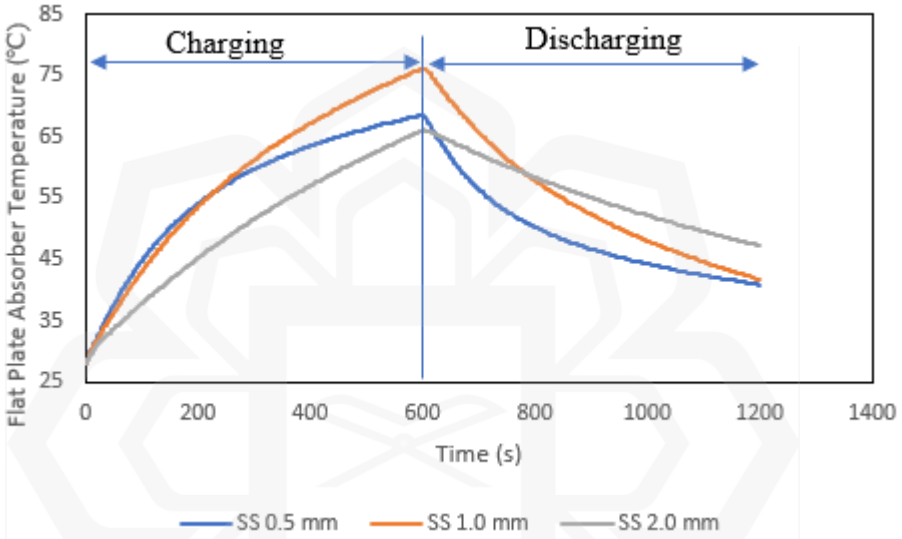

Figure 4.8: Flat plate absorber temperature versus time for different Stainless Steel 304 flat plate thermal cell absorber

Table 4.5 summaries the heat gain rate of different Stainless Steel 304 flat plate thermal cell absorbers. The flat plate thermal cell absorber of 1.0 mm thickness has a higher heat gain rate which is 0.080 ℃/s compared to other configurations. The heat gain rate for the flat plate thermal cell absorber of 0.5 mm and 2.0 mm thickness is 0.067 ℃/s and 0.063 ℃/s. Stainless steel 1.0 mm absorbs high heat energy during the charging period than other configurations. Based on the results, the thickness of 1.0 mm is preferred as the flat plate thermal cell absorber for FPBTCA. In conclusion, stainless steel is an excellent material for use in solar collectors. Its corrosion resistance, durability,has high thermal conductivity, and aesthetic appeal makes it an ideal choice for solar energy applications.

Table 4.5: Summary of heat gain rate of different Stainless Steel 304 flat plate thermal cell absorber

SS thickness (mm)	Heat gain rate (˚C/s)	Maximum absorber temperature (˚C)
0.5	0.067	68.6
1.0	0.080	76.2
2.0	0.063	66.0

4.2.7 FLAT PLATE ABSORBER BASE COLLECTOR

Aluminum flat plate absorber thicknesses of 0.5, 0.8, and 1.0 mm are used in this experiment. The experimental results are presented in Figure 4.9, showing the temperature behavior of different flat plate absorber thicknesses. During the initial stage of the charging period, the temperature of the aluminum 0.5 mm thickness increases rapidly. The pattern showed that a 0.5 mm absorber base collector has a significant effect on the change of solar radiation. The absorber plate is responsible for absorbing the solar radiation and converting it into heat energy, which is then transferred to the drying chamber through the collector. Meanwhile, the flat plate absorber base-collector of 0.5 mm achieves a maximum temperature of 67.2 °C at t = 600 seconds. In contrast, the plate thickness of 0.8 and 1.0 mm achieves a maximum temperature of 66.0 and 64.7 ℃, respectively, at t= 600 seconds.

A thicker absorber plate increases the heat storage capacity of the collector, but it also reduces the heat transfer rate due to the increased thermal resistance. On the other hand, a thinner absorber plate increases the heat transfer rate, but it also reduces the heat storage capacity. This indicates that the geometry of the flat plate absorber collector could affect the performance of the flat plate solar collector. When the solar radiation is increased, then the temperature of the absorber base-collector also increases. In general, the thickness of the absorber plate in a solar collector is chosen based on a trade-off between the heat transfer rate and heat storage capacity. The optimal thickness depends on the specific application, such as the desired operating temperature, the size of the collector, and the local climate conditions.

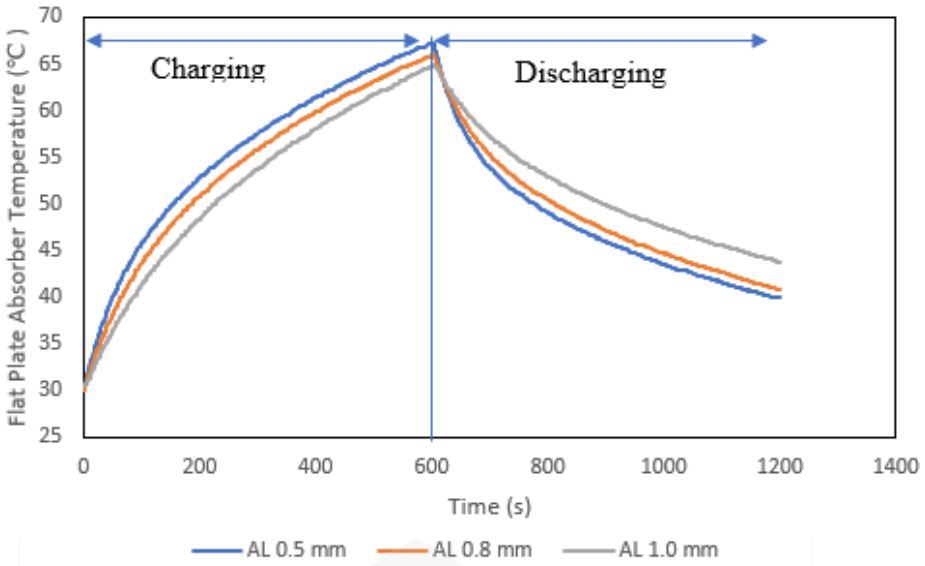

Figure 4.9: Flat plate absorber temperature versus time for different flat plate absorber base collector thicknesses

Table 4.6 summaries the heat gain rate of different flat plate absorber base-collector thicknesses. The heat gain rate for the aluminum flat plate absorber base of 0.5 mm thickness shows the highest temperature than other configurations, with the value of 0.062 ℃/s. Meanwhile, the heat gain rates for the aluminum flat plate absorber base-collector with 0.8 mm and 1.0 mm thickness are 0.060 ℃/s and 0.057 ℃/s. It shows aluminum 0.5 mm absorbed high heat energy during the charging period than other configurations, respectively. In conclusion, the thickness of the absorber plate in a solar collector plays a crucial role in determining the performance of the system. Careful consideration should be given to the material and thickness of the absorber plate to ensure optimal performance and efficiency. Aluminum, 0.5 mm thickness, is selected as the design parameter for FPBTCA.

Table 4.6: Summary of heat gain rate of different flat plate aabsorber base-collector thicknesses

Absorber thickness (mm)	Heat gain rate (℃/s)	Maximum absorber temperature (℃)
0.5	0.062	67.2
0.8	0.060	66.0
1.0	0.057	64.7

4.2.8 GLASS COVER COMPARISON

Figure 4.10 represents flat plate absorber temperature versus time for different glass cover comparisons. A solar collector with a double glass cover typically has two layers of glass that are separated by an air space. The double glass shows a higher flat plate absorber-collector temperature than the single glass, which is 76.3 ℃, at t= 600 seconds. The maximum temperature of flat plate absorber temperature at t = 600 seconds for a single glass configuration is 73.2 ℃. Double glass configuration also has a higher temperature drop than single glass.

The results also indicate that double glass as glass cover for flat plate solar collector could generate a lower top loss on heat transfer coefficient than single glass configuration (Vettrivel & Mathiazhagan, 2017). The double glass cover provides improved insulation, reducing heat loss and increasing the efficiency of the collector. The air space between the two layers of glass acts as an insulating layer, reducing the amount of heat lost through conduction and convection. This helps to maintain a higher temperature inside the collector, improving the overall performance of the system.

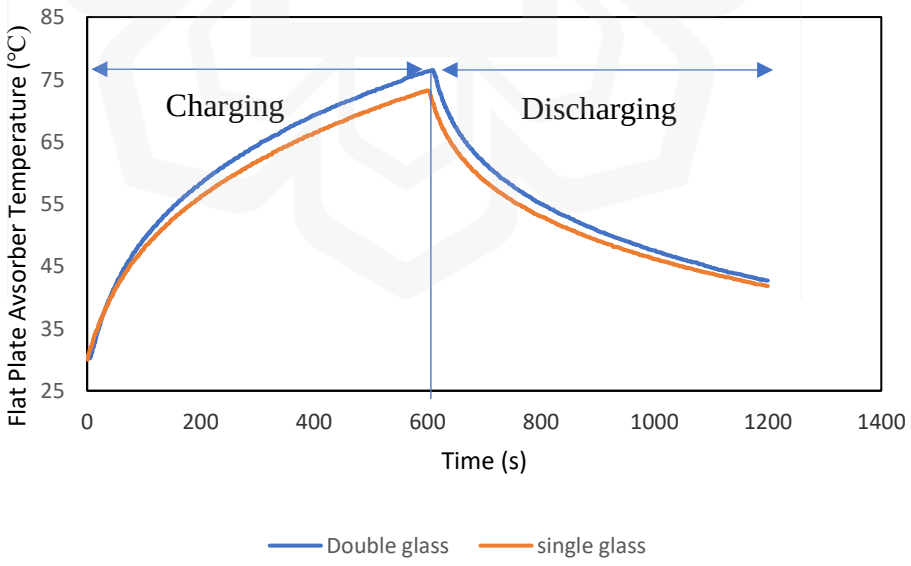

Figure 4.10: Flat plate absorber temperature versus time for different glass cover comparison

Table 4.7 summaries the heat gain rate of different glass covers. The highest heat gain rate is double glass, with a value of 0.077 ℃/s. Meanwhile, the heat gain rate for the single glass is 0.072 ℃/s. It can be concluded that the flat plate absorber-collector for double glass configuration absorbs high heat energy during the charging period from solar radiation as compared to single glass configuration. The advantage of a double glass cover is its reduced heat loss due to condensation. In some climates, the inside of a single glass cover can condense, causing heat loss and reducing the collector's efficiency. A double glass cover helps to prevent condensation by providing a barrier between the hot air inside the collector and the cooler air outside.

In conclusion, a double glass cover provides several benefits to a solar collector, including improved insulation, durability, and protection against environmental factors. The double glass cover also helps to prevent heat loss due to condensation and improves the overall performance and efficiency of the system. Hence, double glass as a glass cover is selected as the design parameter for FPBTCA.

Table 4.7: Summary of heat gain rate of different glass covers

Glass cover	Heat gain rate (℃/s)	Maximum absorber temperature (℃)
Single glass	0.072	73.2
Double glass	0.077	76.3

4.3 DESIGN PARAMETER FOR FLAT PLATE BASE-THERMAL CELL ABSORBER (FPBTCA)

Several design parameters have been determined in this study. However, this research had been specially designed to achieve the highest performance of a Flat Plate Base-Thermal Cell Absorber (FPBTCA) performance. Table 5.8 lists the chosen design parameters of the Flat Plate Base-Thermal Cell Absorber (FPBTCA). The design parameters selected are based on the optimum performance of the flat plate solar collector. Figure 4.11 shows the FPBTCA diagram. The flat plate absorber base-collector is combined with the thermal cell absorber in one unit. This design is applicable for solar radiation of more than 200 W/$m^{2,}$ however during rainy times it

does not operate well. During a normal or good sunshine period, the solar collector can work from 9.00 am to 6.00 pm. The flat plate solar collector will produce higher energy gain with a larger surface area, but the temperature will remain, due to the surface area of the absorber-collector being exposed to solar radiation. The selection done is to obtain a flat plate solar collector with a thermal cell absorber for small energy gain applications.

Table 4.8: Design parameter for Flat Plate Base-Thermal Cell Absorber (FPBTCA)

Design parameter	Parameter
Coating surface	Flat black coating
Air gap distance between flat plate absorber collector and glass cover 1	10.0 mm
Air gap between glass cover 1 and glass cover 2	0.4 mm
Thermal cell absorber (10 cm x 10 cm)	Stainless Steel 1.0 mm
Flat plate base absorber (18.5 cm x 25.5 cm)	Aluminium 0.5 mm
Glass thickness	2.0 mm

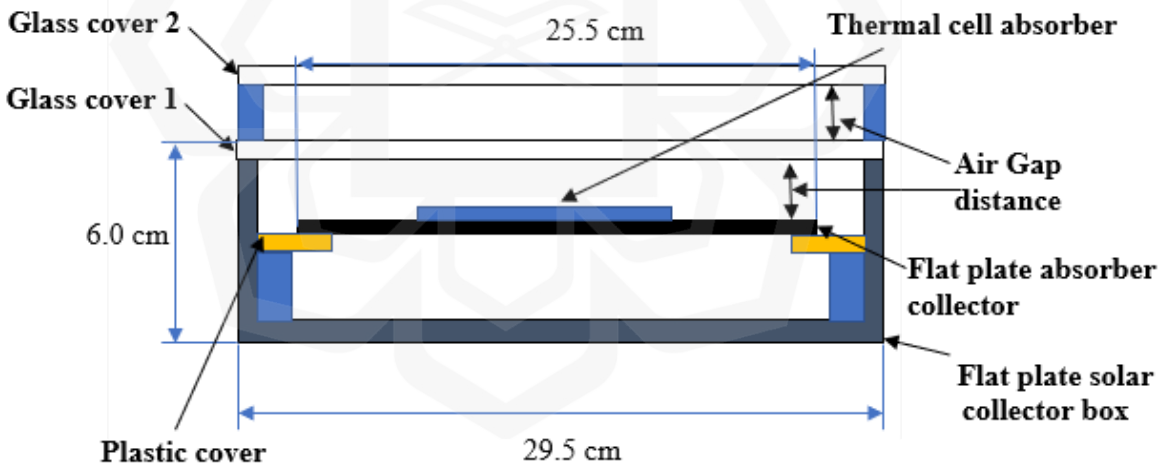

Figure 4.11: Flat Plate Base-Thermal Cell Absorber (FPBTCA) diagram.

4.4 PRELIMINARY EXPERIMENT 1 FOR FLAT PLATE SOLAR COLLECTOR AND FLAT PLATE BASE-THERMAL CELL ABSORBER (FPBTCA)

The flat plate solar collector was exposed to artificial solar radiation for about 300 seconds to stimulate the charging process and a further 300 seconds to stimulate the discharging process when the artificial solar radiation was removed. Table 5.9 and Figure 4.12 shows the maximum temperature within 300 s and temperature versus time for various absorber collector configurations. Temperature T1 refers to the temperature absorbed by aluminum material that attaches at the bottom, which is referred to as a dummy load. The temperature T2 refers to the drying chamber temperature used to dry the product. The temperature T3 refers to the output temperature from the drying chamber to the outside. Therefore T1, T2, and T3 are important when designing the flat plate collector. The temperature depends on the solar radiation exposed to the FPBTCA.

Based on table 4.9, the results show the maximum temperature of T1 at 300 seconds is 33.4˚C, and the absorber is aluminum base absorber with stainless steel cell of 1.0 mm. The temperature T2 shows the maximum temperature at 300 seconds is 37.2˚C, and the absorber is aluminum base absorber with stainless steel cell 1.0 mm. Temperature T3 has the maximum temperature at 300 s of 38.6˚C, and the absorber is aluminum base absorber with stainless steel cell of 1.0 mm. Therefore, it can be concluded that the heat absorbed by the aluminum base absorber with stainless steel cell 1.0 mm absorber is transferred quickly to the drying chamber and to the bottom via conduction and convection heat transfer and thus increased its temperature. The maximum temperature at 300 seconds for T4 is aluminum base absorber with stainless steel cell 0.5 mm, which is 62.4˚C. Aluminum base absorber with aluminum 0.5 mm has the highest temperature for T5 at 300 seconds, which is 63.1˚C. Aluminum base absorber with stainless steel 0.5 mm has highest temperature at 300 seconds for T6 and the value is 65.3˚C. Aluminum base absorber with aluminum 0.5 mm has highest temperature for T7 at 300 seconds which is 57.4˚C, respectively. Aluminum base absorber with stainless steel 0.5 mm has the highest temperature at 300 seconds for T8, which is 45.4˚C. The highest point on each graph illustrates the end of the charging process and the beginning of the discharging process.

Table 4.9: The maximum temperature within 300 seconds of charging process

Absorber types	T1 (˚C)	T2 (˚C)	T3 (˚C)	T4 (˚C)	T5 (˚C)	T6 (˚C)	T7 (˚C)	T8 (˚C)
Aluminum	30.9	36.6	38	61.9	63.1	61.5	57.4	44.1
Aluminum+0.5mm Aluminium cell	30.9	36.6	38	61.9	63.1	61.5	57.4	44.1
Aluminum+1.0mm Aluminium cell	31.1	36.4	37.8	61.5	61	62.3	50.6	43.5
Aluminum + 0.5mm Stainless steel cell	31.7	37.1	38.5	62.4	61	65.3	48	45.4
Aluminum + 1.0mm Stainless steel cell	33.4	37.2	38.6	58.3	57.3	58.6	48	43.2

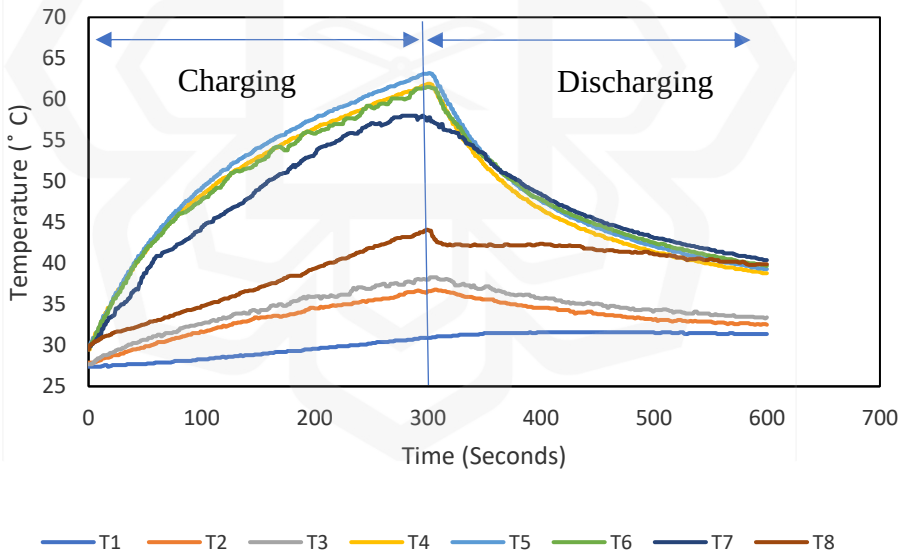

(a)

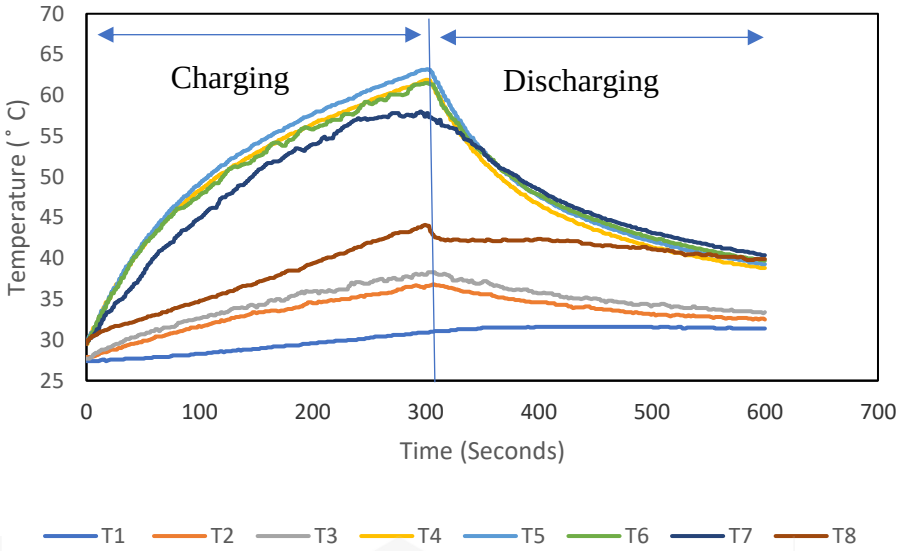
Charging
Discharging
Temperature (° C)
Time (Seconds)
T1 T2 T3 T4 T5 T6 T7 T8

(b)

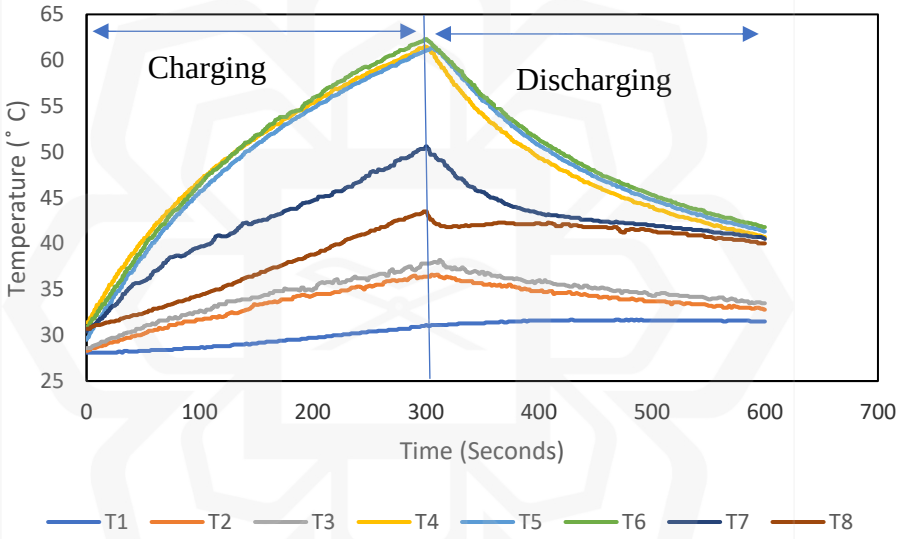
Charging
Discharging
Temperature (° C)
Time (Seconds)
T1 T2 T3 T4 T5 T6 T7 T8

(c)

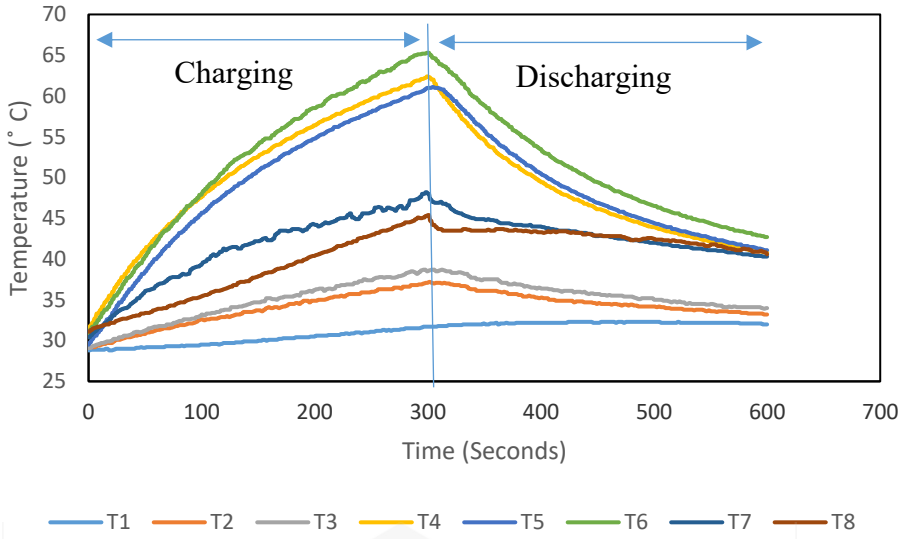

(d)

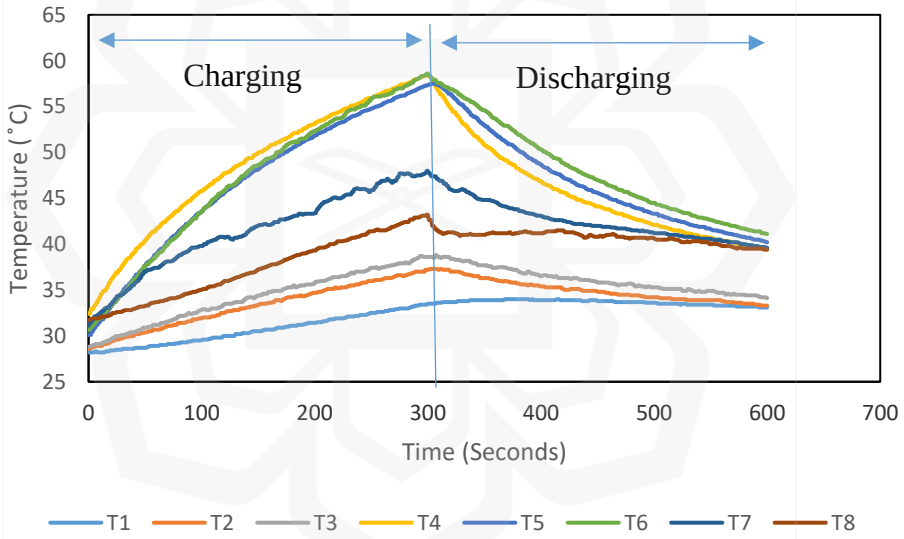

(e)

Figure 4.12: Temperature versus time for various absorber collector configurations,
(a) without cell,

(b) with aluminum 0.5 mm cell,

(c) with aluminum 1.0 mm cell,

(d) with stainless steel 0.5 mm cell and

(e) with stainless steel 1.0 mm cell

4.4.1 PERFORMANCE OUTPUT ANALYSIS OF DRYING CHAMBER

The heat transfer rate of the collector is calculated by the equation (Ahmad Fudholi et al., 2015 and Beckman, 2013):

$$\dot{Q}_{Collector} = \rho A v C_{p(air)}(T_o - T_i) \quad 4.2$$

The heat transfer rate of the thermal absorber storage can be obtained by equation (Ahmad Fudholi et al., 2015 and Beckman, 2013):

$$Q_{Store} = \frac{m_{ab} C_{p(ab)}(T_2 - T_1)}{t_2 - t_1} \quad 4.3$$

Where the efficiency of the collector and storage is presented as:

$$\eta_{Collector+Storage} = \frac{\dot{Q}_{Collector} + Q_{Store}}{G_t A_c} \times 100\% \quad 4.4$$

The solution of **Equation 5.2** and **Equation 5.3** to **Equation 5.4**, then the efficiency of the collector and storage is expressed as:

$$\eta_{Collector+Storage} = \frac{\rho A v C_{p(air)}(T_o - T_i) + \left(\frac{m_{ab} C_{p(ab)}(T_2 - T_1)}{t_2 - t_1}\right)}{G_t A_c} \times 100\% \quad 4.5$$

Where,

ρ = The density of air (kg/m^3)
A = Area of inlet duct (m^2)
v = The velocity of air at inlet duct (m/s)
$C_{p(air)}$ = Specific heat of air (kJ/kgK)
T_o = Air outlet temperature (K)
T_i = Air inlet temperature (K)
G_t = Global solar radiation ($Watt/m^2$)
A_c = Area of the collector (m^2)
m_{ab} = Mass of thermal absorber (kg)
$C_{p(ab)}$ = Specific heat of thermal absorber (kJ/kgK)
T_2 = The temperature of thermal absorber after heat gain (K)
T_1 = The temperature of thermal absorber before heat gain (K)
t_2 = Time after heat gain (s)
t_1 = Time before heat gain (s)

4.4.2 HEAT STORAGE

Table 4.10 presents the details of total heat storage (Q storage) gain for each type of absorber in the drying chamber, respectively. The results, shows that the aluminum absorber base with stainless steel cell 1.0 mm has a higher total heat storage value which is 412 kW compared to the other types of thermal absorber collectors. Correspondingly, the stainless-steel cell absorbs high radiation, then converts it to heat energy and store heat in the drying chamber's system. With higher heat storage, the system becomes less dependent on the availability of sunlight, ensuring a steady and reliable supply of energy even during cloudy or overcast days.There are differences between aluminum absorber base with stainless steel cell of 1.0 mm and aluminum absorber collector without a thermal cell is 231 kW. Aluminum absorber base with stainless steel cell 1.0 mm proved a better performance in terms of heat storage that could be stored during exposure to solar radiation. Based on the situation, the energy efficiency of the solar collector system has also increased. It can be concluded that using a thermal cell could improve the heat storage of the absorber collector more than without a thermal cell.

Table 4.10: Heat storage (Q storage) value (in kW) for each type of absorber in drying chamber

	AL	AL 0.5 mm with AL	AL 1.0 mm with AL	SS 0.5 mm with AL	SS 1.0 mm with AL
Total Heat Storage, Q (kW)	181	236	254	322	412

4.4.3 HEAT TRANSFER RATE ($\dot{Q}$)

Table 4.11 presents the heat transfer rate of the thermal collector ($\dot{Q}$) value (in kW) for the drying chamber by the different types of absorber collectors. The heat transfer rate of a solar collector refers to the amount of heat that is transferred from the solar collector to the storage system or directly to the end-use application per unit of time. The highest total heat transfer rate of the thermal collector collected by the absorber collector is aluminum absorber base with stainless steel cell of 1.0 mm, and the value is 47.05 kW. The results of this experiment indicates that the greater increase value of the heat transfer rate provides high heat transfer in the drying chamber. For discharging period aluminum absorber base with stainless steel cell 1.0 mm has a higher heat transfer rate which is 65.26 kW. The total heat gain for aluminum absorber base with stainless steel cell is 1.0 mm which is 18.21 kW, higher than other configurations. It shows that aluminum absorber base with stainless steel cell 1.0 mm has higher heat energy during discharging and can be used to supply constant heat to the drying chamber. This led to a longer time for the absorber to cool down when the simulator is turned off. The heat transfer rate affects the mass and area of the absorber collector. The larger the surface area of the collector, the higher is the heat transfer rate of the solar collector. While the increasing mass also increased the heat transfer rate of the solar collector system. The intensity of the sunlight falling on the collector determines the heat transfer rate value. The temperature difference between the collector and the storage system or end-use application drives the heat transfer, so a higher temperature difference results in a higher heat transfer rate.

Table 4.11: Heat transfer rate of the collector ($\dot{Q}$) value (in kW) for drying chamber each case of the experiment

	AL	AL 0.5 mm with AL	AL 1.0 mm with AL	SS 0.5 mm with AL	SS 1.0 mm with AL
($\dot{Q}$) Charging (kW)	45.25	45.25	45.25	49.79	47.05
(Q) Discharging (kW)	57.10	57.10	57.10	63.19	65.26
Total (Q) gain (kW)	11.86	11.86	11.86	13.39	18.21

4.4.4 EFFICIENCY (%)

Table 4.12 below illustrates the efficiency (in %) of the collector and storage in the drying chamber of the different types of absorber thermal collectors. The efficiency of a solar collector refers to the percentage of the incident solar energy that is converted into usable thermal energy. Based on the results shows that aluminum absorber base with stainless steel 1.0 mm has a higher value of efficiency in the drying chamber, which is 47.08 percent. The most interesting findings was that the aluminum absorber base with stainless steel cell 1.0 mm could give the best performance in terms of efficiency.

The performance of collector efficiency significantly depends based on the shape factor (Kabeel & Mečárik, 1998) of the absorber collector. A higher efficiency results in more thermal energy being produced per unit area, reducing the size and cost of the system and increasing the overall sustainability of the system. The capacity of the collector is to emit the absorbed energy as thermal radiation. The efficiency is affected by the material and surface texture of the collector and the temperature of the collector.

Table 4.12: Efficiency of the collector and storage in the drying chamber (in %) of the collector and storage in the drying chamber of the different types of absorber thermal collector.

	AL	AL 0.5 mm with AL	AL 1.0 mm with AL	SS 0.5 mm with AL	SS 1.0 mm with AL
Efficiency (%)	25.51	30.40	32.00	39.10	47.08

4.4.5 ENERGY GAIN

Table 4.13 shows the details of the energy gain value (in KJ) of T1 and T2 for a bottom plate for each absorber collector and cumulative energy gain by the different types of absorber collector. The energy gain of a solar collector refers to the amount of thermal energy produced by the collector per unit of time and per unit of surface area. The bottom plate was used as a dummy load to evaluate the heat absorption performance of the drying chamber. The higher total heat gain collected by the dummy load is aluminum absorber base with stainless steel 1.0 mm, and the value of heat gain is 2.85 KW. The higher heat gain collected at the dummy load shows high temperature gain inside drying chamber. The larger the surface area of the collector, the higher is the energy gain absorbed. The difference between an aluminum absorber base with stainless steel 1.0 mm and aluminum without a thermal cell is around 0.19 kW.

Table 4.13: Energy gain value (in KJ) of T1 and T2 for the bottom plate in each case of the experiment after the completion of discharging process

	AL	AL 0.5 mm with AL	AL 1.0 mm with AL	SS 0.5 mm with AL	SS 1.0 mm with AL
Total Energy gain (KJ)	2.66	2.66	1.57	1.7	2.85

Table 4.14 compares the results obtained from the analysis of energy gain value from the drying chamber for each case of the experiment. T1 is referred as temperature at the bottom plate surface, and T ambient is the temperature inlet. The results show the aluminum absorber base with sstainless steel 1.0 mm has higher energy, which is at 300 s and 600s, and the energy gain value is 116.08 J and 102.81 J, respectively, compared

to the other configurations. A higher flow rate can result in higher heat transfer and energy gain. The efficiency of the collector, including its absorption, emission, and heat loss efficiency, affects the energy gain. When T1 is increased, then the energy gain also increases in the solar collector.

Table 4.14: Energy gain value (in J) of absorber for T1 and T ambient in each case of the experiment after the completion of the discharging process.

	AL	AL 0.5 mm with AL	AL 1.0 mm with AL	SS 0.5 mm with AL	SS 1.0 mm with AL
Energy (J) at 300 s	26.82	29.85	36.48	56.38	116.08
Energy (J) at 600 s	41.72	46.43	49.75	66.33	102.81

Table 4.15 provides the energy gain value from the drying chamber for each type of solar thermal collector absorbers. T3 is the temperature outlet for the drying chamber, and T ambient is the temperature inlet. From this data, it can be seen that the drying chamber of an aluminum absorber base with stainless steel 1.0 mm has a higher value of energy gain which is 1279.16 J at 300 s. Aluminum absorber base with stainless steel 1.0 mm also has higher energy at 600 s which is 609.83 J compared to other configurations. The energy storage can be used for drying when the simulator is turned off. The performance of the flat plate collector could be optimized when losses are reduced minimally and by increasing the outlet temperature (Hamed et al., 2014).

Table 4.15: Energy gain value (in J) of absorber for T3 and T ambient in each case of the experiment after the completion of discharging process

	AL	AL 0.5 mm with AL	AL 1.0 mm with AL	SS 0.5 mm with AL	SS 1.0 mm with AL
Energy (J) at 300 s	586.92	763.80	820.08	982.39	1279.16
Energy (J) at 600 s	249.44	324.62	348.53	462.30	609.83

4.5 PRELIMINARY EXPERIMENT 2 FOR FLAT PLATE SOLAR COLLECTOR (FPSC) AND FLAT PLATE BASE-THERMAL CELL ABSORBER (FPBTCA)

The flat plate solar collector was exposed to artificial solar radiation for about 600 seconds to stimulate the charging process and a further 600 seconds to stimulate the discharging process when the artificial solar radiation was removed. Table 4.16 and Figure 4.13 shows the maximum temperature within 600 s and temperature versus time for various absorber collector configurations. Temperature T1 refers to the temperature absorbed by aluminum material that attaches at the bottom, which is referred to as dummy load. The temperature T2 refers to the drying chamber temperature, which is used to dry the product. The temperature T3 refers to the output temperature from the drying chamber to the outside. Therefore T1, T2, and T3 are important when designing the flat plate collector.

Based on the results, it shows the maximum temperature of T1 at 600 seconds is 33.4˚C, and the absorber is aluminum base absorber with stainless steel cell of 1.0 mm. The temperature T2 when the maximum temperature at 600 seconds is 37.2˚C, and the absorber is aluminum base absorber with stainless steel cell of 1.0 mm. Temperature T3 has the maximum temperature of 300 s at 38.6˚C, and the absorber is aluminum base absorber with stainless steel cell of 1.0 mm. Therefore, it can be concluded that the heat absorbed by the aluminum base absorber with stainless steel cell 1.0 mm absorber is transferred fast to the drying chamber and to the bottom via conduction and convection heat transfer and thus increased its temperature.

Table 4.16: The maximum temperature within 600 sseconds of the charging process

Absorber types	T1 (˚C)	T2 (˚C)	T3 (˚C)
Aluminum + 0.5mm Aluminum cell	30.9	36.6	38
Aluminum + 1.0mm Aluminum cell	31.1	36.4	37.8
Aluminum + 0.5mm Stainless steel cell	31.7	37.1	38.5
Aluminum + 1.0mm Stainless steel cell	33.4	37.2	38.6

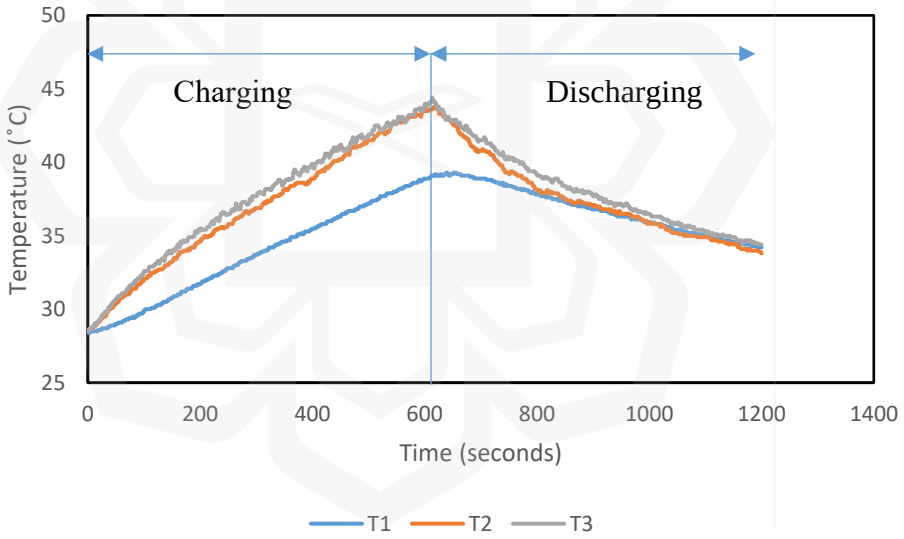

(a)

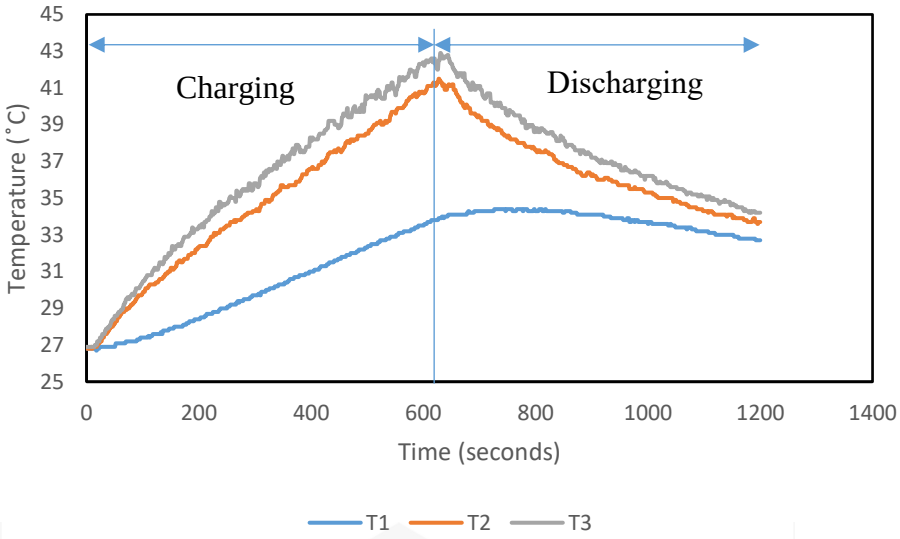
Charging
Discharging
Temperature (°C)
Time (seconds)
T1
T2
T3

(b)

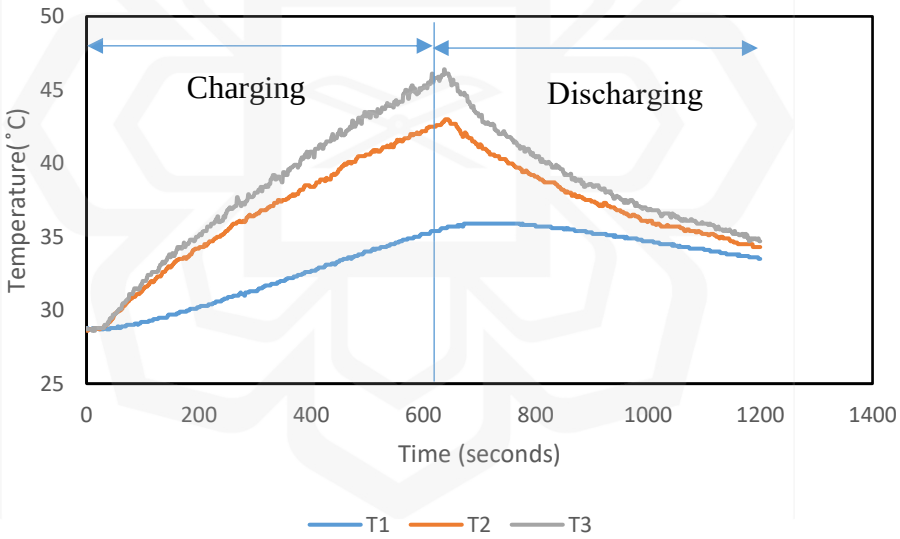
Charging
Discharging
Temperature(°C)
Time (seconds)
T1
T2
T3

(c)

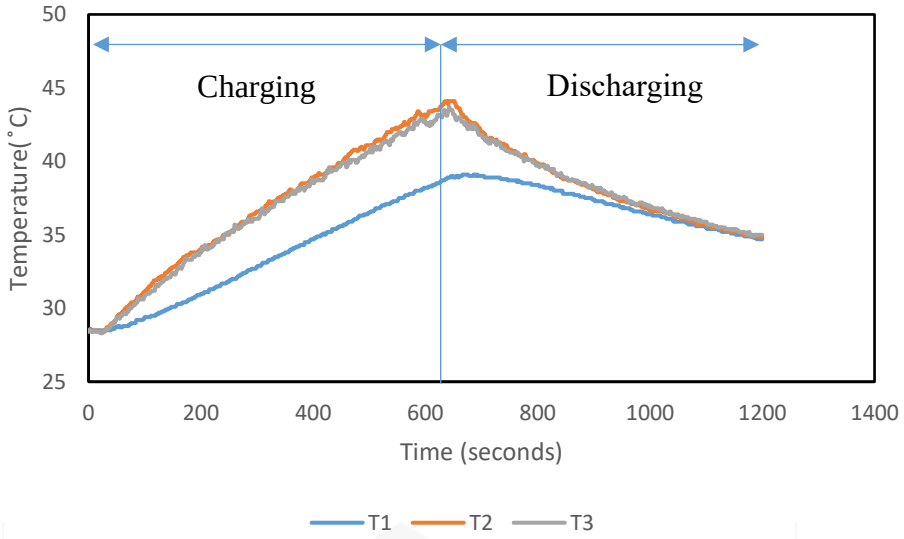

(d)

Figure 4.13: Temperature versus time for various absorber collector configurations,
(a) with aluminum 0.5 mm cell,
(b) with aluminum 1.0 mm cell,
(c) with stainless steel 0.5 mm cell and
(d) with stainless steel 1.0 mm cell

4.5.1 HEAT STORAGE

Table 4.17 presents the details of total heat storage (Q storage) gain for each type of absorber in the drying chamber, respectively. The results, show that the aluminum absorber base with stainless steel cell 1.0 mm has a higher total heat storage value which is 1,196 kW compared to the other types of thermal absorber collectors. Correspondingly, the stainless-steel cell absorbs high radiation, then converts it to heat energy and stores heat in the drying chamber system. The difference between aluminum absorber base with stainless steel cell of 1.0 mm and an absorber without a thermal cell is 335 kW. The heat storage benefits the solar collector in terms of sustainable performance when there are fluctuations of solar radiation and also if the weather is cloudy.

Table 4.17: Heat storage (Q storage) value (in kW) for each type of absorber in a drying chamber

	AL 0.5 mm with AL	AL 1.0 mm with AL	SS 0.5 mm with AL	SS 1.0 mm with AL
Total Heat Storage, Q (kW)	861	749	1,073	1,196

4.5.2 EFFICIENCY (%)

Table 4.18 below illustrates the efficiency (in %) of the collector and storage in the drying chamber of the different types of absorber thermal collectors. Based on the results the aluminum absorber base with stainless steel 1.0 mm has a higher value of efficiency in the drying chamber, which is 67.69 percent. The most interesting findings was that the aluminum absorber base with stainless steel cell 1.0 mm could give the best performance in terms of efficiency than other configurations. The size and mass of the absorber collector contributed to the efficiency of the FPBTCA. When higher mass and larger size of the absorber collector were used, the efficiency could be increased. The air flow of the inlet of the solar collector also affects the efficiency. The efficiency improved with the increasing of air flow.

Table 4.18: Efficiency of the collector and storage in drying chamber (in %) of the collector and storage in the drying chamber of the different types of absorber thermal collector.

	AL 0.5 mm with AL	AL 1.0 mm with AL	SS 0.5 mm with AL	SS 1.0 mm with AL
Efficiency (%)	53.20	46.51	64.11	67.69

4.5.3 ENERGY GAIN

Table 4.19 shows the details of the energy gain value (in KJ) of T1 and T2 for a bottom plate for each absorber collector and cumulative energy gained by the different types of absorber collector. The bottom plate was used as a dummy load to evaluate for heat absorption performance of the drying chamber. The higher total heat gain collected by

the dummy load is aluminum absorber base with stainless steel 1.0 mm, and the value of heat gain is 2.85 KW. The higher heat gain collected at the dummy load shows the high-temperature gain inside the drying chamber. Aluminum base absorber below the thermal cell transfers the heat to the drying chamber effectively to contribute to the increasing drying chamber temperature. Because aluminum has higher thermal conductivity, it has the capability to transfer heat fast to the drying chamber.

Table 4.19: Energy gain value (in KJ) of T1 and T2 for the bottom plate in each case of the experiment after the completion of discharging process

	AL	AL 0.5 mm with AL	AL 1.0 mm with AL	SS 0.5 mm with AL	SS 1.0 mm with AL
Total Energy gain (KJ)	2.66	2.66	1.57	1.7	2.85

Table 4.20 compares the results obtained from the analysis of energy gain value from the drying chamber for each of the experiments. T1 is referred to as the temperature at the bottom plate surface, and T ambient is the temperature inlet. The results show the aluminum absorber base with sstainless steel 1.0 mm has higher energy, which is at 300 s and 600s, and the energy gain value is 291.85 J and 142.61 J, respectively, compared to the other configurations. The bottom plate surface receives the heat via convection and radiation from the absorber base-collector. When the absorber base absorbed high heat energy from solar radiation, it is transferred to the bottom plate faster than stainless steel.

Table 4.20: Energy gain value (in J) of absorber for T1 and T ambient in each case of the experiment after the completion of discharging process

	AL 0.5 mm with AL	AL 1.0 mm with AL	SS 0.5 mm with AL	SS 1.0 mm with AL
Energy (J) at 300 s	291.85	129.34	185.72	291.85
Energy (J) at 600 s	139.29	86.23	109.44	142.61

4.6 OUTDOOR EXPERIMENT PERFORMANCE

The outdoor experiment was done for 7 days (4 – 9 march 2021 and 21 march 2021) from morning until evening. An evaluation of outdoor performance was done to find out the comparison between Flat Plate Solar Collectors (FPSC) and Flat Plate Base-Thermal Cell Absorber (FPBTCA). Based on the results, it will provide the data for the flat plate absorber collector and dummy load.

4.6.1 DAY 1, 4 MARCH 2021

The results of the flat plate absorber, T1, for both FPSC and FPBTCA on Day 1 (Thursday, 4 March 2021) are shown in Figure 4.14. The inconsistent solar radiation profile during the day of experimental work was cloudy, with the radiation value fluctuating between 10.4 – 1022.5 W/m^2. Section (a) refers to the discharge rate value for FPSC and FPBTCA. FPBTCA has a lower temperature discharge rate as compared to the FPSC, which is -0.678 ^{o}C/s and -0.822 ^{o}C/s. The solar radiation drops from 624.5 W/m^2 to 118.5 W/m^2. Section (b) shows the temperature charge rate for FPBTCA is higher than the FPSC configuration with the value of 1.338 ^{o}C/s and 1.319 ^{o}C/s, respectively, with solar radiation having increased by 803.06 W/m^2.

The other results indicate that FPBTCA has a lower temperature discharge rate than FPSC, which is -1.165 ^{o}C/s and -1.51^{o}C/s as shown by section (c), with solar radiation drop of 238.1 W/m^2. Section (d) shows that the temperature discharge rate for FPBTCA is lower than FPSC, which is -0.838 ^{o}C/s and -0.910 ^{o}C/s. The solar radiation drops from 93.3 W/m^2 to 69 W/m^2. Section (a), section (c), and section (d) show the thermal buffer effect for each FPSC and FPBTCA when the solar radiation drops.

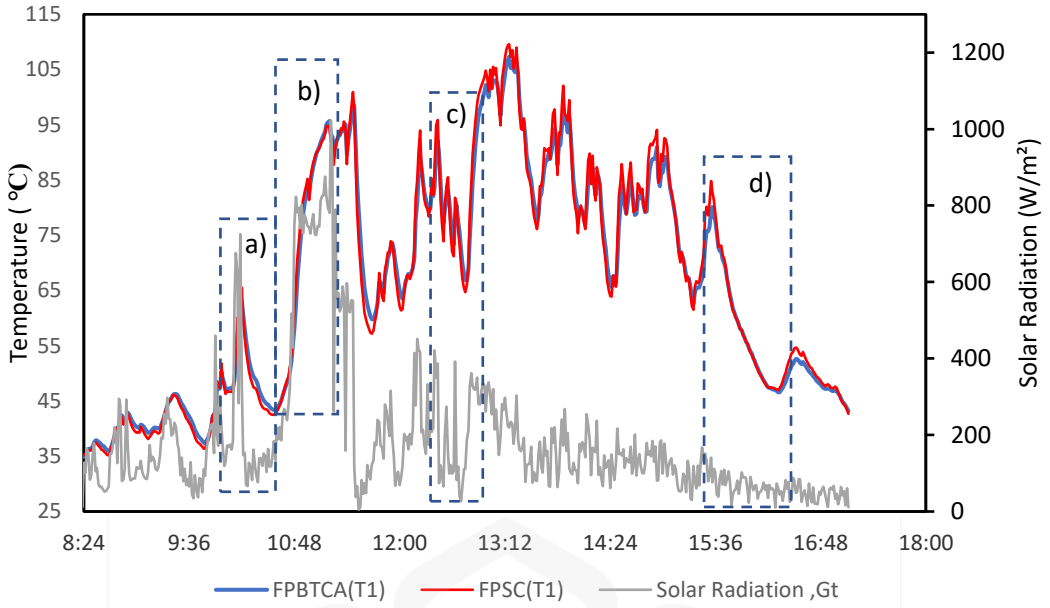

Figure 4.14: Flat plate absorber temperature, T1 for FPSC and FPBTCA

Figure 4.15 represents the dummy load absorber temperature, T3 for both FPSC and FPBTCA on Day 1 (Thursday, 4 March 2021). Section (a) shows the temperature charge rate for FPSC and FPBTCA. Based on the results, FPBTCA has a higher temperature charge rate than FPSC, with values of 0.295 ^{o}C/s and 0.290 ^{o}C/s, respectively. The solar radiation increased from 211.1 W/m^2 to 725.0 W/m^2 with 513.9 W/m^2 increasing. FPTCA also has a higher temperature charge rate than FPSC, as shown by section (b), which is 16.4 ℃/s and 15.6 ^{o}C/s, with 561.5 W/m^2 solar radiation increased. Section (c) provides the results, where temperature discharge rate for FPBTCA is lower than FPSC, which is -0.260 ^{o}C/s and -0.268 ^{o}C/s, with solar radiation dropping from 102.5 W/m^2 to 10.4 W/m^2.

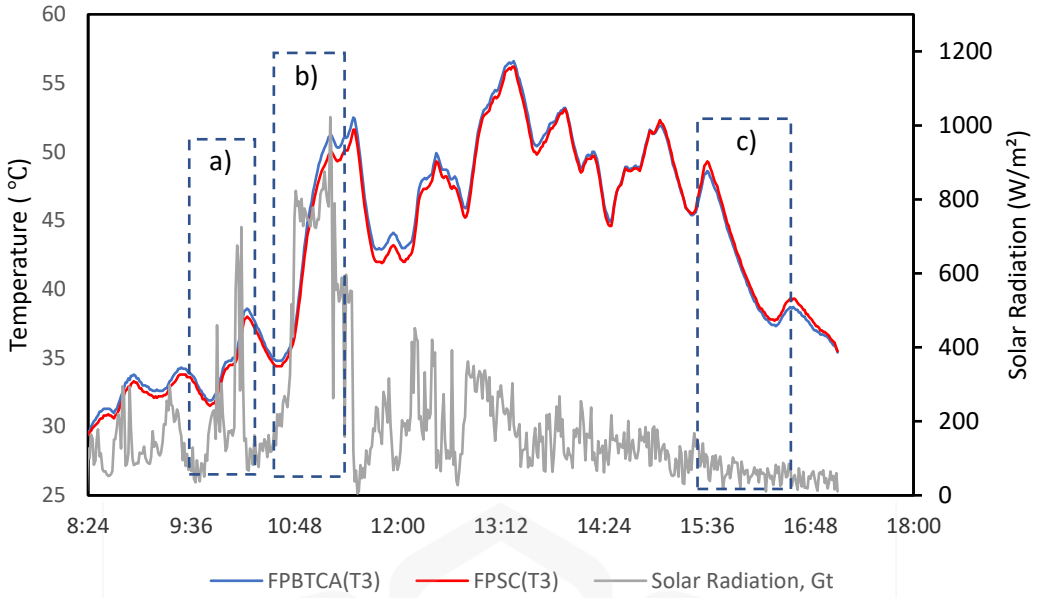

Figure 4.15: Dummy load absorber temperature, T3 for FPSC and FPBTCA

4.6.2 DAY 2, 5 MARCH 2021

The results of the flat plate absorber, T1, for both FPSC and FPBTCA on Day 2 (Friday, 5 March 2021) s is shown in Figure 4.16. The inconsistent solar radiation profile during the day of experimental work was cloudy, with the radiation value fluctuating between 4.0 – 1245.0 W/m^2. Section (a) shows the temperature discharge rate for FPSC and FPBTCA. FPBTCA has a lower temperature discharge rate (with a value of -0.750 ^{o}C/s) than FPSC (with a value of -0.964 ^{o}C/s), with a solar radiation drop of 587.2 W/m^2, from 1102.4 W/m^2 to 515.3 W/m^2. Section (b) represents the FPBTCA has a higher temperature charge rate (with a value of 0.535 ^{o}C/s) than FPSC (with a value of 0.495 ^{o}C/s). The solar radiation increased from 105.1 W/m^2 to 344.9 W/m^2, with an increase of 239.8 W/m^2. FPBTCA (with a value of 0.900 ^{o}C/s) has a higher temperature charge rate than FPSC (with a value of 0.520 ^{o}C/s), as shown in section (c), with solar radiation having increased from 36.0 W/m^{2}to 77.3 W/m^2.

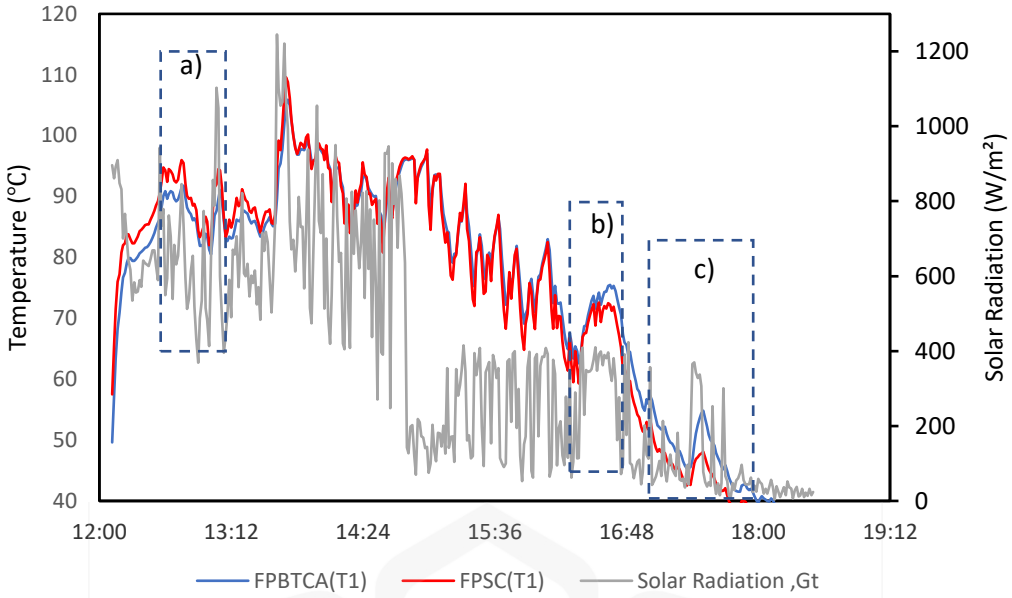

Figure 4.16: Flat plate absorber temperature, T1 for FPSC and FPBTCA

Figure 4.17 represents the dummy load absorber temperature, T3, for both FPSC and FPBTCA on Day 2 (Friday, 5 March 2021). The maximum dummy load absorber temperature, T3, occurred at 13:45 pm for FPBTCA (with a value of 56.2 ^{o}C) and FPSC (with a value of 55.3 ^{o}C). Section (a) represents FPBTCA (with a value of 0.361 ^{o}C/s) which has a higher temperature charge rate than FPSC (with a value of 0.333 ^{o}C/s). The solar radiation increased from 570.8 W/m^2 to 671.5 W/m^2, with increasing of 100.7 W/m^2. Section (c), shows that the FPBTCA (with a value of 0.207 ^{o}C/s) has a higher temperature charge rate than FPSC (with a value of 0.127 ^{o}C/s) configuration, with increasing 34.4 W/m^2 of solar radiation from 346.2 W/m^2 to 380.6 W/m^2.

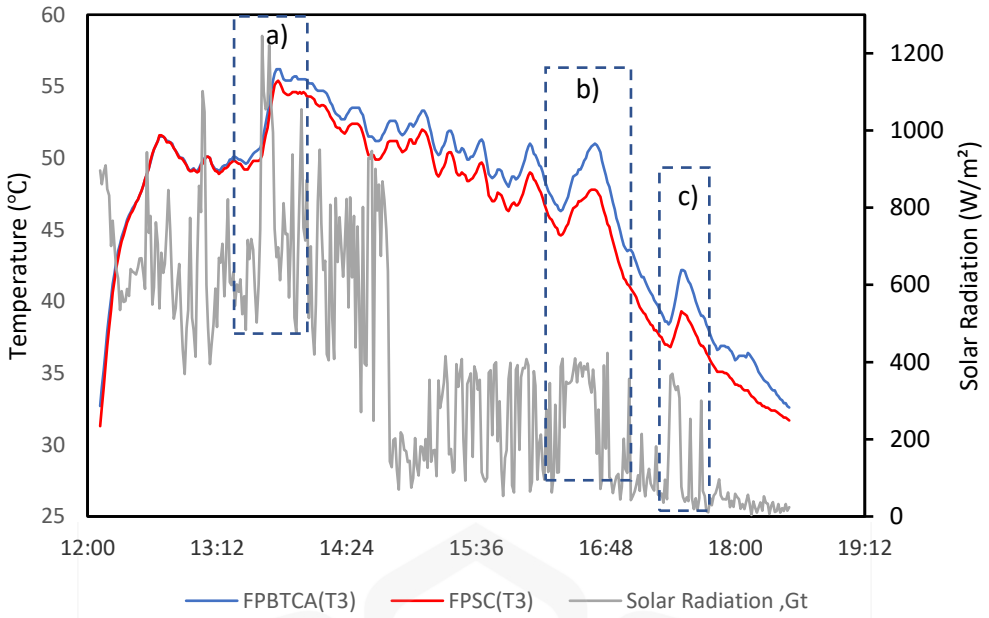

Figure 4.17: Dummy load absorber temperature, T3 for FPSC and FPBTCA

4.6.3 DAY 3, 6 MARCH 2021

The results of the flat plate absorber, T1, for both FPSC and FPBTCA on Day 3 (Saturday, 6 March 2021) are shown in Figure 4.18. The inconsistent solar radiation profile during the day of experimental work was cloudy, with the radiation value fluctuating between 56.5 – 1036.4 W/m^2. Section (a) shows the temperature discharge rate for FPBTCA and FPSC. FPBTCA has a lower temperature discharge rate than FPSC, which is -0.553 ^{o}C/s and -0.724 ^{o}C/s, respectively, with solar radiation dropping 185.7 W/m^2 from 308.3 W/m^2 to 123.0 W/m^2. Section (b) represents the temperature discharge rate for FPBTCA and FPSC. It can be concluded the FPBTCA has a lower temperature discharge rate which is -0.831 ^{o}C/s and -0.934 ^{o}C/s. The solar radiation decreased from 574.0 W/m^2 to 218.8 with a decrease of 355.3 W/m^2. Section (c) shows the FPBTCA has a lower temperature discharge rate than FPSC, which is -0.943 ^{o}C/s and -0.983 ^{o}C/s, with a solar radiation drop of 442.9 W/m^2, from 620.6 W/m^2 to 177.7 W/m^2. Section (d) shows the temperature discharge at the end of the day between FPBTCA and FPSC. FPBTCA has a lower temperature discharge rate than FPSC, which is -0.892 ^{o}C/s and -0.931 ^{o}C/s, with a solar radiation drop of 599.4 W/m^2, from 820. 7 W/m^2 to 221.3 W/m^2.

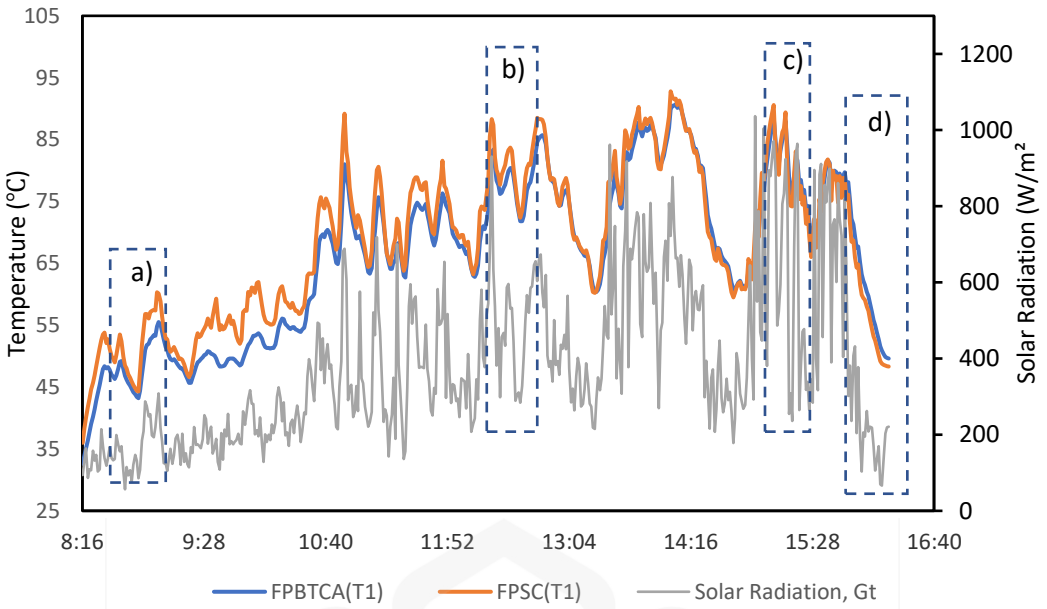

Figure 4.18: Flat plate absorber temperature, T1 for FPSC and FPBTCA

Figure 4.19 represents the dummy load absorber temperature, T3, for both FPSC and FPBTCA on Day 3 (Saturday, 6 March 2021). The maximum dummy load absorber temperature, T3 has, occurred at 14:12 pm for FPBTCA (with a value of 52.5 ^{o}C) and FPSC (with a value of 51.5 ^{o}C). Section (a) shows the temperature discharge rate for FPBTCA and FPSC. Based on the results, FPBTCA has a lower temperature than FPSC, which is -0.131 ^{o}C/s and -0.150 ^{o}C/s, with solar radiation drop of 156.7 W/m^2, from 308.3 W/m^2 to 151.7 W/m^2. While section (b) shows, the FPBTCA has a higher temperature charge rate than FPSC, which is 0.192 ^{o}C/s and 0.177 ^{o}C/s. The solar radiation increased by 273.2 W/m^2 from 787.0 W/m^2 to 801.3 W/m^2. FPBTCA also has a higher temperature charge rate than FPSC in section (c), which is 0.316 ^{o}C/s and 0.274 ^{o}C/s, with solar radiation increased by 14.3 W/m^2, from 787.0 W/m^2 to 801.3 W/m^2. Section (d) represents the temperature discharge rate for FPBTCA and FPSC. It can be concluded that FPBTCA has a higher temperature charge rate than FPSC, which is 0.192 ^{o}C/s and 0.177 ^{o}C/s. The solar radiation has increased by 273.2 W/m^2, from 347.5 W/m^2 to 620.6 W/m^2.

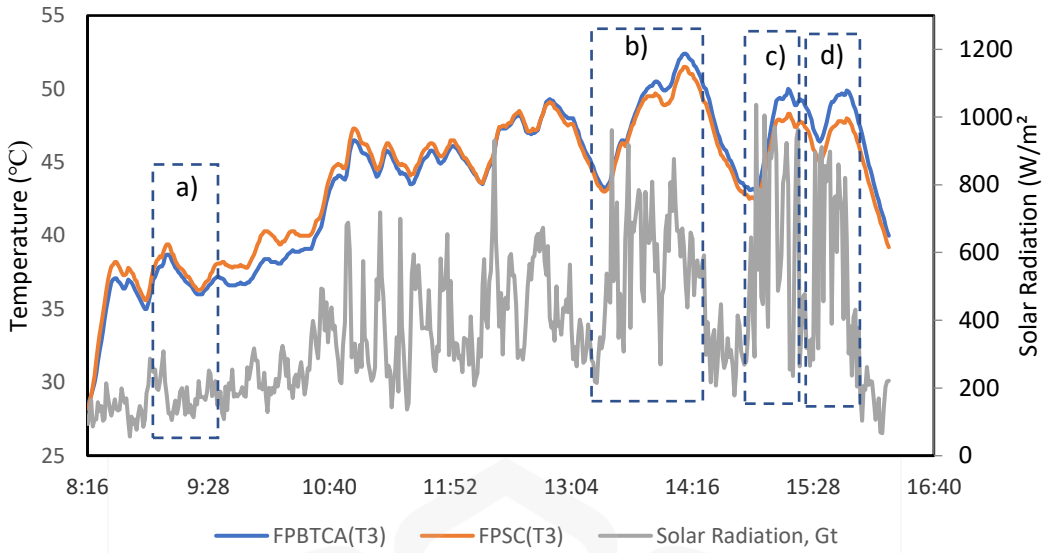

Figure 4.19: Dummy load absorber temperature, T3 for FPSC and FPBTCA

4.6.4 DAY 4, 7 MARCH 2021

The results of the flat plate absorber, T1, for both FPSC and FPBTCA on Day 4 (Sunday, 7 March 2021) are shown in Figure 4.20. The inconsistent solar radiation profile during the day of experimental work was cloudy, with the radiation value fluctuating between 38.2 – 1012.0 W/m^2. Section (a) shows the temperature discharge for FPBTCA and FPSC. FPTCA (with a value of -0.340 ^{o}C/s) represents a lower temperature discharge rate than FPSC (with a value of -0.483 ^{o}C/s), with a solar radiation drop of 333.5 W/m^2, from 416.3 W/m^2 to 82.8 W/m^2. Section (b) shows that FPBTCA (with a value of -1.260 ^{o}C/s) has a lower temperature discharge rate than FPSC (with a value of -1.980 ^{o}C/s) configuration. The solar radiation dropped 455.7 W/m^2 from 702.5 W/m^2 to 246.8 W/m^2, respectively. FPBTCA (with a value of -1.363 ^{o}C/s) also shows a lower temperature discharge rate than FPSC (with a value of -1.963 ^{o}C/s), as shown in section (c), with a solar radiation drop of 625.0 W/m^2, from 921.2 W/m^2 to 296.2 W/m^2. Section (d) denotes that the FPBTCA has a higher temperature drop than FPSC when the solar radiation has decreased from 555.9 W/m^2 to 122.6 W/m^2 from 14:28 pm until 18:04 pm.

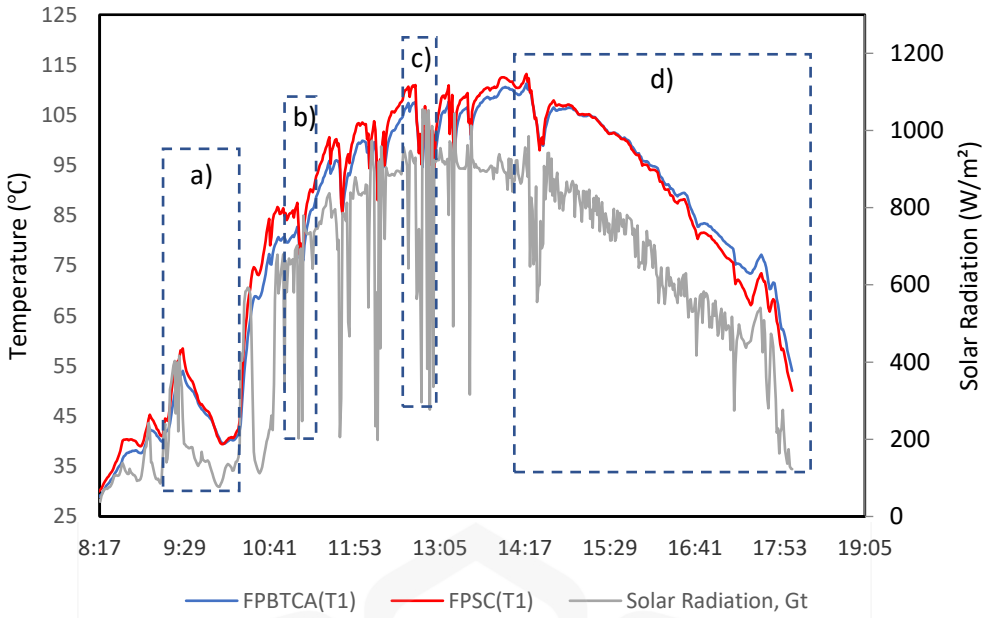

Figure 4.20: Flat plate absorber temperature, T1 for FPSC and FPBTCA

Figure 4.21 represents the dummy load absorber temperature, T3, for both FPSC and FPBTCA on Day 3 (Saturday, 7 March 2021). The maximum dummy load absorber temperature, T3 has, occurred at 14:21 pm for FPBTCA (with a value of 59.0 ^{o}C) and FPSC (with a value of 58.5 ^{o}C) when the solar radiation is 985.5 W/m^2. Section (a) shows the FPBTCA (with a value of -0.090 ^{o}C/s) has a lower temperature discharge rate than FPSC (with a value of -0.112 ^{o}C/s), with solar radiation drop of 255.9 W/m^2, from 398.8 W/m^2 to 143.0 W/m^2. Section (b) represents the temperature discharge rate for FPBTCA and FPSC. FPBTCA (with a value of -0.112 ^{o}C/s) has a lower temperature discharge rate than FPSC (with a value of -0.113 ^{o}C/s), with a solar radiation drop of 455.7 W/m^2, from 702.5 W/m^2 to 246.8 W/m^2. Section (c) shows that the FPBTCA has a higher temperature drop when the solar radiation is decreased from 616.4 W/m^2 to 122.6 W/m^2 from 14:28 pm to 18:04 pm.

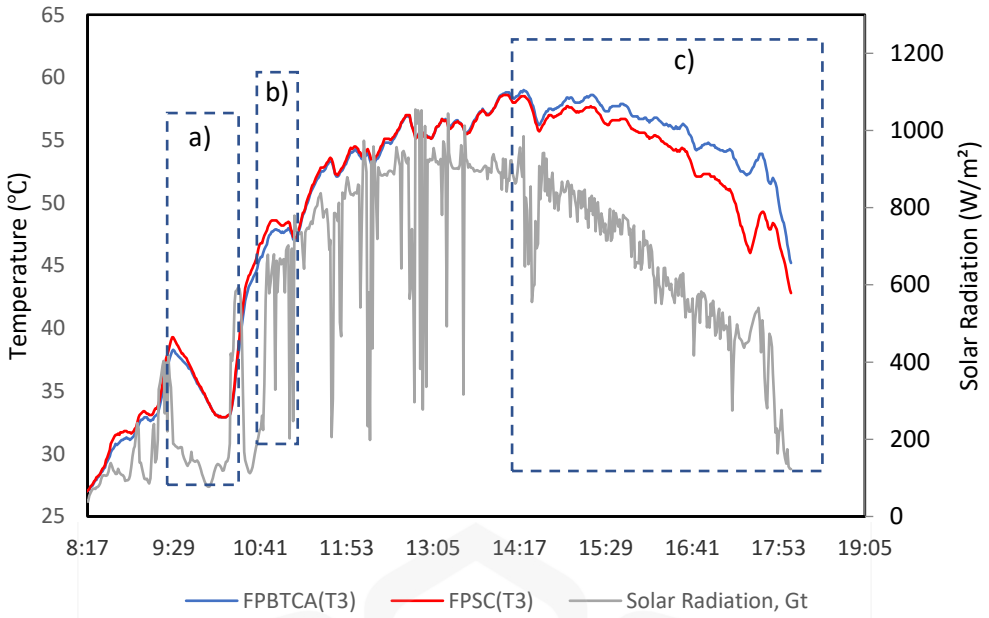

Figure 4.21: Dummy load absorber temperature, T3 for FPSC and FPBTCA

4.6.5 DAY 5, 8 MARCH 2021

The results of the flat plate absorber, T1, for both FPSC and FPBTCA on Day 5 (Monday, 8 March 2021) are shown in Figure 4.22. The solar radiation during the experiment fluctuated between 43.5 W/m^2 to 982.7 W/m^2. Section (a) shows the temperature discharge rate for both FPTCA and FPSC. The FPTCA has a lower temperature discharge rate than FPSC, which is -1.030 ^{o}C/s and -1.58 ^{o}C/s, with solar radiation dropping 494.8 W/m^2 from 748.2 W/m^2 to 253.4 W/m^2. FPBTCA also has a lower temperature discharge rate than FPSC in section (b), which is -1.220 ^{o}C/s and -1.78 ^{o}C/s. The solar radiation dropped 293.1 W/m^2, from 900.4 W/m^2 to 607.4 W/m^2. Section (c) denotes that FPBTCA has a higher temperature drop than FPSC during decreasing of solar radiation from 770.0 W/m^2 to 380.6 W/m^2.

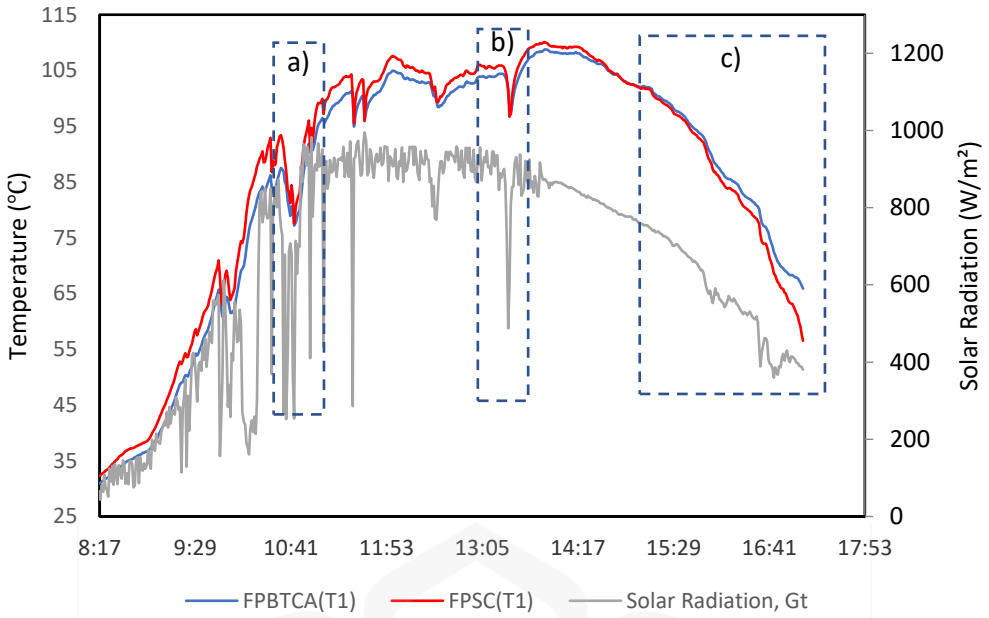

Figure 4.22: Flat plate absorber temperature, T1 for FPSC and FPBTCA

Figure 4.23 represent the dummy load absorber temperature, T3, for both FPSC and FPBTCA on Day 5 (Monday, 8 March 2021). The maximum dummy load absorber temperature, T3, occurred at 14:21 pm for FPBTCA (with a value of 59.3 ^{o}C) and FPSC (with a value of 58.8 ^{o}C). Section (a) represents the temperature discharge rate for FPBTCA and FPSC. FPBTCA has a lower temperature discharge rate than FPSC, which is -0.052 ^{o}C/s and -0.058 ^{o}C/s. The solar radiation dropped 42.1 W/m^2, from 919.5 W/m^2 to 877.3 W/m^2. Section (b) shows that FPBTCA has a higher temperature drop from 14:21 pm to 17:07 pm, with solar radiation dropping 452.1 W/m^2, from 832.7 W/m^2 to 380.6 W/m^2. It can be concluded that FPBTCA has stored excessive heat energy compared to FPSC and pprovides a longer time for the temperature to cool down when there is no sun shine

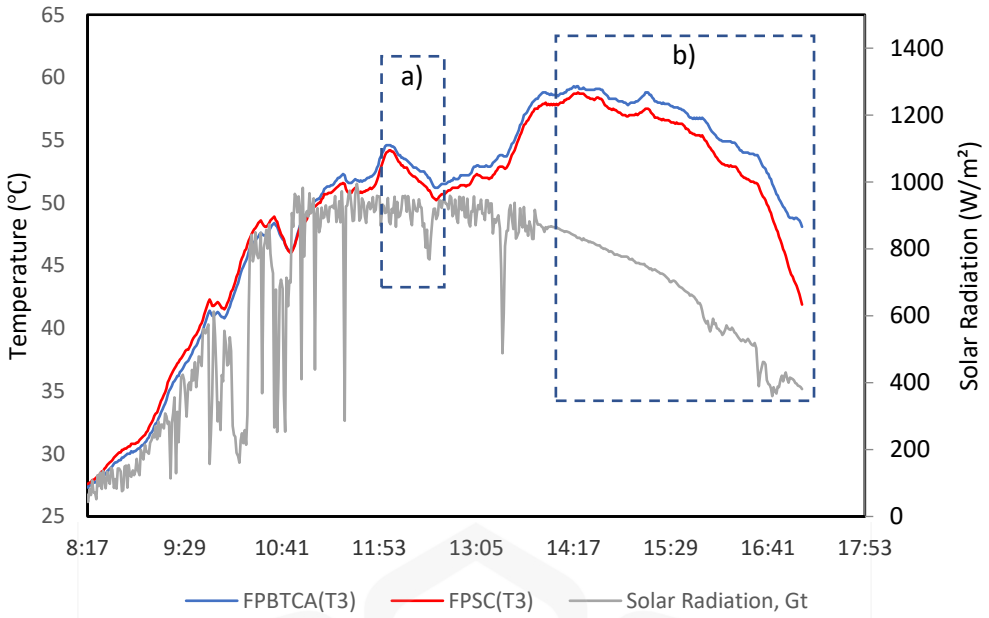

Figure 4.23: Dummy load absorber temperature, T3 for FPSC and FPBTCA

4.6.6 DAY 6, 9 MARCH 2021

The results of the flat plate absorber, T1, for both FPSC and FPBTCA on Day 6 (Tuesday, 9 March 2021) are shown in Figure 4.24. The solar radiation during the experiment fluctuates between 27.9 W/m^2 to 981.0 W/m^2. Section (a) represents the temperature discharge rate for FPBTCA and FPSC. FPBTCA (with a value of -0.667 ^{o}C/s) has a lower temperature discharge rate than FPSC (with a value of -0.876 ^{o}C/s), with solar radiation drop 340.5 W/m^2, from 424.0 W/m^2 to 83.5 W/m^2. FPBTCA (with a value of -1.093 ^{o}C/s) also has a lower temperature discharge rate than FPSC (with a value of -1.614 ^{o}C/s), as seen in section (b), with solar radiation decreased from 711.7 W/m^2 to 97.8 W/m^2. Section (c) shows the FPBTCA ^{o}C/s has higher temperature drop than FPSC. The temperature discharge rate for FPBTCA (with a value of -0.257) is lower than FPSC (with a value of -0.284 ^{o}C/s).

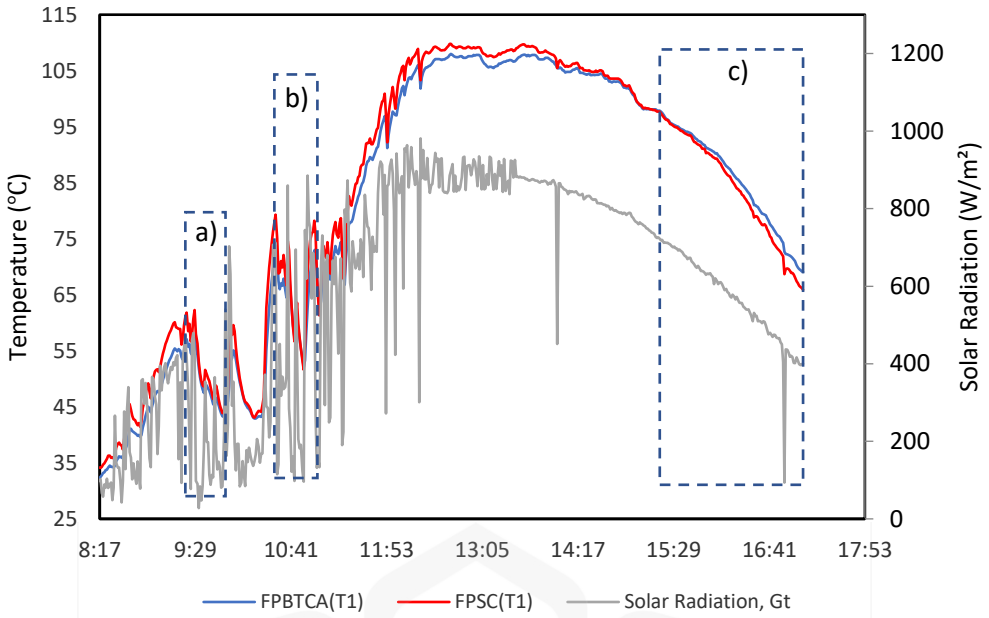

Figure 4.24: Flat plate absorber temperature, T1 for FPSC and FPBTCA

Figure 4.25 represents the dummy load absorber temperature, T3, for both FPSC and FPBTCA on Day 6 (Tuesday, 9 March 2021). The maximum dummy load absorber temperature, T3, occurred at 13:45 pm for FPBTCA (with a value of 57.7 ^{o}C) and FPSC (with a value of 57.5^{o}C) when the solar radiation is 872.6 W/m^2. FPBTCA (with a value of -0.227 ^{o}C/s) has a lower discharge rate than FPSC (with a value of -0.273 ^{o}C/s) on section (a), with solar radiation dropping 372.6 W/m^2, from 479.3 W/m^2 to 106.8 W/m^2. The section (c) represents that FPBTCA has higher temperature drop than FPSC. The temperature discharge rate for FPBTCA (with a value of -0.033^{o}C/s) is lower than FPSC (with a value of -0.048 ^{o}C/s).

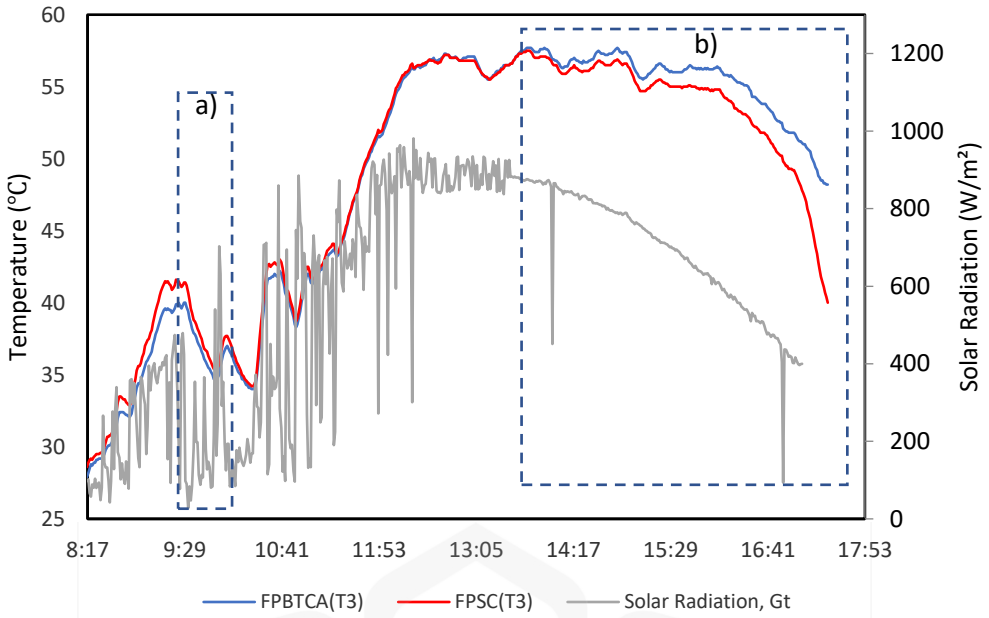

Figure 4.25: Dummy load absorber temperature, T3 for FPSC and FPBTCA

4.7.7 DAY 7, 21 MARCH 2021

The results of the flat plate absorber, T1, for both FPSC and FPBTCA on Day 7 (Sunday, 21 March 2021) are shown in Figure 4.26. FPBTCA and FPSC were closed with a box to prevent solar radiation from finding the heat storage capability for both solar collectors. Section (a) indicates that FPBTCA and FPSC were close within 10 minutes from solar radiation. Based on the results shown, FPBTCA has a lower temperature discharge rate than FPSC, which is -1.620 ^{o}C/s and -1.800 ^{o}C/s, with solar radiation drop of 524.7 W/m^2 to 0 W/m^2. Section (b), section (c), and section (d) show that the FPBTCA was closed within 30 minutes of solar radiation. FPBTCA has a lower temperature discharge rate than FPSC, which is -1.803 ^{o}C/s and -1.960 ^{o}C/s, with solar radiation decreasing from 789.7 W/m^2 to 0 W/m^2 in section (b). Section (c) denotes that FPBTCA has a lower temperature discharge rate than FPSC, which is -2.073 ^{o}C/s and -2.167 ^{o}C/s, with solar radiation drop from 823.3 W/m^2 to 0 W/m^2. FPBTCA also has lower temperature drops on section (d) than FPSC, which is -1.887 ^{o}C/s and -1.900 ^{o}C/s, with solar radiation decreasing from 851.7 W/m^{2}to 0 W/m^2.

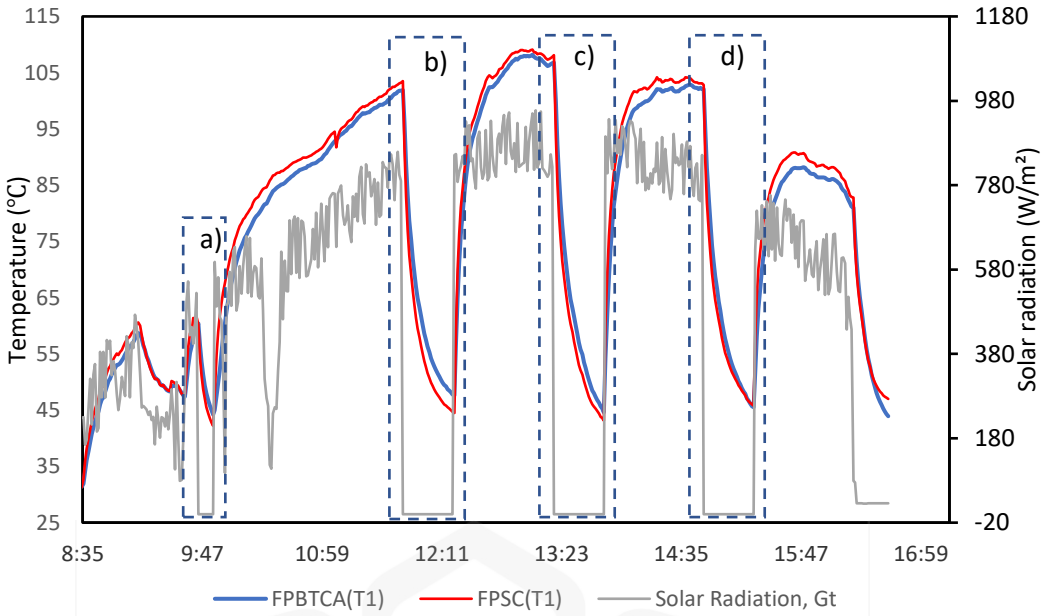

Figure 4.26: Flat plate absorber temperature, T1 for FPSC and FPBTCA

Figure 4.27 represents the dummy load absorber temperature, T3, for both FPSC and FPBTCA on Day 7 (Sunday, 21 March 2021). Section (a) was closed for 10 minutes with a box for FPTCA and FPSC. The results show that FPBTCA has a lower temperature discharge rate than FPSC, which is -0.010 ^{o}C/s and -0.070 ^{o}C/s, with solar radiation dropping from 443.3 W/m^2 to 0 W/m^2. Sections (b), (c), and (d) were close to 30 minutes from solar radiation. Section (b) shows that FPBTCA has a lower temperature discharge rate, which is -0.400 ^{o}C/s and -0.447 ^{o}C/s, with solar radiation decreased from 789.7 W/m^2 to 0 W/m^2. FPBTCA has a lower temperature discharge rate on section (c) than FPSC, which is -0.553 ^{o}C/s and -0.560 ^{o}C/s, with solar radiation dropping to 823.3 W/m^2. FPBTCA also has a lower temperature discharge rate on section (d) than FPSC, which is -0.507 ^{o}C/s and -0.550 ^{o}C/s, with solar radiation decreased by 851.7 W/m^2.

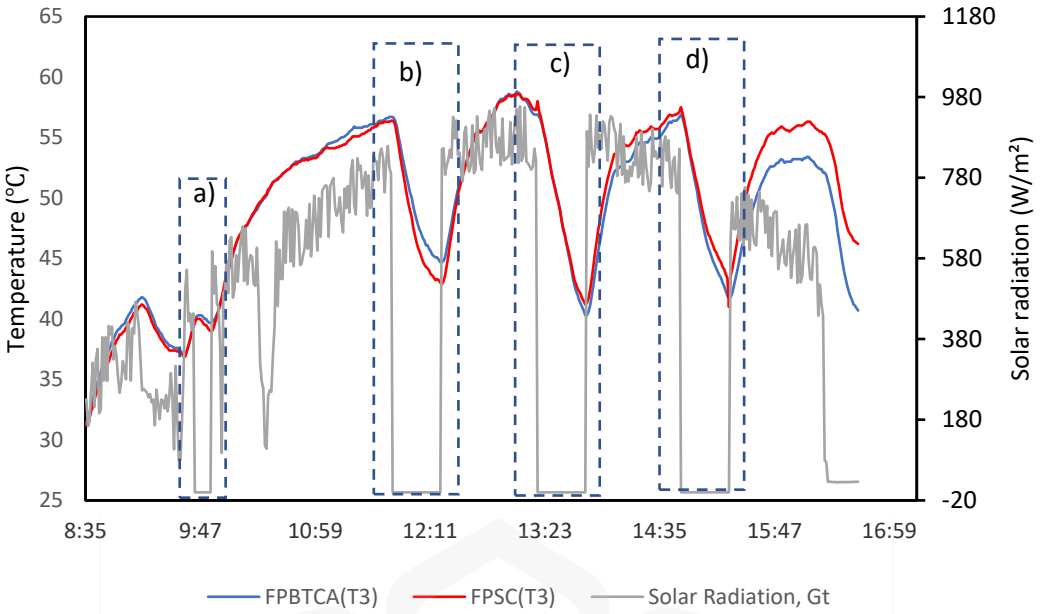

Figure 4.27: Dummy load absorber temperature, T3 for FPSC and FPBTCA

4.8 DAILY PERFORMANCE COMPARISON

Figure 4.28 shows the daily heat absorption (Q) for Flat Plate Solar Collector (FPSC) and Flat Plate Base-Thermal Cell Absorber (FPBTCA). The heat absorption is taken from 4 March 2021 to 9 March 2021. There are six days of comparison data to analyse to determine the performance of FPSC and FPBTCA. FPBTCA showed the highest heat absorption (Q), which was 96079.37 J on 4 March 2021, compared to FPSC, which was 49187.07 J.

The heat absorption (Q) for FPSC on 5 March 2021 is 47488.79 J which is lower than FPTCA. Heat absorption (Q) for FPBTCA is 63656.89 J. For 6 March 2021 shows, the FPTCA has the highest heat absorption (Q), which is 59128.00 J, than FPSC. FPSC has 53697.85 J as compared to FPBTCA. Based on the graph it shows that FPBTCA performed high heat absorption (Q) on 7 March 2021, which is 44646.22 J. FPSC showed a heat absorption (Q) of 41620.16 J. FPSC has the lower heat absorption (Q) than FPBTCA for the rest of the day. The comparison of heat absorption on 8 March 2021 shows the FPCA has the highest, which is 27128.01 J than FPSC, which is 24827.54 J. Heat absorption (Q) on 9 March shows the FPSC has the lowest heat

absorption (Q), which is 35685.80 J as compared to the FPBTCA. FPBTCA shows heat absorption of 38184.78 J.

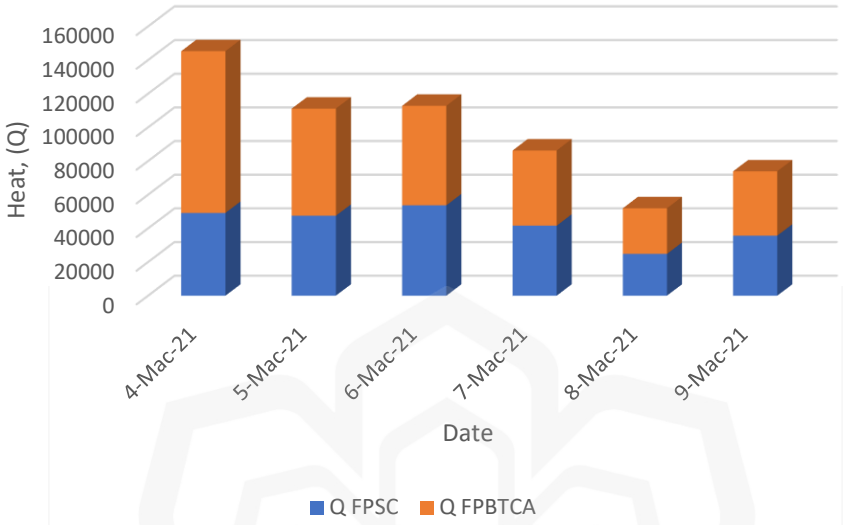

Figure 4.28: Daily heat absorption for FPSC and FPBTCA.

The heat absorption of a solar collector refers to the ability of the collector to absorb and transfer the energy from the sun into usable heat. The heat absorption also depends on the surface area, type of collector, the materials used in the collector, the angle and orientation of the collector, and the weather conditions. When the absorber collector absorbs high heat energy from solar radiation, it can be transferred to the drying chamber. So that the design of FPTCA is integrated with drying chamber, which is located below the absorber collector. The advantage is that heat energy loss can be reduced.

4.9 EVALUATION OF THERMAL CELL MODULE PERFORMANCE

The thermal cell will be used to develop a solar thermal collector, which will be integrated with the absorber base collector. The thermal cell module is a combination of a multi-number of thermal cells and will be used to develop solar thermal collectors. Based on previous findings it was evident that using a single thermal cell could improve the performance of a Flat Plate Base Thermal Cell Absorber (FPBTCA). Furthermore,

a thermal cell can be used to develop a solar collector array at the absorber base-collector surface.

4.8.1 MATHEMATICAL MODELLING ANALYSIS

Mathematical modelling analysis was done over 60 minutes period where the Solar radiation was higher at 860.034 W/m^2. Based on the results, iteration was done to compare between heat inlet and heat outlet. The iteration applied in this analysis was done until energy balanced inlet and outlet had an error below 5 %. Table 4.21 shows the error between *Qin* and *Qout* for the overall Flat Plate Base-Thermal Cell Absorber (FPBTCA). Glass cover 1, glass cover 2, thermal cell, and absorber base-collector has an error of 4.81 %, 2.51 %, 3.98 %, 3.67 %, respectively. Based on the results shown, the energy balance for the thermal cell contributed to the thermal performance of the Flat Plate Base-Thermal Cell Absorber (FPBTCA). It can be concluded that the heat inlet increased as the solar radiation increased.

Table 4.21: Error between Qin and Qout

Solar collector component	Qin (J)	Qout(J)	Error (%)
Glass Cover 1	106.90	101.75	4.81
Glass Cover 2	112.58	109.75	2.51
Thermal Cell	446.25	428.47	3.98
Absorber base collector	1522.01	1466.14	3.67

4.8.2 EFFICIENCY (%) COMPARISON BETWEEN FPBTCA AND FPSC

Figure 4.29 represents the Efficiency (%) versus Time (Minutes) and Solar Radiation for the comparison between the model Flat Plate Base-Thermal Cell Absorber (FPBTCA) and Flat Plate Solar Collector (FPSC). Based on the graph, it shows that the highest efficiency for FPBTCA is 30.24 % at 360 minutes. The highest efficiency for FPSC is also the same at 360 minutes, and the efficiency is 21.81 %. Based on the graph, it shows the efficiency of FPBTCA is consistent while the solar radiation is decreased

within 120 minutes and 180 minutes. It can be concluded that the increase in solar radiation could increase the efficiency of FPBTCA and FPSC. FPBTCA performance is better when operating at outdoors as compared to the FPSC.

FPBTCA design is focused more on the cell absorber attached at the top of the absorber collector. The main factor involved when designing the FPBTCA is the thickness and mass of the cell absorber. When the thickness and mass is increased, then the performance of FPTCA is also increased, this is because the cell absorber absorbs high heat energy from solar radiation. Thermal cell absorber will absorb the heat from the solar radiation and store the heat inside the absorber. Thermal cell absorber's design should be carried out with the best thickness and mass, also depending on the FPBTCA size, because it affects the cell absorber's performance. Having cell absorber thickness and mass which are extreme, results in the cell absorber temperature dropping and this affects the absorber's base temperature. Based on the configuration, the drying chamber temperature also drops. Temperature difference at the cell absorber surface will affect the performance of FPBTCA. When the temperature difference is high, then the heat gain by the cell absorber also increases as compared to FPSC.

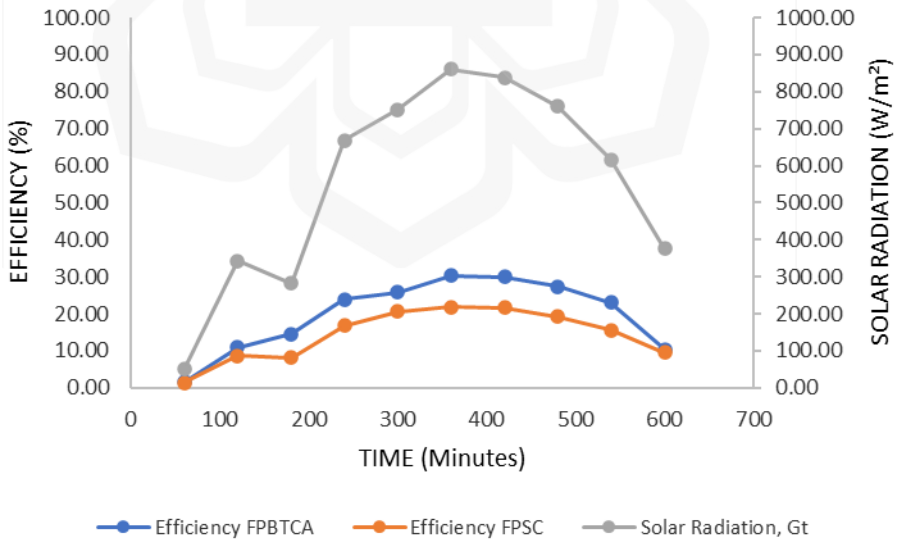

Figure 4.29: Efficiency (%) versus Time (Minutes) and Solar Radiation (W/m^2)

4.8.3 HEAT CONDUCTION, *Q* (J) BETWEEN FPBTCA AND FPSC

Heat conduction in a solar collector refers to the transfer of thermal energy from a hot surface to a cooler one through direct contact. It occurs when there is a temperature difference between two materials, and heat moves from the hotter material to the cooler one until they reach thermal equilibrium. The rate of heat conduction in a solar collector is influenced by several factors, including the material properties of the collector, the temperature difference, and the area of contact between the materials. Figure 4.30 shows the heat conduction, *Q* (J) versus Time (Minutes), and solar radiation between FPBTCA and FPSC. Based on the graph, the FPTCA shows the highest heat conduction, which is 2424.91 J at 360 minutes, while at the same time, FPSC also shows the most increased heat conduction and the value is 1749.06 J.

The heat conduction difference between FPBTCA and FPSC is 675.85 J. The condition occurs when the solar radiation is at elevated condition, which is 860.03 W/m^2. It can be concluded that the performance of FPBTCA and FPSC depends on the solar radiation absorbed by the absorber collector. If the solar radiation is decreased, then heat conduction for FPBTCA and FPSC also decreases.

Furthermore, the FPBTCA represents a high value of heat conduction all day than FPSC. Heat energy is stored in the cell absorber and then transferred to the absorber base. The cell absorbs the stored heat energy, and then it can be used when the solar radiation has dropped, and it will then be transferred to the drying chamber. A cell absorber is designed to store the heat energy from solar radiation and could be used during cloudy weather conditions.

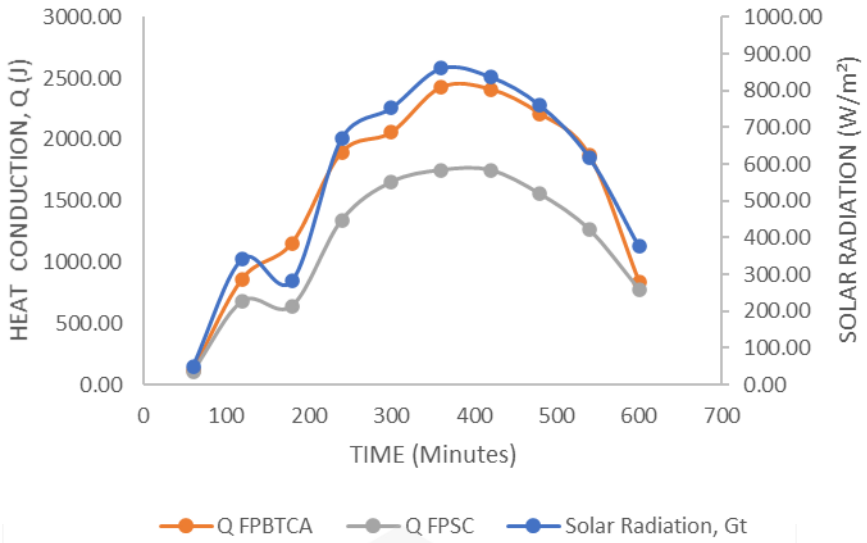

Figure 4.30: Heat conduction, Q (J) versus Time (Minutes) and Solar Radiation (W/m^2).

4.9 TECHNO-ECONOMICS EVALUATION OF THE FLAT PLATE BASE-THERMAL CELL ABSORBER (FPBTCA)

The main costing factor involved in Flat Plate Solar Collectors is the design itself. Flat Plate Collector efficiency and performance depend on the weather conditions such as the fluctuation of solar energy sources. Using Flat Plate Solar Collector (FPSC) with active system such as a fan for air flow will increase power consumption usage. A flat plate Base-Thermal cell Absorber (FPBTCA) will overcome the power consumption by using a passive system which does not use any mechanical devices in the design.

Based on the design, it has advantages as compared to the active system of Flat Plate Solar Collector. The short-and long-term cost, such as installation and operating, should be done to evaluate the financial effect of FPBTCA. So, the future application of FPBTCA is more reliable than FPSC. The economic evaluation in this research is focused on the collector and the thermal absorber only, as other components used in the experiments are for experimental purposes.

4.10 FPBTCA ECONOMIC EVALUATION: COST SAVINGS

Beckman, Klein, and Duffie (1977) introduced the concept of solar savings, which is the difference between the utilized cost of a conventional system and a solar system. It can be summarized as:

$$Solar\ savings = costs\ of\ conventional\ energy - \ costs\ of\ solar\ energy \quad 5.6$$

In this case, the comparison was made between FPBTCA and Flat Plate Solar Collector (A A Razak, 2017) (power consumption: 18 W). The comparison was made based on a low voltage commercial tariff of 0.44 RM/kWh (TNB, 2014), with estimated working hours of 8 hours. The initial cost of FPBTCA, is RM 12.93, considering the cost of structure and fabrication. Then the other is the maintenance cost of FPBTCA based on the work required to be performed at the FPBTCA annually was estimated as RM 50, including cost of labor. Based on the calculation from Equation 5.6, it was determined that the total solar savings within the first year of operation were 92.93 % lower than the conventional electrical household dryer.

FPBTCA was developed as a passive solar collector without using mechanical components and power consumption. There is an advantage to the maintenance of FPBTCA over FPSC, which is lower in maintenance. The maintenance of FPBTCA only involves touchup painting work, cleaning of dust, and insulation replacement (if required in the 1st year). The maintenance of FPSC is expensive, such as electrical component replacement and mechanical component replacement. Table 4.22 presents the detailed cost projection for these two devices based on the first year of device installation.

Table 4.22: Cost projection of conventional electrical household dryer and FPBTCA for the first year of installation and cost-saving by solar energy

Description	Solar Collector	FPBTCA
Power consumption, W	18	0
Operating hours, h	8	8
Hourly power consumption, kWh	0.144	0
Electricity price, RM/kWh	0.44	0
Cost for 1 day, RM	0.055	0
Cost for 1 year, RM	16.5	0
Maintenance cost per year, RM/year	100	50
Initial cost, RM	773	12.93
Total cost (first-year), RM	889.5	62.93
Cost savings, RM	826.57	
Saving rate, %	92.93	

4.11 EVALUATION OF FPBTCA COST-EFFECTIVENESS

The cost involved in fabricating of FPBTCA, is the thermal absorber collector cost. The cost of workmanship and material influences the thermal absorber collector. Table 4.23 shows the cost of thermal absorber for FPBTCA and FPSC. The cost of FPSC is the cheapest because it only involves a simple design and only the cutting process of the thermal absorber collector. The cost of FPBTCA involves cutting the thermal cell absorber attached to the absorber base-collector.

Table 4.23: The cost of thermal absorber

Thermal absorber type	Flat Plate Solar Collector (FPSC)	Flat Plate Base-Thermal Cell Absorber (FPBTCA)
Absorber base area, m^2	0.0441	0.0441
Thermal cell area, m^2		0.01
Price absorber base per area, RM/m^2	31.24	31.24
Price Thermal cell per area , RM/m^2		54
Absorber base price per area, RM	1.38	1.38
Thermal cell price per area RM		0.54
Cost of Workmanship,	10	12
Thermal absorber material cost, RM	1.38	1.92
Total thermal absorber cost, RM	11.38	13.92

Cost-effectiveness numerical calculations were implemented with the value for global solar radiation of 700 W/m2 and average ambient temperature at 28 ºC. Collector's effective operational time for a year was estimated at 300 days and 8 hours per day.

The FPBTCA cost includes the cost of glass cover (RM6), cost of thermal absorber (RM6), cost of structure (RM3), costs of insulation (RM3), cost of electricity (RM 0.44 / kWh), cost of fabrication (RM12) and cost of maintenance (10%CI). The Interest rate was assumed at 10 % per year, and the collector’s life duration was estimated at up to 10 years. Table 4.24 shows the details of the parameters for cost-effectiveness.

Table 4.24: Cost effective parameter for FPBTCA

Parameters	Value
Annual average radiation intensity	700 W/m2
Operational time	top=300 $days$ / year, 8 hours /day
Cost of glass cover	RM6
Cost of thermal absorber material	RM13.92
Cost of structure	RM3
Cost of insulation	RM3
Cost of electricity	RM 0.44 / kWh
Cost of fabrication	RM12
Cost of maintenance	10 % CI
Interest rate (i)	10%
Collector life time (n)	10 years Absorber base area, m2

4.12 DISCUSSION

There are several parameters that should be considered when designing a new Flat Plate Solar Collector (FPSC). The parameters such as absorber base materials, absorber base thickness, air gap distance, double glass, glass thickness, thermal cell thickness, and material. The parameter affects the efficiency and performance of Flat Plate Solar Collectors (FPSC). This study's focus is to develop Flat Plate Base-Thermal Cell (FPBTCA) based on parameter configuration. The experiment was done indoor by using artificial solar radiation, and several discussions are made as follows:

i) Stainless Steel 304 flat plate absorber-collector has a higher heat charging capacity than Aluminum flat plate absorber capacity. Stainless Steel 304 flat plate absorber also has the highest total heat gain. It showed that Stainless Steel absorbed high heat during exposure to solar radiation and stored the heat energy inside the absorber collector. Heat energy is used when solar radiation drops. Stainless steel has high heat resistance, meaning it can withstand high temperatures without losing its strength or durability. This makes it ideal for use in applications when exposed to high temperatures.

By storing excess heat, a solar collector with heat storage can provide a consistent source of space heating, even during periods of low or no solar radiation. By reducing the need for additional energy generation during periods of high demand, heat storage in a solar collector can lead to cost savings. Stainless steel could be used as thermal cell material and aluminum as absorber base-collector material.

ii) Coated surfaces in solar collectors refer to surfaces that have been treated with a coating material to enhance their performance in absorbing and converting solar radiation into heat. The coat shows a significant effect on the performance of the absorber collector. Aluminum-coated plate showed the highest flat plate absorber temperature than non-coated aluminum. It also represents a higher heat gain rate than a non-coated aluminum absorber collector. Coating materials, such as black or selective coatings, can be designed to have high absorbance, allowing the collector to absorb more of the incoming solar radiation and converting it into heat. Coated surfaces can also be designed to have low reflectance, which reduces the amount of incoming solar radiation that is reflected away from the collector, increasing the energy gain of the collector. By improving the absorption and reducing the reflection of incoming solar radiation, coated surfaces can increase the overall efficiency of the collector, resulting in more usable heat being generated from a given amount of solar radiation.

iii) One of the key components of a solar collector is the cover or glazing, which protects the internal components and helps to retain heat within the collector. The thickness of the glass used as a cover can have a significant impact on the performance of the solar collector. The different configurations of glass thickness show the different performances of flat plate absorber collectors. Based on the result, 2.0 mm glass thickness has a higher maximum flat plate absorber collector and higher heat gain rate than other glass thickness configurations. It can be concluded that the glass thickness of 2.0 mm received high solar radiation through the glass to be absorbed by the absorber collector. One of the main effects of glass thickness on solar

collectors is its impact on heat loss. Thicker glass provides greater insulation, reducing the amount of heat that is lost from the collector. This results in a higher temperature of the fluid being heated and a higher energy output from the collector. On the other hand, thinner glass allows for more heat to escape, resulting in a lower temperature of the fluid and a lower energy output. The thickness of the glass also affects the transmission of solar radiation into the collector. Thicker glass can reduce the amount of solar radiation that is transmitted, reducing the energy gain of the collector. However, this effect can be offset by using low-iron or high-transmission glass, which provides better transmission of solar radiation compared to regular glass. Another factor to consider is the structural integrity of the collector. Thicker glass provides greater strength and stability, making it less likely to break or deform under normal operating conditions. Proper handling should be considered when using lesser thickness of glass as flat plate solar collector glazing.

iv) The air gap distance in a solar collector refers to the distance between the cover or glazing and the absorber plate. This space is typically filled with air, which acts as an insulating layer, reducing the amount of heat that is lost from the collector. The air gap distance between the glass and absorber collector affects the flat plate absorber's collector temperature. The flat plate absorber temperature for an air gap distance of 10.0 mm is selected as the suitable parameter because it increases rapidly and has a higher heat gain rate when exposed to solar radiation. By controlling the air gap distance, it is possible to optimize the thermal performance of the collector. A larger air gap provides greater insulation, reducing heat loss and increasing the temperature of the fluid being heated. However, a larger air gap also results in a lower rate of heat transfer from the absorber plate to the air, reducing the energy output of the collector. By adjusting the air gap distance, it is possible to optimize the trade-off between thermal performance and structural stability, thus reducing the cost of the collector.

v) Thermal cell absorber collector thickness contributes to the performance of FPSC. Stainless steel material with 1.0 mm thickness showed better flat plate absorber collector temperature and higher heat gain rate than other thickness configurations. Stainless steel has a high thermal conductivity, which helps to transfer heat from the absorber plate to the fluid being heated. This results in higher energy output from the collector and improved thermal performance. Stainless steel is highly resistant to corrosion, which is important for ensuring the longevity and performance of the solar collector. This is particularly important in areas with high humidity or high levels of pollutants, where other materials may degrade over time. Stainless steel is a strong and durable material that can withstand harsh weather conditions and high temperatures, making it an ideal choice for use in solar collectors. By using stainless steel in a solar collector, it is possible to create a long-lasting, efficient, and cost-effective means of harnessing the power of the sun.

vi) Flat plate absorber base-collector thickness is selected based on its performance when exposed to solar radiation. Aluminum, 0.5 mm thickness, increased rapidly during the charging period and also has a higher heat gain rate. Aluminum is a popular choice for absorbers in solar collectors due to its high thermal conductivity and durability. Aluminum has a high thermal conductivity, which allows it to quickly transfer heat from the absorbing surface to the fluid that is being heated. This results in a more efficient solar collector, as more of the absorbed solar radiation is converted into usable heat. Another benefit of using aluminum as the absorber in solar collectors is its durability. Aluminum is a corrosion-resistant material, which means that it can withstand the elements and last for many years without degradation. Additionally, aluminum is a lightweight material, which makes it easier to handle and install compared to heavier materials such as copper. The use of aluminum as the absorber in solar collectors also has some drawbacks. One of the main disadvantages is that aluminum is a reflective material, which means that some of the incoming solar radiation will be reflected away from the absorber, reducing the energy gain of the collector.

vii) Double glazing in a solar collector refers to the use of two layers of glass to create an insulated barrier. Double glass and a single glass of glazing could affect the performance of FPSC. By using double glass as a glazing material, the flat plate absorber collector temperature is higher than single glass. Double glass also has high heat gain rate than single glass. Double glass traps the heat from the absorber collector to the surroundings. The double glazing provides an insulating layer that helps to reduce heat loss from the collector. This results in a higher temperature of the fluid being heated and a higher energy output from the collector. The double glazing provides additional protection against weather and physical damage, making the solar collector more durable and long-lasting. Double glazing helps to reduce condensation, which can lead to corrosion and other problems in the collector. Double glazing provides a clean, modern appearance that can enhance the aesthetic appeal of the solar collector.

Based on the preliminary experiments done under simulation (300 seconds charging and 300 seconds discharging, 600 seconds charging and 600 seconds discharging) shows the results of the performance for different types of thermal absorber collectors. There are several conclusions which can be made:

i) Thermal cell absorbers have a more significant effect on the performance of FPBTCA than FPSC. Thermal cells affect the thermal performance of FPBTCA. By using a thermal cell attached to the top surface of FPSC, it will increase the overall performance of FPBTCA.

ii) Aluminum absorber base with stainless steel cell 1.0 mm thickness is selected as a design parameter for FPBTCA. Aluminum absorber base with stainless steel cell 1.0 mm thickness has good performance in terms of outlet temperature, which is, it has a high outlet temperature inside the drying chamber compared to the other absorber collector configurations.

iii) Aluminum absorber base with stainless steel cell 1.0 mm has better performance in terms, of heat storage ($Q_{storage}$), the heat transfer rate of the collector ($\dot{Q}$) and efficiency of the collector (%). It can be concluded that FPBTCA has improved its performance over FPSC. The efficiency of a solar collector refers to the ratio of the amount of thermal energy collected and converted to useful energy compared to the total amount of solar radiation received by the collector. In other words, it is a measure of how well the collector converts solar radiation into thermal energy. To maximize the efficiency of a solar collector, it is important to have a high-quality absorber plate with a high absorption coefficient and low emission coefficient.

iv) Aluminum absorber with stainless steel cell of 1.0 mm has higher energy gain at the bottom plate, which is known as a dummy load. The Absorber collector absorbs the energy gained during exposure to solar radiation. The energy gain increases when solar radiation is increased. To increase the energy gain, it is important to have a high-quality absorber plate with a high absorption coefficient and low emission coefficient. The surface of the absorber plate should also be treated to minimize the reflection of solar radiation. The temperature of the air-drying chamber should be maintained at a suitable level to ensure efficient heat transfer.

v) The research proved the performance of the thermal cell absorber attached to a flat plate absorber collector (FPBTCA) could be used to produce modest thickness design and lightweight, as well as could be utilized for portable collector application. FPBTCA produces better thermal performance and efficiency than FPSC.

The outdoor experiment was done for 7 days (4 – 9 march 2021 and 21 march 2021) from morning until evening. The results from the outdoor experiment shows that Flat Plate Base-Thermal Cell Absorber performs better than Flat Plate Solar Collectors (FPSC). Based on outdoor experimental works, the discussions are as follows:

i) FPBTCA had better performances in terms of heat absorption as compared to FPSC. Thermal cell absorbers absorb and store heat from solar radiation. The heat absorption could be improved by the use of an absorber plate, which is made of a material with high thermal conductivity and high absorption capacity for solar radiation. The absorbed solar energy is then transferred to air that circulates through the collector to transfer the thermal energy to a storage system or to be used directly for heating.

ii) FPBTCA shows a low discharge rate when the solar radiation drops. It also illustrates better thermal absorber heat storage, which provides consistent heat discharge rate as compared to FPSC. A low discharge rate in a solar collector refers to a situation where the rate at which thermal energy is transferred from the collector to the storage system or to the end-use application is lower than expected. This can result in lower thermal energy output and reduced efficiency of the solar thermal system. When the heat transfer system is not designed or installed properly, it may result in low heat transfer efficiency, leading to a low discharge rate.

iii) The fluctuation of solar radiation is advantageous to FPTCA performance over FPSC. FPBTCA performance was consistent because the design of the thermal cell absorber could be used to solve the heat storage capability of FPSC. FPBTCA has advantages because it has a thermal cell absorber attached at the top surface of the absorber base-collector and can store high heat energy from solar radiation. It could be used when there is an absence of solar radiation.

iv) FPBTCA was designed to meet the requirement of Good Manufacturing Practice (GMP) for drying food, whereby a selective surface could be coated outside on a thermal absorber to avoid direct contact with drying material. The advantage is, the portable FPBTCA has potential in drying food.

4.13 CHAPTER SUMMARY

An experiment was done to determine the suitable parameters and materials to consider when designing FPBTCA. FPBTCA was designed as a portable solar collector by reducing the weight with the lesser thickness of the thermal cell absorber collector. The experimental results proves that FPBTCA had greater efficiency in terms of heat storage capability, discharge rate, and thermal absorption response time as compared to FPSC. Both FPBTCA and FPSC use aluminum as an absorber base material to increase the high discharge rate that could be transferred to the drying chamber.

Stainless steel thermal cell is attached at the top surface of the absorber base-collector to solve the heat storage of FPSC. When the weather is cloudy, the solar radiation drops and affects the performance of the solar collector. Thermal cells absorb and store the heat energy from solar radiation and then it could be used when there is fluctuation of solar radiation. Stainless steel thermal cell has a low discharge rate when transferred to the surrounding. It shows that stainless steel thermal cell has the capability to store heat energy more than other materials.

FPBTCA as a portable solar collector has advantages and could be introduced as the new design of solar thermal collector to strengthen the conventional FPSC. There are three categories of solar drying which are natural convection solar dryers, force convection dryers, and hybrid solar dryers. Based on that, it can be concluded Flat Plate Base-Thermal Cell Absorber (FPBTCA) can be used for drying products.

CHAPTER FIVE

CONCLUSION AND RECOMMENDATION

5.1 CONCLUSIONS

There were different techniques and methods applied with a focus to improve the performance of the Flat Plate Solar Collectors (FPSC). The purpose of this study is to investigate the theory behind Flat Plate Solar Collectors and the potential techniques that could be used to enhance performance. This chapter discusses the findings based on the results and discussion to overcome the objectives of this study. An experimental test rig was created with the aim of examining how the performance of the flat plate solar collector with an enhancement of the absorber collector using different types of material and thickness.

Conclusion for objective (i), which is to design and develop Flat Plate Base-Thermal Cell Absorber (FPBTCA) is given as follows:

i. To improve Flat Plate Solar Collector design which is to have a compact design with lesser thickness compared to conventional solar air heating systems such as V-Groove, corrugated, cross design, and fin type absorber solar collector absorber design. FPBTCA is designed by combining a drying chamber with an air collector to reduce the heat energy transfer from the air collector to the drying chamber. By combining a solar air collector and a drying chamber, it could increase the drying air temperature and reduce process time (Tuncer et al., 2020). The flat plate solar thermal collector integrated with the drying chamber has an advantage which is it has the stability of the air temperature in the absence of solar radiation (Jain & Tiwari, 2003). Integrated heat exchanger furthermore increases this performance and efficiency. In addition, this design does not require to use air circulation system such as a fan, and it will apply to natural convection.

ii. FPBTCA was designed and developed based on a design parameter experiment. Table 6.1 represents the chosen design parameters for Flat Plate Base-Thermal Cell Absorber (FPBTCA). By referring to the figure, matt black coating was used as the coating surface for the absorber collector. The air gap between the flat plate absorber collector and glass cover 1 is 10.0 mm. The air gap between glass cover 1 and glass cover 2 is 0.4 mm. The thermal cell absorber collector is stainless steel material with 1.0 mm thickness. For the flat plate absorber base-collector material is aluminum with a thickness of 0.5 mm. Glass thickness of 2.0 mm was used for glass cover 1 and glass cover 2.

Table 5.1: Chosen design parameters for Flat Plate Base-Thermal Cell Absorber (FPBTCA)

Design parameter	**Parameters**
Coating surface	Matt black coating
Air gap between flat plate absorber collector and glass cover 1	10.0 mm
Air gap between glass cover 1 and glass cover 2	0.4 mm
Thermal cell absorber (10 cm x 10 cm)	Stainless Steel 1.0 mm
Flat plate base absorber (18.5 cm x 25.5 cm)	Aluminium 0.5 mm
Glass thickness	2.0 mm

iii. There are two preliminary experiments that was conducted outdoors by using a solar simulator. Preliminary experiment 1 was done to FPBTCA by charging for 300 seconds and discharging for 300 seconds. Preliminary experiment 2 was done to FPBTCA by charging for 600 seconds and discharging for 600 seconds. The fan speed used in this experiment is 0.62 m/s. The flat plate absorber base-collector material is aluminum with 0.5 mm thickness. Four types of thermal cell absorber thickness were applied in the experiment, which is aluminum 0.5 mm, aluminum 1.0 mm, stainless steel 0.5 mm, and stainless steel 1.0 mm. By referring to the results in terms of heat storage ($Q_{storage}$), the heat transfer rate of the collector ($\dot{Q}$) and efficiency of the collector and storage shows that Stainless steel 1.0 mm with aluminium base absorber has a higher value.

iv. The higher total energy gain collected at the bottom plate as a dummy load in the drying chamber is stainless steel 1.0 mm with aluminum absorber base-collector. It also has a better temperature than other configurations. Stainless steel 1.0 mm with aluminum absorber base-collector has the maximum value of energy gain at 300 seconds for the bottom plate. The performance of the outlet temperature in the drying chamber of stainless steel with aluminum absorber has a higher value of energy gain which is at 300 seconds. The results show that the thermal cell absorber has significant effect on the performance of FPBTCA as compared to FPSC. A thermal cell absorber thickness of 1.0 mm is selected as the design parameter for FPBTCA. FPBTCA design focuses on reducing the thickness of the absorber base-collector and thermal cell absorber while maintaining its performance. This design involved has no mechanical component, and it's called natural convection.

To evaluate the effect of design parameters (such as absorber base materials, absorber base thickness, air gap distance, double glass, glass thickness, thermal cell thickness, and material) on the performance of the FPBTCA in objective (ii), draws the following conclusions:

i. The design parameter of flat plate solar collector (FPSC) that affects the performance and efficiency could be determined based on experimental and literature review. Aluminum materials are chosen as absorber base-collector because it is faster in charging than stainless steel material when exposed to solar radiation. The need for FPBTCA design also affects the absorber base material. Based on the FPBTCA design, the thermal cell absorber attaches at the top of the absorber base. So that the absorber base is closed from solar radiation. When the absorber base material has the capability to absorb solar radiation rapidly, the performance of FPTCA is enhanced as compared to FPSC.

ii. Aluminum absorber base thickness of 0.5 mm is selected as the absorber base thickness. The reason aluminum 0.5 mm is selected is when exposed to solar radiation, the aluminum 0.5 mm absorber base temperature increases rapidly.

iii. The air gap distance between the absorber collector and glass is an important factor that cannot be ignored when designing FPBTCA. It contributes to the overall performance of FPBTCA because the absorber collector temperature will be increased or decreased when the air gap is either low or high from the absorber collector.

iv. Double glass configuration also affects the performance of FPTCA. There are significant effects of using double glass when setting up a new design of FPBTCA. The double glass shows the highest temperature for flat plate absorber collector than single glass.

v. Thermal cell materials are selected based on their capability to store heat energy when exposed to solar radiation. The thermal cell materials also should have low discharge rate than other materials. Stainless steel 304 is applied to the FPBTCA because it has the advantage to store heat energy over other materials and can be used during cloudy weather conditions. Based on the experiment, the 1.0 mm stainless steel plate has a higher flat plate absorber-collector temperature than other stainless steel thickness . A thermal cell has been introduced to be attached to the absorber base-collector to enhance the performance and efficiency of the solar thermal collector system. This application of using thermal cells enhanced the new design of solar thermal collectors with a compact design.

To develop and validate the mathematical model for FPBTCA in passive condition objective (iii) projected the following conclusions:

i. The mathematical modelling was developed based on heat transfer analysis. The energy balance of the FPBTCA is developed to conduct the mathematical modelling. The mathematical modelling showed that the error between Qin and Qout is below 5 %. It can be concluded that the energy balance equation proved that significant results between *Q*in and *Q*out of the FPBTCA.

ii. Based on the mathematical modelling a comparison will be made between FPBTCA and FPSC. The results also shows that the highest efficiency for FPBTCA is at 360 minutes .

iii. The heat conduction difference between FPBTCA and FPSC is 675.85 J. The condition occurs when the solar radiation is at high condition, which is 860.03 W/m^2. It can be concluded that the thermal cell absorber thickness and mass contribute to the performance of FPBTCA. Using the highest thickness and mass as thermal cell absorber, results in the highest efficiency and heat conduction, but the temperature of the drying chamber would slowly drop so that these should be considered when choosing the right thermal cell thickness and mass configuration.

5.2 RECOMMENDATIONS

In future, with the design of a Flat Plate Base-Thermal Cell Absorber (FPBTCA) as a new method to enhance its performance and efficiency, the study can be further extended based on the following:

i. To study the efficiency and performance by using more than one Thermal Cell attached at the top of the base absorber collector and increasing the size of the Flat Plate Solar Collector.

ii. To extend the application of FPBTCA towards the drying of specific agricultural products, the study includes a comparison study on the drying kinetics and the development of a mathematical model of respective products.

iii. To perform a theoretical study on the heat distribution inside the Thermal Cell material during the charging and discharging cycle of the FPBTCA by using commercial software.

iv. To investigate the other possibilities of Thermal Cell material attached at the top surfaces of the base absorber collector.

REFERENCES

A A Razak. (2017). *TitlePerformance of Bi-Metallic Cross Matrix Absorber in Air Based Solar Collector,*. Universiti Kebangsaan Malaysia.

Ab Ghani, M. R., Affandi, R., Gan, C. K., Raman, S. H., & Zanariah, J. (2014). The influence of concentrator size, reflective material and solar irradiance on the parabolic dish heat transfer. *Indian Journal of Science and Technology*, *7*(9), 1454–1460.

Abbas, R., Muñoz-Antón, J., Valdés, M., & Martínez-Val, J. M. (2013). High concentration linear Fresnel reflectors. *Energy Conversion and Management*, *72*, 60–68.

Abene, A., Dubois, V., Le Ray, M., & Ouagued, A. (2004). Study of a solar air flat plate collector: Use of obstacles and application for the drying of grape. *Journal of Food Engineering*, *65*(1), 15–22.

Abu-Hamdeh, N. H., Bantan, R. A. R., Khoshvaght-Aliabadi, M., & Alimoradi, A. (2020). Effects of ribs on thermal performance of curved absorber tube used in cylindrical solar collectors. *Renewable Energy*, *161*, 1260–1275.

Ahmad, S., & Ilham, M. M. (2018). Absorber Thickness Effect on The Effectiveness of Solar Collectors to Production Hot Air For Drying. 04028, 1–6.

Akhtar, N., & Mullick, S. C. (2012). Effect of absorption of solar radiation in glass-cover(s) on heat transfer coefficients in upward heat flow in single and double glazed flat-plate collectors. *International Journal of Heat and Mass Transfer*, *55*(1–3), 125–132.

Akpinar, E. K., & Koçyiĝit, F. (2010). Energy and exergy analysis of a new flat-plate solar air heater having different obstacles on absorber plates. *Applied Energy*, *87*(11), 3438–3450.

AL-Khaliffajy, M. and Mossad, R. (2011). Optimization of the Air Gap Spacing In a Solar Water Heater with Double Glass. *9th Australasian Heat and Mass Transfer Conference-9AHMTC*, *1*.

Álvarez, A., Tarrío-Saavedra, J., Zaragoza, S., López-Beceiro, J., Artiaga, R., Naya, S., & Álvarez, B. (2016). Numerical and experimental study of a corrugated thermal collector. *Case Studies in Thermal Engineering*, *8*, 41–50.

Amankwah, E. A. Y., Dzisi, K. A., van Straten, G., van Willigenburg, L. G., & van Boxtel, A. J. B. (2017). Distributed mathematical model supporting design and construction of solar collectors for drying. *Drying Technology*, *35*(14), 1675–1687.

Amer, B. M. A., Hossain, M. A., & Gottschalk, K. (2010). Design and performance evaluation of a new hybrid solar dryer for banana. *Energy Conversion and Management*, *51*(4), 813–820.

Anirudh, K., & Dhinakaran, S. (2020). Numerical study on performance improvement of a flat-plate solar collector filled with porous foam. *Renewable Energy*, *147*, 1704–1717.

Ardente, Fulvio & Beccali, Giorgio & Cellura, Maurizio & Lo Brano, V. (2005). Life cycle assessment of a solar thermal collector. *Renewable Energy, Elsevier*, *30(7)*, 1031–1054.

B. Norton. (1992). *Solar Energy Thermal Technology*. Springer-Verlag London Limited.

Bahadori, A., & Nwaoha, C. (2013). A review on solar energy utilisation in Australia. *Renewable and Sustainable Energy Reviews*, *18*, 1–5.

Bakos, G. C. (2006). Design and construction of a two-axis Sun tracking system for parabolic trough collector (PTC) efficiency improvement. *Renewable Energy*, *31*(15), 2411–2421.

Bande, Y. M., & Mariah, N. A. (2014). Flat plate solar collectors and applications: A review. *Pertanika Journal of Science and Technology*, *22*(2), 365–386.

Beckman, J. A. D. and W. A. (2013). *Solar engineering of thermal process*.

Belessiotis, V., & Delyannis, E. (2011). Solar drying. *Solar Energy*, *85*(8), 1665–1691.

Bellos, E. (2019). Progress in the design and the applications of linear Fresnel reflectors – A critical review. *Thermal Science and Engineering Progress*, *10*(January), 112–137.

Billy Anak Sup. (2010). *Effect Of Absorber Plate Material On Flat Plate Collector Efficiency*.

Blanco, M. J., & Miller, S. (2017). Introduction to concentrating solar thermal (CST) technologies. *Advances in Concentrating Solar Thermal Research and Technology*, 3–25.

Brinkworth, B. J. (1974). Solar energy. *Nature*, *249*(5459), 726–729.

Buker, M. S., & Riffat, S. B. (2015). Building integrated solar thermal collectors - A review. *Renewable and Sustainable Energy Reviews*, *51*, 327–346.

Cengel, Y. A. (2007). *Introduction to Thermodynamics and Heat Transfer, Second Edition.* McGraw-Hill Science/Engineering/Math.

Chafie, M., Ben Aissa, M. F., & Guizani, A. (2018). Energetic end exergetic performance of a parabolic trough collector receiver: An experimental study. *Journal of Cleaner Production*, *171*, 285–296.

Chang, C. (2016). Tracking solar collection technologies for solar heating and cooling systems. *Advances in Solar Heating and Cooling*, 81–93.

Cherif, H., Ghomrassi, A., Sghaier, J., Mhiri, H., & Bournot, P. (2019). A receiver geometrical details effect on a solar parabolic dish collector performance. *Energy Reports*, *5*, 882–897.

Chieruzzi, M., Cerritelli, G. F., Miliozzi, A., & Kenny, J. M. (2013). Effect of nanoparticles on heat capacity of nanofluids based on molten salts as PCM for thermal energy storage. *Nanoscale Research Letters*, *8*(1), 1–9.

Choi, S U.S., & Eastman, J. A. (1963). Thermal Conductivity of Fluids. Ethane. In *Journal of Chemical and Engineering Data* (Vol. 8, Issue 3, pp. 281–285).

Choudhary, S., Sachdeva, A., & Kumar, P. (2020). Influence of stable zinc oxide nanofluid on thermal characteristics of flat plate solar collector. *Renewable Energy*, *152*, 1160–1170.

Colangelo, G., Favale, E., Miglietta, P., & De Risi, A. (2016). Innovation in flat solar thermal collectors: A review of the last ten years experimental results. *Renewable and Sustainable Energy Reviews*, *57*, 1141–1159.

Collado, F. J., & Guallar, J. (2019). Quick design of regular heliostat fields for commercial solar tower power plants. *Energy*, *178*, 115–125.

Dixon-hardy, D. W., Heggs, P., & Al-damook, M. (2019). *CFD Modelling of Solar Air Heaters School of Chemical and Process Engineering MSc . Advanced Chemical Engineering CAPE5000M Research Project Final Report CFD modelling of solar air heaters Author : Abdulaziz Doukhi Supervisor (s): Dr . Darron Dixon-Hard*. *May 2020*.

Dobriyal, R., Negi, P., Sengar, N., & Singh, D. B. (2020). A brief review on solar flat plate collector by incorporating the effect of nanofluid. *Materials Today: Proceedings*, *21*(xxxx), 1653–1658.

Duffie, J. A., & Beckman, W. A. (1991). *Solar Engineering Of Thermal Processes, Photovoltaics and Wind* (2nd Edition).

El-Sebaii, A. A., & Shalaby, S. M. (2012). Solar drying of agricultural products: A review. *Renewable and Sustainable Energy Reviews*, *16*(1), 37–43.

Essalhi, H., Tadili, R., & Bargach, M. N. (2018). Comparison of thermal performance between two solar air collectors for an indirect solar dryer. *Journal of Physical Science*, *29*(3), 55–64.

Fakoor Pakdaman, M., Lashkari, A., Basirat Tabrizi, H., & Hosseini, R. (2011). Performance evaluation of a natural-convection solar air-heater with a rectangular-finned absorber plate. *Energy Conversion and Management*, *52*(2), 1215–1225.

Fan, M., You, S., Gao, X., Zhang, H., Li, B., Zheng, W., Sun, L., & Zhou, T. (2019). A comparative study on the performance of liquid flat-plate solar collector with a new V-corrugated absorber. *Energy Conversion and Management*, *184*(January), 235–248.

Ferahta, F. Z., Bougoul, S., Ababsa, D., & Abid, C. (2011). *Numerical Study of the Convection in the Air Gap of a*. *6*, 176–184.

Fudholi, A., & Sopian, K. (2019). A review of solar air flat plate collector for drying application. *Renewable and Sustainable Energy Reviews*, *102*(December 2017), 333–345.

Fudholi, A., Sopian, K., Gabbasa, M., Bakhtyar, B., Yahya, M., Ruslan, M. H., & Mat, S. (2015). Techno-economic of solar drying systems with water based solar collectors in Malaysia: A review. *Renewable and Sustainable Energy Reviews*, *51*,

809–820.

Fudholi, A., Sopian, K., Othman, M. Y., Ruslan, M. H., & Alghoul, M. A. (2008). Heat Transfer Correlation for the V-Groove Solar Collector. *8th WSEAS International Conference on SIMULATION, MODELLING and OPTIMIZATION (SMO '08) Santander, Cantabria, Spain, September 23-25, 2008 Heat*, *October 2014*, 177–182.

Gao, D., Gao, G., Cao, J., Zhong, S., Ren, X., Dabwan, Y. N., Hu, M., Jiao, D., Kwan, T. H., & Pei, G. (2020). Experimental and numerical analysis of an efficiently optimized evacuated flat plate solar collector under medium temperature. *Applied Energy*, *269*(April), 115129.

Gao, Y., Zhang, Q., Fan, R., Lin, X., & Yu, Y. (2013). Effects of thermal mass and flow rate on forced-circulation solar hot-water system: Comparison of water-in-glass and U-pipe evacuated-tube solar collectors. *Solar Energy*, *98*(PC), 290–301.

Gomesh, N., Daut, I., Irwanto, M., Irwan, Y. M., & Fitra, M. (2013). Study on Malaysian's perspective towards renewable energy mainly on solar energy. *Energy Procedia*, *36*, 303–312.

Gordon, J. M. (1986). Nonimaging solar energy concentrators (CPC's) with fully illuminated flat receivers: A viable alternative to flat-plate collectors. *Journal of Solar Energy Engineering, Transactions of the ASME*, *108*(3), 252–256.

Hafez, A. Z., Soliman, A., El-Metwally, K. A., & Ismail, I. M. (2016). Solar parabolic dish Stirling engine system design, simulation, and thermal analysis. *Energy Conversion and Management*, *126*, 60–75.

Hakam, M., Ichsani, D., & Suroso, C. (2016). Numerical investigation of heat transfer and fluid flow characteristic of V-corrugated plate solar air collector with prismatic fin as an extended surface. *AIP Conference Proceedings*, *1778*(2016).

Hamed, M., Fellah, A., & Ben Brahim, A. (2014). Parametric sensitivity studies on the performance of a flat plate solar collector in transient behavior. *Energy Conversion and Management*, *78*, 938–947.

Hawwash, A. A., Abdel Rahman, A. K., Nada, S. A., & Ookawara, S. (2018). Numerical Investigation and Experimental Verification of Performance Enhancement of Flat Plate Solar Collector Using Nanofluids. *Applied Thermal Engineering*, *130*, 363–374.

Hottel, H.C., Whillier, A. (1958). No Title. *Evaluation of Flat-Plate Solar Collector Performance.*, *2*, 74–104.

Hottel, H.C., Woertz, B.B. (1942). No Title. *The Performance of Flat-Plate Solar-Heat Collectors.*, *62*, 91–104.

Huff, R., Layfield, B., Leitner, S., Zhang, X., Alharbi, A., Yao, W., & Science, C. (1950). *ECE 421 / 599 Group Presentation Solar Energy*.

Hussein, A. K. (2016). Applications of nanotechnology to improve the performance of solar collectors - Recent advances and overview. *Renewable and Sustainable Energy Reviews*, *62*, 767–792.

Ion, V., & Martins, G. (2006). Design, developing and testing of a solar air collector. *The Annals of "Dunarea de Jos" University of Galati. ...*, *2*(1), 7–10. http://xa.yimg.com/kq/groups/23188191/1434267579/name/design+of+a+solar+collector.pdf

Ismail, K. A. R., & Henr, J. R. (2003). *Modeling and simulation of a simple glass window*. *80*, 355–374.

J.Shbailat, S., & A. Jassim, N. (2018). Energy and Exergy Analysis of Dual Channel Solar Air Collector with Perforating "V" Corrugated Absorber Plate. *Basrah Journal of Engineering Science*, *18*(1), 10–15.

Jain, D., & Tiwari, G. N. (2003). Thermal aspects of open sun drying of various crops. *Energy*, *28*(1), 37–54.

Jiang, C., Yu, L., Yang, S., Li, K., Wang, J., Lund, P. D., & Zhang, Y. (2020). A review of the compound parabolic concentrator (CPC) with a tubular absorber. *Energies*, *13*(3), 1–31.

John A. Duffie and William A. Beckman. (2006). *Solar Engineering of Thermal Processes*.

Kabeel, A. E., Khalil, A., Shalaby, S. M., & Zayed, M. E. (2016). Investigation of the Thermal Performances of Flat, Finned, and v-Corrugated Plate Solar Air Heaters. *Journal of Solar Energy Engineering, Transactions of the ASME*, *138*(5).

Kabeel, A. E., & Mečárik, K. (1998). Shape optimization for absorber plates of solar air collectors. *Renewable Energy*, *13*(1), 121–131.

Kalogirou, S. (2003). The potential of solar industrial process heat applications. *Applied Energy*, *76*(4), 337–361.

Kalogirou, S. A. (2002). Low Temperature Solar Collectors. *Encyclopedia of Life Support Systems, I.*

Kalogirou, S. A. (2004). Solar thermal collectors and applications. In *Progress in Energy and Combustion Science* (Vol. 30, Issue 3).

Kalogirou, S. A. (2008). Thermal performance, economic and environmental life cycle analysis of thermosyphon solar water heaters. *Journal of Solar Energy*.

Kaminski, K., Znaczko, P., Lyczko, M., Krolikowski, T., & Knitter, R. (2019). Operational properties investigation of the flat-plate solar collector with poliuretane foam insulation. *Procedia Computer Science*, *159*, 1730–1739.

Kim, Y., & Seo, T. (2007). Thermal performances comparisons of the glass evacuated tube solar collectors with shapes of absorber tube. *Renewable Energy*, *32*(5), 772–795.

Kodama, T. (2003). High-temperature solar chemistry for converting solar heat to chemical fuels. In *Progress in Energy and Combustion Science* (Vol. 29, Issue 6).

Kumar, M., Sansaniwal, S. K., & Khatak, P. (2016). Progress in solar dryers for drying various commodities. *Renewable and Sustainable Energy Reviews*, *55*, 346–360.

Kumar, N., Tyagi, A., Yadav, T., Prakash, O., Singh, V., & Tiwari, S. (2019). Heat Transfer Analysis of Flat Plate Air Collector. *IOP Conference Series: Materials Science and Engineering*, *691*(1).

Kumar, R., & Rosen, M. A. (2010). Thermal performance of integrated collector storage solar water heater with corrugated absorber surface. *Applied Thermal Engineering*, *30*(13), 1764–1768.

Kumaresan, G., Sridhar, R., & Velraj, R. (2012). Performance studies of a solar parabolic trough collector with a thermal energy storage system. *Energy*, *47*(1), 395–402.

Kürklü, A., Özmerzi, A., & Bilgin, S. (2002). Thermal performance of water-phase change material solar collector. *Renewable Energy*, *26*(3), 391–399.

Li, C., Zhai, R., & Yang, Y. (2017). Optimization of a heliostat field layout on annual basis using a hybrid algorithm combining particle swarm optimization algorithm and genetic algorithm. *Energies*, *10*(11).

Lin, M., Sumathy, K., Dai, Y. J., Wang, R. Z., & Chen, Y. (2013). Experimental and theoretical analysis on a linear Fresnel reflector solar collector prototype with V-shaped cavity receiver. *Applied Thermal Engineering*, *51*(1–2), 963–972.

M. Faizal Fauzan. (2015). *Energy , Heat Transfer And Economic Analysis Of Flat-Plate Solar Collector Utilizing Sio 2 Nanofluid Faculty Of Engineering*.

M. Kehrer, H. M. K. A. K. S. (2003). *Ecological Insulation Materials À Does Sorption Moisture Affect their*. *26*(3), 207–212.

Ma, L., Lu, Z., Zhang, J., & Liang, R. (2010). Thermal performance analysis of the glass evacuated tube solar collector with U-tube. *Building and Environment*, *45*(9), 1959–1967.

Makhanlall, D., & Jiang, P. (2015). Performance Analysis and Optimization of a Vapor-filled Flat-plate Solar Collector. *Energy Procedia*, *70*, 95–102.

Manikandan, J., & Sivaraman, B. (2016). Comparative studies on thermal efficiency of single and double glazed flat plate solar water heater. *ARPN Journal of Engineering and Applied Sciences*, *11*(9), 5521–5526.

Mawire, A., & Taole, S. H. (2014). Experimental energy and exergy performance of a solar receiver for a domestic parabolic dish concentrator for teaching purposes. *Energy for Sustainable Development*, *19*(1), 162–169.

Mekhilef, S., Safari, A., Mustaffa, W. E. S., Saidur, R., Omar, R., & Younis, M. A. A. (2012). Solar energy in Malaysia: Current state and prospects. *Renewable and Sustainable Energy Reviews*, *16*(1), 386–396.

Mintsa Do Ango, A. C., Medale, M., & Abid, C. (2013). Optimization of the design of a polymer flat plate solar collector. *Solar Energy*, *87*(1), 64–75.

Moghadam, A. J., Farzane-Gord, M., Sajadi, M., & Hoseyn-Zadeh, M. (2014). Effects of CuO/water nanofluid on the efficiency of a flat-plate solar collector. *Experimental Thermal and Fluid Science*, *58*, 9–14.

Mohamad, A. A. (1997). Integrated solar collector-storage tank system with thermal diode. *Solar Energy*, *61*(3), 211–218.

Mohammadi, K., & Sabzpooshani, M. (2013). Comprehensive performance evaluation and parametric studies of single pass solar air heater with fins and baffles attached over the absorber plate. *Energy*, *57*, 741–750.

Mokhtar, G., Boussad, B., & Noureddine, S. (2016). A linear Fresnel reflector as a solar system for heating water: Theoretical and experimental study. *Case Studies in Thermal Engineering*, *8*, 176–186.

Muhammad-Sukki, F., Ramirez-Iniguez, R., Abu-Bakar, S. H., McMeekin, S. G., & Stewart, B. G. (2011). An evaluation of the installation of solar photovoltaic in residential houses in Malaysia: Past, present, and future. *Energy Policy*, *39*(12), 7975–7987.

Musembi, M. N., Kiptoo, K. S., & Yuichi, N. (2016). Design and Analysis of Solar Dryer for Mid-Latitude Region. *Energy Procedia*, *100*(September), 98–110.

Nabnean, S., Janjai, S., Thepa, S., Sudaprasert, K., Songprakorp, R., & Bala, B. K. (2016). Experimental performance of a new design of solar dryer for drying osmotically dehydrated cherry tomatoes. *Renewable Energy*, *94*, 147–156.

Naik, H., Baredar, P., & Kumar, A. (2017). Medium temperature application of concentrated solar thermal technology: Indian perspective. *Renewable and Sustainable Energy Reviews*, *76*(February 2016), 369–378.

Nasir, A. (2004). Design, Construction and Experimental Study of the Thermal Performance of a Parabolic Cylindrical Trough Solar Air Heater. *Au J.T*, *8*(1), 21–26.

Nixon, J. D., Dey, P. K., & Davies, P. A. (2010). Which is the best solar thermal collection technology for electricity generation in north-west India? Evaluation of

options using the analytical hierarchy process. *Energy*, *35*(12), 5230–5240.

Norton, B. (2006). Anatomy of a solar collector. Developments in Materials, Components and Efficiency Improvements in Solar Thermal Collector Systems. *Refocus*, *7*(3), 32–35.

Pandey, K. M., & Chaurasiya, R. (2017). A review on analysis and development of solar flat plate collector. *Renewable and Sustainable Energy Reviews*, *67*, 641–650.

Panwar, N. L., Kaushik, S. C., & Kothari, S. (2011). Role of renewable energy sources in environmental protection: A review. *Renewable and Sustainable Energy Reviews*, *15*(3), 1513–1524.

Pekez, J., Lambić, M., & Stojadinović, S. (2013). Materials for flat plat solar collectors. *Metalurgia International*, *18*(2), 77–80.

Polvongsri, S., & Kiatsiriroat, T. (2011). Enhancement of Flat-Plate Solar Collector Thermal Performance with Silver Nano-fluid. *The Second TSME International Conference on Mechanical Engineering*, *2*, 1–7.

Ramalingam Senthil and Marimuthu Cheralathan. (2017). Effect of the Pcm in a Solar Receiver on Thermal. *Thermal Science*, *21*(6), 2803–2812.

Saghafifar, M. (2016). *Thermo-economic Optimization of Hybrid Combined Power Cycles Using Heliostat Field Collector*. *January*.

Said, Z., Ghodbane, M., Hachicha, A. A., & Boumeddane, B. (2019). Optical performance assessment of a small experimental prototype of linear Fresnel reflector. *Case Studies in Thermal Engineering*, *16*, 100541.

Saleh, A. M. (2012). Eksperyment Modeling Of Flat-Plate Solar Collector Operation In Transient States + mod mat + MATLAB + exp. May.

Sarma, D., Barua, P. B., & Hatibaruah, D. (2014). Optimization of Glazing Cover Parameters of a Solar Flat Plate Collector (FPC). *International Journal of Engineering Trends and Technology (IJETT)*, *14*.

Sato, A. I., Scalon, V. L., & Padilha, A. (2012). Numerical analysis of a modified evacuated tubes solar collector. *Renewable Energy and Power Quality Journal*, *1*(10), 384–389.

Shafie, S. M., Mahlia, T. M. I., Masjuki, H. H., & Andriyana, A. (2011). Current energy usage and sustainable energy in Malaysia: A review. *Renewable and Sustainable Energy Reviews*, *15*(9), 4370–4377.

Sharafeldin, M. A., Gróf, G., & Mahian, O. (2017). Experimental study on the performance of a flat-plate collector using WO3/Water nanofluids. *Energy*, *141*, 2436–2444.

Sharol, A. F. (2021). Integrated Cross-Matrix Absorber_Phase Change Material In Double_Pass Solar Air Heater.

Shojaee, S. M. N., Moradian, M. A., & Mashhoodi, M. (2015). Numerical Investigation of Wind Flow around a Cylindrical Trough Solar Collector. *Journal of Power and Energy Engineering*, *03*(01), 1–10.

Su, D., Jia, Y., Lin, Y., & Fang, G. (2017). Maximizing the energy output of a photovoltaic–thermal solar collector incorporating phase change materials. *Energy and Buildings*, *153*, 382–391.

Subiantoro, A., & Ooi, K. T. (2013). Analytical models for the computation and optimization of single and double glazing flat plate solar collectors with normal and small air gap spacing. *Applied Energy*, *104*, 392–399.

Tchinda, R. (2009). A review of the mathematical models for predicting solar air heaters systems. *Renewable and Sustainable Energy Reviews*, *13*(8), 1734–1759.

Thirugnanasambandam, M., Iniyan, S., & Goic, R. (2010). A review of solar thermal technologies. *Renewable and Sustainable Energy Reviews*, *14*(1), 312–322.

Tian, M., Su, Y., Zheng, H., Pei, G., Li, G., & Riffat, S. (2018). A review on the recent research progress in the compound parabolic concentrator (CPC) for solar energy applications. *Renewable and Sustainable Energy Reviews*, *82*(June 2016), 1272–1296.

Tian, Y., & Zhao, C. Y. (2013). A review of solar collectors and thermal energy storage in solar thermal applications. *Applied Energy*, *104*, 538–553.

Timilsina, G. R., Kurdgelashvili, L., & Narbel, P. A. (2012). Solar energy: Markets, economics and policies. *Renewable and Sustainable Energy Reviews*, *16*(1), 449–465.

Tsilingiridis, G. & Martinopoulos, G. & Kyriakis, N. (2004). Life cycle environmental impact of a thermosyphonic domestic solar hot water system in comparison with electrical and gas water heating. *Renewable Energy, Elsevier*, *29(8)*, 1277–1288.

Tuncer, A. D., Sözen, A., Khanlari, A., Amini, A., & Şirin, C. (2020). Thermal performance analysis of a quadruple-pass solar air collector assisted pilot-scale greenhouse dryer. *Solar Energy*, *203*(April), 304–316.

Tzivanidis, C., Bellos, E., Korres, D., Antonopoulos, K. A., & Mitsopoulos, G. (2015). Thermal and optical efficiency investigation of a parabolic trough collector. *Case Studies in Thermal Engineering*, *6*, 226–237.

Utekar, G., & Navadagi, V. (2016). *Performance analysis of solar collector with Inline and perforated W shape rib roughened absorber plate for air heating applications*. *June*, 170–178.

Vafaei, L. E., & Sah, M. (2017). Predicting efficiency of flat-plate solar collector using a fuzzy inference system. *Procedia Computer Science*, *120*, 221–228.

Varun, Saini, R. P., & Singal, S. K. (2008). Investigation of thermal performance of solar air heater having roughness elements as a combination of inclined and transverse ribs on the absorber plate. *Renewable Energy*, *33*(6), 1398–1405.

Vengadesan, E., & Senthil, R. (2020). A review on recent developments in thermal performance enhancement methods of flat plate solar air collector. *Renewable and Sustainable Energy Reviews*, *134*(August), 110315.

Venu, A., & Arun, P. (2013). Simulation studies on porous medium integrated dual purpose solar collector. *International Journal of Renewable Energy Research*, *3*(1), 114–120.

Vestlund, J. (2012). *Gas-filled, flat plate solar collectors*.

Vettrivel, H., & Mathiazhagan, P. (2017). Comparison study of solar flat plate collector with single and double glazing systems. *International Journal of Renewable Energy Research*, *7*(1), 267–274.

Wahida Khalili, N. N., Othman, M., Abu Bakar, M. N., Sakidin, H., & Abdullah, M. L. (2019). Mathematical Modelling and Simulation of the Performance of PV/T Air Solar Collector. *Journal of Physics: Conference Series*, *1366*(1).

Winston, R. (1974). Principles of solar concentrators of a novel design. *Solar Energy*, *16*(2), 89–95.

Wuryanti, S., & Megawati. (2019). Fin flat-plate type tetragon solar collector design based on convection radiation mechanism. *Cogent Engineering*, *6*(1), 1–12.

Xu, B., Xu, J., & Chen, Z. (2020). Heat transfer study in solar collector with energy storage. *International Journal of Heat and Mass Transfer*, *156*.

Yahya, M., Fudholi, A., & Sopian, K. (2017). Energy and exergy analyses of solar-assisted fluidized bed drying integrated with biomass furnace. *Renewable Energy*,

105, 22–29.

Youcef-Ali, S. (2005). Study and optimization of the thermal performances of the offset rectangular plate fin absorber plates, with various glazing. In *Renewable Energy* (Vol. 30, Issue 2, pp. 271–280).

Zhang, H., Chen, H., Han, Y., Liu, H., & Li, M. (2017). Experimental and simulation studies on a novel compound parabolic concentrator. *Renewable Energy*, *113*, 784–794.

Zima, W., & Dziewa, P. (2010). Mathematical modelling of heat transfer in liquid flat-plate solar collector tubes. *Archives of Thermodynamics*, *31*(2), 45–62.

APPENDIX I

LIST OF PUBLICATIONS

Journals

1. Harun, M. A., Abdul Majid, Z. A., Zakaria, Z. A., Ismail, A. F., Ihsan, S. I., Sopian, K., Sharol, A. F., & Abdul Razak, A. (2021). Study on Selection of a Suitable Material and The Parameters for Designing a Portable Flat Plate Base-Thermal Cell Absorber (FPBTCA). *Journal of Advanced Research in Fluid Mechanics and Thermal Sciences*, *85*(1), 71–92. https://doi.org/10.37934/arfmts.85.1.7192.
2. Muhammad Amin Harun, Zafri Azran Abdul Majid, Zairul Azrul Zakaria, Ahmad Faris Ismail, Sany Izan Ihsan, Kamaruzzaman Sopian, Amir Abdul Razak, & Ahmad Fadzil Sharol. (2022). Performance Analysis of Flat Plate Base-Thermal Cell Absorber (FPBTCA): Low Thickness Design. *Journal of Advanced Research in Fluid Mechanics and Thermal Sciences*, *96*(2), 122–133. https://doi.org/10.37934/arfmts.96.2.122133
3. Zakaria, Z. A., Majid, Z. A. A., Harun, M. A., Ismail, A. F., Ihsan, S. I., Sopian, K., Abdul Razak, A., & Sharol, A. F. (2021). Investigation on The Thermal Performance of Evacuated Glass-Thermal Absorber Tube Collector (EGATC) for Air Heating Application. Journal of Advanced Research in Fluid Mechanics and Thermal Sciences, 79(2), 48–64. https://doi.org/10.37934/arfmts.79.2.4864
4. Zairul Azrul Zakaria, Zafri Azran Abdul Majid, Muhammad Amin Harun, Ahmad Faris Ismail, Sany Izan Ihsan, Kamaruzzaman Sopian, Amir Abdul Razak, & Ahmad Fadzil Sharol. (2022). Experimental Investigation of Integrated Energy Storage on Thermal Performance Enhancement of Evacuated Glass-Thermal Absorber Tube Collector (EGATC) for Air Heating Application. *Journal of Advanced Research in Fluid Mechanics and Thermal Sciences*, *96*(1), 137–152. https://doi.org/10.37934/arfmts.96.1.137152

5. Zairul Azrul Zakaria, Zafri Azran Abdul Majid, Muhammad Amin Harun, Ahmad Faris Ismail, Sany Izan Ihsan, Kamaruzzaman Sopian, Amir Abdul Razak, & Ahmad Fadzil Sharol. Experimental Investigation of Integrated Energy Storage on Thermal Performance Enhancement of Evacuated Glass-Thermal Absorber Tube Collector (EGATC) for Air Heating Application. 5th INTERNATIONAL CONFERENCE ON MECHANICAL, AUTOMOTIVE AND AEROSPACE ENGINEERING 2021 (ICMAAE 2021), 22nd– 23rd June 2021, International Islamic University Malaysia, Kuala Lumpur.
6. Zairul Azrul Zakaria, Zafri Azran Abdul Majid, Muhammad Amin Harun, Ahmad Faris Ismail, Sany Izan Ihsan, Kamaruzzaman Sopian, Amir Abdul Razak, Ahmad Fadzil Sharol, Mohd Syahriman Mohd Azmi. Mathematical Model Development of Evacuated Glass-Thermal Absorber Tube Collector (EGATC) for Air Heating Application. International Conference on Science, Technology, Engineering & Mathematics (ICSTEM2022) in conjunction with 10th International Postgraduate Conference on Science & Mathematics 2022 (IPCSM2022), 24 September 2022, Sultan Idris Education University, Muallim, Perak.
7. Zairul Azrul Zakaria, Zafri Azran Abdul Majid, Muhammad Amin Harun, Ahmad Faris Ismail, Sany Izan Ihsan, Kamaruzzaman Sopian, Amir Abdul Razak, Ahmad Fadzil Sharol, Mohd Syahriman Mohd Azmi. Mathematical Model Development of Evacuated Glass-Thermal Absorber Tube Collector (EGATC) for Air Heating Application. Journal of Science and Mathematics Letter, JSML. (Manuscript draft: Accepted for publication)
8. Zairul Azrul Zakaria, Zafri Azran Abdul Majid, Muhammad Amin Harun , Ahmad Faris Ismail , Sany Izan Ihsan , Kamaruzzaman Sopian , Amir Abdul Razak , Ahmad Fadzil Sharol , Mohd Syahriman Mohd Azmi. Experimental Investigation of Pre-Heating Double Pass Flow Arrangement on Thermal Performance Enhancement of Evacuated Glass-Thermal Absorber Tube Collector (EGATC) for Air Heating Application. 3rd International Conference on Innovative Technology & Science (IC.ITS’22), 6 th - 7 th December 2022, University College of Yayasan Pahang (UCYP), Kuantan, Pahang.
9. Zairul Azrul Zakaria, Zafri Azran Abdul Majid , Muhammad Amin Harun , Ahmad Faris Ismail , Sany Izan Ihsan , Kamaruzzaman Sopian , Amir Abdul

Razak , Ahmad Fadzil Sharol , Mohd Syahriman Mohd Azmi. (2022). Experimental Investigation of Pre-Heating Double Pass Flow Arrangement on Thermal Performance Enhancement of Evacuated Glass-Thermal Absorber Tube Collector (EGATC) for Air Heating Application. Engineering, Agricultural, Science and Technology Journal (EAST-J). (Manuscript draft: Accepted for publication)

10. A.F. Sharol, A.A. Razak, Z.A.A. Majid, M.A.A. Azmi, M.A.S.M. Tarminzi, Y.H. Ming, Z.A. Zakaria, M.A. Harun, A. Fazlizan, K. Sopian. (2022). Effect of thermal energy storage material on the performance of double-pass solar air heater with cross-matrix absorber. *Journal of Energy Storage*, Volume 51, 104494, ISSN 2352-152X, https://doi.org/10.1016/j.est.2022.104494.

Conferences

1. Muhammad Amin Harun, Zafri Azran Abdul Majid, Zairul Azrul Zakaria, Ahmad Faris Ismail, Sany Izan Ihsan, Kamaruzzaman Sopian, Amir Abdul Razak, Ahmad Fadzil Sharol. (2021). Performance analysis of Flat Plate Base-Thermal Cell Absorber (FPBTCA): Low Thickness Design, 5th International Conference on Mechanical, Automotive and Aerospace Engineering 2021 (ICMAAE 2021), 22nd– 23rd of June 2021, International Islamic University Malaysia, Kuala Lumpur.

2. Zairul Azrul Zakaria, Zafri Azran Abdul Majid, Muhammad Amin Harun, Ahmad Faris Ismail, Sany Izan Ihsan, Kamaruzzaman Sopian, Amir Abdul Razak, Ahmad Fadzil Sharol. (2021). Experimental Investigation of Integrated Energy Storage on Thermal Performance Enhancement of Evacuated Glass-Thermal Absorber Tube Collector (EGATC) for Air Heating Application, 5th International Conference on Mechanical, Automotive and Aerospace Engineering 2021 (ICMAAE 2021), 22nd– 23rd of June 2021, International Islamic University Malaysia, Kuala Lumpur.

APPENDIX II

INTELECTUAL PROPERTY

Industrial Design Certification

INVOIS CUKAI DIPERMUDAHKAN

PERBADANAN HARTA INTELEK MALAYSIA
Unit 1-7 Aras Bawah Tower B
Menara UOA Bangsar
No 5 Jalan Bangsar Utama 1,
59000, Kuala Lumpur, Malaysia.
Tel: 603-2299 8400 Faks: 603-2299 8989
GST NO: 000869019648

MyIPO

RESIT RASMI

Diterima Daripada	**Butiran Resit Rasmi**
ZAFRI AZRAN ABDUL MAJID RADTEC ENTERPRISE PERAMU BARU LOT 352, Kuantan 26060 (MY)	Nombor Resit : RST/PHG-000670-2019 Tarikh : 15/07/2019 12:37:27 Jumlah : 290.00

Rujukan		**Butiran Bayaran**			
Pusat Bayaran	: PAHANG-	Cara Bayaran	No Doc	Tarikh Doc	Amaun (RM)
No. Invois	: 1889095	KAD DEBIT	000331000231	15/07/2019	290.00
Catatan	:				

Keterangan	No pendaftaran	Kuantiti	Kos Per Unit	GST	Jumlah
PM1	PI2019004062	1.00	290.00	0.00	290.00

Cetakan Berkomputer Tidak Perlu Tandatangan

*Resit ini akan dianggap batal sekiranya cek tidak dapat ditunaikan.
Pelanggan di bawah Seksyen 56(3)(b) Akta Cukai Barangan dan Perkhidmatan 2014

NURAIN BINTI OTHMAN
SALINAN PELANGGAN

PERBADANAN HARTA INTELEK MALAYSIA
INTELLECTUAL PROPERTY CORPORATION OF MALAYSIA
(Agensi di bawah KPDNHEP)
Unit 1-7 & Mezzanine, Aras 12–19
Tower B, Menara UOA Bangsar
No. 5, Jalan Bangsar Utama 1
59000 KUALA LUMPUR
MALAYSIA

Tel : +603 - 2299 8400
Faks (Fax) : +603 - 2299 8989
Laman Web (Web) : www.myipo.gov.my

CERTIFICATE OF FILING

APPLICANT	:	1) ZAFRI AZRAN ABDUL MAJID 2) ZAIRUL AZRUL BIN ZAKARIA 3) MUHAMMAD AMIN BIN HARUN 4) AHMAD FARIS ISMAIL 5) SANY IZAN IHSAN 6) KAMARUZZAMAN SOPIAN
APPLICATION NO	:	PI2019004062
REQUEST RECEIVED ON	:	15 JULY 2019
FILING DATE	:	15 JULY 2019
AGENT'S/APPLICANT'S FILE REF.	:	-

Please find attached, a copy of the Request Form relating to the above application, with the filing date and application number marked thereon in accordance with Regulation 25(1).

Date : 16 JULY 2020

(NOORHISHAM BIN OTHMAN)
for Registrar of Patents
✉ noorhisham@myipo.gov.my
☎ 03-22998812

To : ZAFRI AZRAN ABDUL MAJID
RADTEC ENTERPRISE PERAMU BARU LOT 352
26060 KUANTAN
PAHANG DARUL MAKMUR
MALAYSIA

INVOIS CUKAI DIPERMUDAHKAN

PERBADANAN HARTA INTELEK MALAYSIA
Unit 1-7 Aras Bawah Tower B
Menara UOA Bangsar
No 5 Jalan Bangsar Utama 1,
59000, Kuala Lumpur, Malaysia.
Tel: 603-2299 8400 Faks: 603-2299 8989
GST NO: 000869018648

MyIPO

RESIT RASMI

Diterima Daripada	Butiran Resit Rasmi		
ZAFRI AZRAN BIN ABDUL MAJID RADTEC ENTERPRISE, PERAMU BARU LOT 352, 26060 KUANTAN, PAHANG DARUL MAKMUR,	Nombor Resit	:	RST/PHG-001289-2020
	Tarikh	:	15/12/2020 08:46:41
	Jumlah	:	1,100.00

Rujukan			Butiran Bayaran			
Pusat Bayaran	:	PAHANG-	Cara Bayaran	No Doc	Tarikh Doc	Amaun (RM)
No. Invois	:	-	KAD DEBIT	001081000706	15/12/2020	1,100.00
Catatan	:					

Keterangan	No pendaftaran	Kuantiti	Kos Per Unit	GST	Jumlah
PME	PI 2019004052	1.00	1,100.00	0.00	1,100.00

Cetakan Berkomputer Tidak Perlu Tandatangan

NUR SAIDATUN SHEILA BINTI TALIB
SALINAN PELANGGAN

*Resit ini akan dianggap batal sekiranya cek tidak dapat ditunaikan.
Pelepasan di bawah Seksyen 56(3)(b) Akta Cukai Barangan dan Perkhidmatan 2014

PERBADANAN HARTA INTELEK MALAYSIA
INTELLECTUAL PROPERTY CORPORATION OF MALAYSIA
(Agensi di bawah KPDNHEP)
Unit 1-7 & Mezzanine, Aras 12–19
Tower B, Menara UOA Bangsar
No. 5, Jalan Bangsar Utama 1
59000 KUALA LUMPUR
MALAYSIA

Tel : +603 - 2299 8400
Faks (Fax) : +603 - 2299 8989
Laman Web (Web) : www.myipo.gov.my

APPLICATION NO : PI2019004062

APPLICANT : 1) ZAFRI AZRAN ABDUL MAJID
2) ZAIRUL AZRUL BIN ZAKARIA
3) MUHAMMAD AMIN BIN HARUN
4) AHMAD FARIS ISMAIL
5) SANY IZAN IHSAN
6) KAMARUZZAMAN SOPIAN

APPLICANT'S/AGENT'S REF. : -

DATE OF MAILING : 16 JULY 2020

PRELIMINARY EXAMINATION - ADVERSE FORMALITIES REPORT

Please find attached a copy of the Preliminary examination report under Section 29 of the Patents Act, relating to the following deficiencies :

☐ **ANNEX A**: Deficiencies as to Regulation 5 to 11,50 and 51

☒ **ANNEX D**: Deficiencies as to Regulation 18.

You are invited to correct the deficiencies. Corrections should be received at the above Office or Branch Offices in Sabah or Sarawak within 3 months of the above date of mailing, otherwise the application may be refused.

Date : 16 JULY 2020

(NOORHISHAM BIN OTHMAN)
for Registrar of Patents
✉ noorhisham@myipo.gov.my
☎ 03-22998812

To : ZAFRI AZRAN ABDUL MAJID
RADTEC ENTERPRISE PERAMU BARU LOT 352
26060 KUANTAN
PAHANG DARUL MAKMUR
MALAYSIA